

The Cenozoic salt diapir near Eyvanekey and Garmsar, Iran: New insights from structural investigations and analogue modeling

Dissertation
zur Erlangung des Doktorgrades
der Naturwissenschaften

vorgelegt beim Fachbereich Geowissenschaften
der Johann Wolfgang Goethe–Universität
in Frankfurt am Main

von

Shahram Baikpour
aus Teheran (Iran)

Frankfurt am Main, 2010

This is dedicated to my parents

&

To whom I love

CONTENTS

ZUSAMMENFASSUNG.....	1
ABSTRACT.....	4
ACKNOWLEDGMENTS.....	7
1. INTRODUCTION.....	8
2. REGIONAL GEOLOGY.....	9
3. METHODS.....	10
3.1. Field investigations.....	10
3.2. Interferometry	11
3.3. Geophysics.....	12
4.3. Analogue modelling.....	12
4. RESULTS.....	13
5. CONCLUSIONS.....	17
6. REFERENCES.....	19
7. MANUSCRIPTS RELATED TO THESIS.....	20
7.1. InSAR maps and time series observations of surface displacements of rock salt extruded near Garmsar, northern Iran.	
7.2. The Garmsar salt nappe and seasonal inversions of surrounding faults imaged on SAR Interferograms, Northern Iran.	
7.3. Analogue and geophysical modeling of the Garmsar Salt Nappe, Iran: constraints on the evolution of the Alborz Mountains.	
7.4. Hazardous waste disposal in Iran: Results from a pre-site study of the Garmsar Salt basin.	

CURRICULUM VITAE



Shahram Baikpour

Personal Information:

Date of Birth: 10th Jan 1976
Marital Status: Single
Nationality: Iranian
E-mail address: baikpour@em.uni-frankfurt.de
baikpour2004_rsgsi@yahoo.com

Education:

- Ph.D (student) in Structural Geology (Tectonics) – Frankfurt University (2005-2010), Frankfurt, Germany.
- M.Sc in Structural Geology (Tectonics) – Shahid Beheshti University (2001-2004), Tehran, Iran.
- B.Sc in Geology Science_ Shahid Beheshti University (1996- 2000), Tehran, Iran.
- High school Diploma in Natural Branch, Shahid Beheshti High school.

Academic Achievements:

- Obtained the score (16.25 out of 20) and thesis's score (18.5 out of 20), in M.Sc degree (2004).
- Obtained the score (15.65 out of 20) in B.Sc. degree (2000).

PhD Thesis Title:

- The Cenozoic salt diapir near Eyvanekey and Garmsar, Iran: New insights from structural investigations and analogue modelling

M.Sc. Thesis Title:

- Structural analysis of Ipack Fault in South of Eshtehard and seismicity of the area.

Publications:

- Baikpour, S., Zulauf, G., Dehghani, M. & Bahroudi, A., 2010, *InSAR maps and time series observations of surface displacements of rock salt extruded near Garmsar ,Northern Iran*, **Journal of the Geological Society**, London, 167, 171-181.
- "Shahram Baikpour,Gernold Zulauf, Arash Sebti, Hassan Kheirolahi and Carlo Dietl, 2010, *Analogue and geophysical modelling of the Garmsar Salt Nappe, Iran: constraints on the evolution of the Alborz Mountains*. **Geophysical Journal International**, 182, PP 599-612
- Baikpour, S., Talbot, C.J., 2010, The Garmsar salt nappe and seasonal inversions of surrounding faults imaged on SAR interferograms, northern Iran, Edited by Ian Alsop in, **Salt Tectonics, Sediments and Prospective. Geological Society, London, Special publications (in press)**.
- Baikpour, S., Zulauf, G., Abdolahifard, I., 2010, Hazardous waste disposal in Iran: Results from a pre-site study of the Garmsar Salt basin. *Manuscript submitted to journal of Sciences, Islamic Republic of Iran*.
- "Folding and Boudinage under constriction based on analogue modeling", **26th conference (GSI)**, Iran, 2008.
- "InSAR maps and time series observations of Garmsar Salt Nappe" **ESA conference, Fringe 2009**, Frascati, Italy, 2009.
- "Target modeling by geology structures", **MapIndia2005** conference, India, 2005.
- "Remote sensing studies in South of Khorasan", **Map Middle East 2005** conference, Dubai, 2005.
- "Remote sensing studies in South of Khorasan ", **23rd conference (GSI)**, Iran, 2005.
- "Structural analysis of Ipack Fault ", **22nd conference (GSI)**, Iran, 2004.
- "Seismicity of Eshtehard Area ", **22nd conference (GSI)**, Iran, 2004.

Work Experiences:

- Working as private teacher (Tutor).
- Working as Remote Sensing specialist in Remote Sensing Group of Geological Survey of Iran (GSI) in following fields:
 - Mineral Exploration (Involved with several mineral exploration projects)

- Digital Image Pre-Processing and Processing (Including optical and RADAR images).
- Working as Heavy mineral study Group in Geological Survey of Iran (GSI) since 2003.
- Cooperation with Keyhan Exploration and Production Services (KEPS).

Activities:

- Member of Iranian RS & GIS Society (IRSGS).

Research Interests:

- Digital image processing
- Alteration areas and structures extraction in mineral exploration
- Cooperation with GSI group in field works.

Skills:

- Knowledge of Computer:
 - Digital image processing and GIS softwares (PCI, ERDAS, ENVI, Arcview, AutoCAD, ImagJ)
 - General softwares: Office (Microsoft word, PowerPoint...)
- Language:
 - English (well in all abilities "LSRW")
 - German (Elementary)
 - Persian (Mother tongue)

ZUSAMMENFASSUNG

Die Alborz-Ketten bilden einen ~ 100 km breiten E-W streichenden Gebirgsgürtel mit bis zu 5000 m hohen Gipfeln im nördlichen Iran. Das Gebirge ist Teil des alpinen Gebirgsgürtels und erstreckt sich 2000 km südlich des Kaspischen Meeres. Die Alborz-Berge bestehen aus neogenen Sedimenten, die verfaltet und gestört sind. In den westlichen Alborz-Bergen streichen die Falten und Störungen NW-SE, in den östlichen Alborz-Bergen streichen sie NE-SW. GPS Untersuchungen belegen eine N-S Verkürzung mit dextraler Blattverschiebungskomponente entlang von ESE-WNW streichenden Störungen und sinistralen Bewegungen entlang von ENE-WSW streichenden Störungen.

Die vorliegende Arbeit beschäftigt sich mit der aktiven Garmsar-Salzdecke, deren fragmentiertes Dach von Salzgesteinen durchstoßen wird, die im Bereich der Alborz-Deformationsfront extrudieren. Während der vergangenen 5 Ma verlagerte sich die Alborz-Deformationsfront nach SSW und überfuhr dabei eine Salzabfolge im Garmsar-Becken. Dabei wurde das Salz nach SSW ausgequetscht, um auf der Oberfläche des Great Kavir Platz zu nehmen. Das „ausgeflossene“ Salz bildet das Eyvanekey-Plateau zwischen den Städten Eyvanekey und Garmsar. Die Garmsar-Salzdecke und das Eyvanekey-Plateau sind möglicherweise entlang der Zirab-Garmsar-Störung um ca. 9 km dextral versetzt worden.

Die struktureologische Aufnahme der Garmsar-Salzdecke ergibt drei verschiedene Gruppen von Klüften, die senkrecht und parallel zur lokalen mechanischen Anisotropie angeordnet sind. Die Falten im Arbeitsgebiet sind kongruent (Typ 2 und 3 nach Ramsay) und resultieren aus viskosem, irregulärem Fließen.

Die Ergebnisse der InSAR-Untersuchungen zeigen, dass die zentralen Alborz-Berge mit einer Geschwindigkeit von ca. 1 cm/a gehoben und mit 8 ± 2 mm/a verkürzt werden. Diese Werte stimmen mit den GPS-Daten überein. Basierend auf neun „Advanced Synthetic Aperture Radar“ (ASAR) Szenarien, die vom Satelliten ENVISAT der Europäischen Weltraumagentur zwischen 2003 und 2006 erstellt wurden, haben wir Interferogramme zur Kartierung des Versatzes über 22 Inkremente im Verlauf von 2 bis 18 Monaten erstellt.

Die Ergebnisse lassen vermuten, dass die Höhe der Salzoberfläche kontinuierlichen Schwankungen unterliegt, die saisonal bedingt sind. Der Oberflächenversatz über die gesamte Region reicht von reiner Subsidenz um -40 bis -50 mm/a bis hin zu einem Aufstieg von 20 mm/a. Um das zeitabhängige Deformationsverhalten mit einer hohen räumlichen Auflösung zu untersuchen, wurden Algorithmen auf der Grundlage kleiner Basislinien-Datensätze (SBAS) benutzt. Damit wurden interferometrische SAR-

Zeitreihenanalysen durchgeführt. Das Arbeitsgebiet sinkt demnach kontinuierlich mit einer jährlich variierenden Rate ab.

Die Karte der mittleren LOS-Deformationsgeschwindigkeiten zeigt hingegen an, dass die Subsidenz im oberen Teil der Salzdecke nach unten bis hin zu den landwirtschaftlichen Flächen im Tiefland zunimmt. Der Großteil der Subsidenz kann vermutlich der Subrosion des Salzes durch die jährlichen Niederschläge von ca. 100 mm/a zugerechnet werden. Die räumlichen Änderungen in der Subsidenzrate werden möglicherweise von der Verteilung von Brunnen, von Bergbautätigkeit am Rande des Salzgletschers und von Störungen und Brüchen im Salz selbst gesteuert.

Die auffälligsten saisonalen Effekte können auf den landwirtschaftlichen Flächen rund um die Garmsar-Salzdecke beobachtet werden. Diese Nutzflächen sinken im Summer und im Frühjahr schnell ab, also dann, wenn sie unter Entnahme von Grundwasser bewässert werden. Die maximale Subsidenzrate (40-50 mm/a) liegt östlich und westlich des Eyvanekey-Plateaus vor, wo Ackerflächen jeden Frühling und Sommer aus grundwassergespeisten Brunnen bewässert werden.

Die maximale Oberflächendeformationsrate liegt bei 20 mm/a im Ackerland und bei 5 mm/a im Zentrum der Salzdecke.

Tiefenabschätzungen mit Hilfe der Euler-Dekonvolution für Schwere- und Magnetikdaten machen deutlich, dass das Salz aus einer Tiefe von weniger als 2000 m extrudiert. Das Schwerefeld im Arbeitsgebiet ist durch starke Anomalien im SW und schwache Anomalien im NE charakterisiert. Eine deutlich negative Anomalie im N zeigt an, dass der nördliche Teil abgesunken ist, während die Südseite asymmetrisch angehoben wurde.

Die seismischen Profile zeigen drei dominierende Horizonte in den miozänen Sedimenten : die Untere Rot-Formation, die Qom-Formation und die Obere Rot-Formation. In den seismischen Profilen vom Westteil des Arbeitsgebietes liegen keine Hinweise für aufsteigendes Salz und damit verbundene Salzdome vor. Entlang der NE- und NW-streichenden Störungen sind die Schichten jedoch im oberen Teil der Qom-Formation ausgedünnt. An einigen Stellen zeigen die Reflektoren steile Störungen nahe der Sattelkerne. Es überwiegen NE-SW- bzw. NW-SE und E-W-streichende Störungen.

Analogexperimente wurden durchgeführt, um unser Wissen über die Entwicklung des Garmsar-Saldomes zu erweitern. Zur Modellierung diente ein skaliertes Modell mit den Dimensionen 34 cm * 25 cm * 2,5 cm (Länge * Breite * Höhe), welches senkrecht zu seiner Längsseite verkürzt wurde. Die Keilform der Alborz-Berge im Kartenbild wurde durch einen Styroporkeil simuliert. Als Analogmaterial für Steinsalz wurde

Polydimethylsiloxan (PDMS) verwendet, ein linearviskoses (Newtonisches) Material mit einer Viskosität von $2,3 \cdot 10^4$ Pa s und einer Dichte von $0,96 \text{ g/cm}^3$ bei Raumtemperatur. Als Analogmaterial für siliziklastische Krustengesteine wurde trockener Quarzsand benutzt.

Die Experimentalergebnisse lassen sich heranziehen, um die strukturelle Entwicklung des Arbeitsgebietes zu simulieren: Während ihres Fortschreitens nach SSW überfuhr die Alborz-Deformationsfront die Salzfolge im Garmsargebiet. Auch im Modell entstanden ein Salzbecken und eine Salzextrusion.

Einige Schnitte durch das keilförmige Analogmodell zeigen N- und S-einfallende Auf- und Überschiebungen, die in guter Übereinstimmung mit der Keilform der Alborz-Gebirgskette stehen. Darüber hinaus wurden sinistrale Scherung entlang ENE-WSW-streichender Störungen der Alborz-Berge, sowie dextrale Blattverschiebungen entlang ESE-WNW-streichender Störungen mit einer N-S-Verkürzung während des Miozän in Verbindung gebracht. Strukturelle Vorzeichnungen, die im Modell zu Z-Falten auf dem „westlichen“ und zu S-Falten auf dem „östlichen“ Faltenschenkel gelegt wurden, sind vergleichbar mit den Falten im Arbeitsgebiet.

Die neuen Ergebnisse können herangezogen werden, um mögliche Endlager für radioaktiven und sonstigen giftigen Abfall zu bewerten. Die Entsorgung dieses Abfalls ist ein zentrales Problem für die Gesellschaft. Salzgesteine haben gute Eigenschaften was die Einlagerung von gefährlichen Stoffen anbelangt. Es ist nahezu impermeabel und verfügt aufgrund seiner plastischen Verformbarkeit bereits unter geringen Temperaturen über einen ‚Selbstverschließungsmechanismus‘. Das Qom und Garmsar Becken stellen mit den hier vorhanden Salzdiapiren aufgrund ihrer engen Nachbarschaft zu Theheran gute Kandidaten für die Einlagerung von gefährlichen Stoffen dar.

Aufgrund der vorliegenden Daten läßt sich feststellen, dass eine Einlagerung von gefährlichen Stoffen in tieferen Abschnitten des Salzdiapires möglich sein könnte, wohingegen eine Entsorgung in oberflächennahen Salzgesteinen nicht empfohlen werden kann, da hier die Wegsamkeit für zirkulierende Fluide erheblich größer ist als in tieferen Stockwerken.

ABSTRACT

The Alborz Mountains are forming a ~100 km wide, E-W trending mountain chain where individual summits are up to 5000 m in elevation. The Alborz Mountains range are part of the Alpine orogen and are straddling a 2000 km wide area S of the Caspian Sea.

The rocks of the Alborz Mountains consist of Neogen sediments, which are affected by folding and faulting. In the western part of the Alborz Mountains the folds and faults are trending NW-SE, whereas in the eastern part they are trending NE-SW. GPS data confirm N-S shortening including dextral strike-slip along ESE-WNW trending faults, and sinistral strike-slip along ENE-WSW trending faults.

The present thesis is focusing on the active Garmsar salt nappe, the fragmented roof of which is pierced by rock salt which extruded near the front of the Alborz Mountains Range. During the past 5 m.y. the front of the Alborz chain migrated towards SSW on top of the salt of the Garmsar basin. The salt was squeezed towards SSW and took place at the Great Kavir.

The extruded salt is forming the Eyvanekey plateau between the cities of Eyvanekey and Garmsar. Both the Garmsar salt nappe and the Eyvanekey plateau are dextrally displaced for ca. 9 km along the Zirab-Garmsar fault.

Structural analyses of the Garmsar salt nappe indicate three different groups of joints which are trending perpendicular and parallel to the local mechanical anisotropy. The folds of the study area are congruent (type 2 and 3 after Ramsay) resulting from viscose inhomogeneous flow.

InSAR-Investigations suggest the Alborz Mountains to be lifted up by ca. 1 cm/a, while horizontal shortening is active at a rate of 8 ± 2 mm/a. These values are consistent with GPS data. Based on nine „Advanced Synthetic Aperture Radar“ (ASAR) scenarios, produced by the ENVISAT satellite of the European space agency between 2003 and 2006, we used interferograms to map the displacement via 22 increments during 2 – 18 months. The results suggest that the topographic height of the surface of the salt is changing at a rate which is controlled by the season. The displacement ranges from subsidence at -40 to -50 mm/a to uplift of 20 mm/a. In order to investigate the time-dependent deformation with high spatial resolution, we used algorithms which are based on data of small base lines (SBAS). The resulting interferometric SAR time series analyses also suggest that the study area is largely subsiding at a rate that is controlled by the seasons.

The map with the averaged LOS deformation velocities, on the other hand, suggests the subsidence to increase from the upper part of the salt nappe towards deeper topographic

levels of the agricultural lowlands. The major part of subsidence is probably caused by the annual rainfall which results in subsidence of salt. The spatial changes in the subsidence rate are probably controlled by the distribution of fountains, mining activity at the margin of the salt glacier, and faults and fractures inside the salt.

Striking seasonal imprints are obvious along the agricultural areas which are surrounding the Garmsar salt nappe. These areas are rapidly subsiding in summer and spring when groundwater is used for irrigations. The maximum rate of subsidence (40-50 mm/a) is located E and W of the Eyvanekey plateau, where large areas are irrigated. The maximum displacement is 20 mm/a in the farmland and 5 mm/a in the center of the salt nappe.

Depth estimates using Euler deconvolution method for gravimetric and magnetic data suggest the salt to extrude from a depth less than ca. 2000 m. The gravity field of the study area is characterized by strong anomalies in the SW and weak anomalies in the NE. A considerable negative anomaly in the N indicates that the northern part subsided, whereas the southern part was lifted up.

The seismic data show three major horizons inside the Miocene sediments: the Lower Red Formation, the Qom Formation, and the Upper Red Formation. The western part of the study area seems to be free from salt domes. The layers of the upper part of the Qom Formation show thinning along the NE and NW trending faults. In some areas the seismic reflectors indicate steep faults close the saddle of the folds. NE-SW-, NW-SE and E-W-trending faults prevail.

Analogue experiments have been carried out to extend our knowledge about the evolution of the Garmsar salt dome. We used a scaled model (34 cm * 25 cm * 2.5 cm) that was shortened perpendicular to its long side. The wedge shape of the Alborz Mountains was simulated by a wedge consisting of Styrofoam. Rock salt was simulated using Polydimethylsiloxan (PDMS), a linear viscous material with a viscosity of $2.3 \cdot 10^4$ Pa s and a density of 0.96 g/cm^3 at room temperature. Other sediments were modeled using dry quartz sand. The experimental results can be used to simulate the structural evolution of the study area: The Alborz deformation front was emplaced on top of the salt rocks in the Garmsar area while migrating towards SSW. A salt basin and a salt extrusion have also been produced in the model. Cross sections through the wedge shaped analogue model indicate N- and S-dipping reverse faults, which are in line with the wedge shape of the Alborz chain. Moreover, ENE-WSW trending sinistral and ESE-WNW trending dextral strike-slip faults led to N-S shortening during the Miocene. Structural marker horizons,

which have been turned into Z-folds on the western fold limbs and to S-folds on the eastern fold limbs, are comparable with the folds of the study area.

Solving the problem of waste is one of the central tasks of environmental protection. It is becoming increasingly difficult to find suitable sites that are acceptable to the public. Salt and salt formations have relevant properties to be utilizing as a repository for each kind of waste. The favorable properties make rock salt highly suitable as a host rock, in particular for nonradioactive and radioactive wastes.

The Qom and Garmsar basins are the nearest salt diapirs to the Tehran province, and there are suitable repositories for waste disposal.

Based on surface and subsurface data, the Garmsar salt diapir has been investigated as a case example for its suitability as a host and repository for various types of waste. The data used are based on field studies, interferometry, and geophysical investigations.

The results of this study suggest the deep bedded salt of the Garmsar Salt Basin to be an appropriate host for the deposition of industrial waste. Rock salt of surficial layers or domes, on the other hand, is not regarded as an appropriate candidate for waste disposal.

ACKNOWLEDGMENTS

The author would like to express his sincere gratitude to Prof. Gernold Zulauf for his supervision, encouragement, guidance and inspiration provided during the course of this research. Prof. Georg Kleinschmidt, my second advisor, is also greatly acknowledged. Thanks for his helping and kindness.

I would also like to express my sincere thanks to Dr. Carlo Dietl for his advice, encouragement. I wish to express my sincere thanks and appreciation for helpful contributions made by the following professionals during this study: Dr. Abbas Bahroudi, Dr. Maryam Dehghani. I also would like to thank the Geomatics staff in the Geological Survey of Iran, especially, Arash Sebti and Hassan Kheirolahi for their geophysics contribution, Dr. Fariborz Gharib, Davoud Refahi, Ali Kiani, Ali Hosseinmardi, Mahasa Rousta. Special thanks to Pedram Aftabi for his field work leadership and thanks to Mark Peinl, he has always taken the time to explain and resolve my problems.

The Geophysics Group (National Iranian Oil Company) is thanked for their contributions, in particular Dr. Iraj Abdolahi Fard, Gholamreza Peyrovian, and Rahman Javaherian.

Very special thanks to Prof. Christopher J. Talbot for setting up my papers and giving me the possibility to work easily. I wish to express my profuse gratitude to Justin Parker, for Editing and setting up the thesis.

I would like to express my deepest thanks to my parents and members of my family in Iran who have provided continued support throughout this study and indeed for my entire life.

This study would not have been finished without support and encouragement from all my Iranian and German friends at the University of Frankfurt (Susanne Fondacaro, Annette Schlapp, M. Ghobadi, David Storz, Michael Seitz, Stefanie Lode, Michael Doblner, Gutier Nejimak, Thomas Klein, also my Iranian and German friends and their families in Frankfurt (Aref & Sara, Reza Ghodsi, Manouchehr & Maryam Danesh, A. Mohamadi, Sara & Mehrdad).

I would like to thank European Space Agency for supplying the ENVISAT data, the Geological Survey of Iran for supplying the hardware and software and logistical support for preparation and analysis of the data. I have also benefited greatly from the National Iranian Oil Company who supplied Geophysical data, special thanks to them.

I would like to acknowledge with sincere appreciation the financial support of the DAAD (for 6 months) and Carl Duisburg Centeren. I have also benefited greatly from the Semnan Regional Water Company who supplied well locations, special thanks to them.

1. Introduction

The Garmsar salt nappe is a major constituent of the Alborz Mountains in northern Iran.

The main aim of this thesis is to establish whether the Garmsar salt nappe is still active and whether salt is still extruding at the Alborz Mountain front. Some salt diapirs at the Alborz Mountain front probably supplied the Garmsar salt nappe and are still active. This may also be the case with diapirs behind the front. Current data are ambiguous and it is unclear if the salt that extruded to the surface is expanding or shrinking due to seasonal changes.

From an economical point of view, the study area has recently been investigated by many miners and discoveries. However, there is still a significant unexploited potential, for instance, using the Garmsar salt basin as a repository for different kind of waste.

There are many ambiguities concerning stratigraphy and structure. Different structural trends have been distinguished in the area and their priority and relationship to each other and to the salt nappe are unknown. The present thesis attempts to describe the structural elements based on field investigations, interferometry and geophysics. The purpose is to realize the source and the depth of the salt to utilize for waste disposal in the future.

InSAR uses the phase differences between two SAR images of the same area acquired at different times to map surface displacement in the Line Of Sight (LOS) of the satellite. Data for this InSAR study of the Garmsar area were collected by the European Space Agency (ESA) Environmental Satellite (ENVISAT) that imaged the area between August 2003 and February 2006.

Understanding of the distribution pattern of dominant faults and igneous rocks at the top of the basement, studying of the depth and relief of the main density interfaces have been constrained using geophysical analyses.

Analogue models have been used as a small-scale structure to unravel the kinematics of large-scale tectonics.

The more detailed aims of this study are:

- 1) to determine the geometry of structures beneath the salt nappe and other units based on geophysical data, the latter obtained by National Iranian Oil Company;
- 2) to understand the effect of different parameters of surface deformation of salt glacier based on Interferometry SAR (InSAR) ;
- 3) using analogue modeling as an experimental method to constrain the geometry, dimensions and evolution of the salt diapir of Garmsar. The latter should be integrated into large-scale tectonic reconstructions and inversion modeling. Since the experimental

technique can be used to obtain solutions for three-dimensional problems, it can offer invaluable new insights into geological problems, which are intrinsically three dimensional and often involve large amounts of strain;

4) to realize the relationship between surface and sub-surface structures in the study area.

5) to check if hazardous waste can be deposited in the Garmsar salt basin.

The most important results of the present PhD thesis have already been published in international journals or have been submitted for publication in international journals. A summary of the content of these publications is presented in the following sections.

The following four papers are attached to the present summary and support the thesis:

- Baikpour, S., Zulauf, G., Dehghani, M. & Bahroudi, A., 2010. InSAR maps and time series observations of surface displacements of rock salt extruded near Garmsar, northern Iran, *Journal of the Geological Society, London*, 167, 171-181.
- Baikpour, S., Talbot, C.J., 2010. The Garmsar salt nappe and seasonal inversions of surrounding faults imaged on SAR Interferograms, Northern Iran. *Geological Society, London, Special publications (in press)*.
- Shahram Baikpour, Gernold Zulauf, Arash Sebti, Hassan Kheirolahi and Carlo Dietl, 2010. Analogue and geophysical modeling of the Garmsar salt nappe, Iran: constraints on the evolution of the Alborz Mountains. *Geophysical Journal International, UK, Volume 182, Issue 2, PP 599-612*.
- Shahram Baikpour, Gernold Zulauf, Iraj Abdolahifard, 2010, Hazardous waste disposal in Iran: Results from a pre-site study of the Garmsar Salt basin. Manuscript submitted to: *Journal of Sciences, Islamic Republic of Iran*.

2. Regional Geology

The Alborz Mountains represent a composite orogenic belt which results from oblique crustal shortening between central Iran and Eurasia. For the last 5 ± 2 m.y this oblique shortening is partitioned along range-parallel, sinistral strike-slip and thrusting, the latter with thrust planes dipping inwards from the margins of the range (Allen *et al.*, 2003; Ritz *et al.*, 2006).

The kinematic pattern of the Alborz Mountains is affected by salt-bearing Neogen sediments that underwent shortening and uplift during the Cenozoic (*Alavi, 1996*).

Unlike most Iranian salt extrusions that probably gravity-spread for tens or hundreds of millennia from diapirs that reached the surface along faults (*Talbot et al., 2000*), the salt sheet that underlies the Eyvanekey Plateau differs in having been squeezed to the surface, while the frontal part of the Alborz Mountains advanced southward over the Garmsar basin. Some salt may remain at place beneath the deformation front of the Alborz Mountains and its foreland and several small diapirs extrude along faults in the foothills (*Safaei, 2001*). Several extrusions of salt in the hills north of Garmsar mark where the Alborz deformation front is offset about 9 km by the 130 km long SW-NE trending Zirab-Garmsar transtensional fault.

The Garmsar basin is one of a series of basins in the foredeep of the Alborz Mountains forming an embayment in the northern periphery of the Great Kavir from which it is separated by the Kuh-e-Gachab and Dulasian swell. The oldest Cenozoic strata in the region are marine Eocene sediments associated with volcanic rocks resting unconformably on top of folded Mesozoic strata. The age of the evaporitic sequence is unclear because of the lack of fossils. However, lithological similarities with rocks from Qom Kuh and with the diapirs in the Great Kavir (*Jackson et al., 1990*) suggest the Garmsar rocks to include evaporites of both upper Eocene and Oligocene age.

The upper part of the Oligocene sequence, the Lower Red Formation, is made of gyprock, sandy shale and some volcanics. A similar sequence, referred to as Upper Red Formation, was deposited in the Miocene. Between the Lower and Upper Red Formations there is a sequence of limestone, marl, shale and sandstone which is called the Qom Formation. The age of the latter is upper Oligocene to lower Miocene.

3. Methods

3.1. Field investigations

Field investigations were carried out to map and measure the major structural elements, such as bedding, fold axes, faults, and joints. Analyses of geological structures help to interpret the conditions of deformation of salt rocks in the study area.

The field work started from 25th of June 2007 until 5th of July 2007. It was included, walking on the surface of salt nappe in S and N directions of the study area, and finding the outcrops to obtain some structures to measuring and taking photos. Outcrops on salt rock and salt caprock were not sufficient for next investigations. Totally 48 stations visited

during 10 days and in any case we measured the structural elements in outcrops for next interpretation. Joints and fractures were measured in every station, but the traces of major faults were not sufficient. Probably the faults in the study area are blind faults and covered by sediments.

We were also focusing on folds and boudins to realize the directions of stress and strain. Although the acquired data are not sufficient for next interpretations, owing to lack of outcrops on salt nappe and ductile properties of salt; we utilized the acquired data and structural elements to process by RockWork 2006 software (supply in Geological Survey of Iran).

3.2. Interferometry

Interferometric analyses of SAR images have become a widespread, valuable technique to measure subtle displacements of the ground surface (*Massonnet and Feigl, 1998*). When two radar scenes are made at different times from the same viewing angle, a small change in the position of the target (ground surface) may create a detectable change in the phase of the backscattered signals. The resulting difference of phase is expressed in an interference map (interferogram), which the resulting fringe pattern reflects the ground displacement that occurred between the two acquisitions, and the product is referred to as a “change interferogram”. Rather than using the primary data to generate our own DEM, we used the DEM provided by the Shuttle Radar Topography Mission (SRTM) with the spatial resolution of 90 m.

In the case of the ENVISAT SAR satellite each fringe or colour cycle in a change interferogram corresponds to a map contour of displacement equivalent to half the radar wavelength. The mean incidence angle of this satellite is 23°. Thus, in the case of pure vertical movement, one fringe cycle represents 31 mm of displacement.

The phase change in the interferogram is the composite of topographic information, φ_{topo} , and surface displacement, between the two acquisitions, φ_{disp} , atmospheric delay, φ_{delay} , and noise, φ_{noise} . Successful InSAR generation requires the removal of the topographic phase contribution and so as to isolate the ground displacement component. The φ_{topo} can be simulated and eliminated by introducing DEM information.

$$\varphi = \varphi_{\text{topo}} + \varphi_{\text{disp}} + \varphi_{\text{delay}} + \varphi_{\text{noise}}$$

The atmospheric component, ϕ_{delay} , is primarily due to fluctuations of water content in the atmosphere between the satellite and the ground. The atmospheric delay can be identified using the fact that the fringe structure is independent over several interferograms; alternatively, it can be modeled by using data from a GPS network. It is also possible to reduce the atmospheric disturbance to the displacement phase term by using the ‘interferogram stacking technique’. The atmospheric effect can be estimated by plotting the phase against the height for each pixel; it is strong if there is a good correlation between height and phase. Maps displaying the mean displacement velocity were produced using MATLAB software.

3.3. *Geophysics*

We applied geophysical (gravity and magnetic) processed data for next interpretations. These data were collected by the National Iranian Oil Company. Their workload was $\sim 4674 \text{ km}^2$ and a total of 13270 G/M stations had been acquired. Many analysis methods have been developed to process raw magnetic and/or gravity data; the latter we utilized these processed data by using the Geosoft software (supply in Geological Survey of Iran) to estimate the depth of the Garmsar salt basin.

The Euler deconvolution is a common and approved method in magnetic and gravity interpretation all over the world. The Geosoft software uses the same strategy for solution and gives the results as a database including x, y, z (depth), and the error of calculations as dx, dy, dz. Generally the depths are calculated for magnetic or gravity source boundaries. Therefore after this geophysical calculation we used them for geological and structural interpretation.

3.4. *Analogue modeling*

We used Polydimethylsiloxane (PDMS) to model the ductile layers of evaporite deposits in the region. Pure PDMS is a transparent Newtonian viscous fluid with a viscosity of $2.3 \times 10^4 \text{ Pa/s}$ and a density of 0.964 g/cm^3 at a temperature of 20°C . Dry quartz sand with a grain size of 0.5 mm was used to simulate brittle sedimentary rocks. The sand has negligible cohesion, an angle of internal friction of about 30° , and a density of about 1.44 g/cm^3 . Sand is a good analog for most sedimentary rocks in the upper continental crust, which obey Mohr-Coulomb behaviour (*Byerlee, 1978; Weijermars et al., 1997*).

In this study a brittle sedimentary overburden of laterally varying thickness is resting on top of a relatively weak viscous salt layer; therefore we used clean Polydimethylsiloxane (PDMS) to model the ductile layers of evaporite in the region.

The dimensions of the model are 34 x 25 x 2.5 cm. It was shortened from one end perpendicular to the width. The overall chevron or V-shape of the Alborz Mountain Range on a map was initially simulated by casting a V-Shaped slab out of Styrofoam. The limbs of the chevron were 20 cm long and the hinge began 13 cm wide, the western wing was 13 cm in width and the eastern limb was 12 cm in width.

Dry sand was deposited to a depth of 2.5 cm around the Styrofoam chevron and then removed. In the hole left by the Styrofoam, sands of different colour were deposited to simulate the stratigraphy of Alborz Mountains Range.

In order to model the evolution of a salt sheet in front of the advancing Alborz Mountains a tiny triangular layer (1 x 1 x 0.5 cm) of PDMS, was placed below the apex of the 'V'. This triangle of PDMS layer was covered by sand.

The prepared chevron-shaped model was placed into the thermo-mechanical apparatus designed and built at the Department of Earth Sciences, Frankfurt University, and compressed between two movable plates. The two plates [x] and [y] were driven by two horizontal screws driven by a step motor.

The model was subjected to 25 % shortening at a rate of 1 mm/hr for 30 hours. It was then sliced as indicated in the block diagram. The geometric scaling of our experiment was chosen that 1 cm in the experiment represents 10 km in nature and 1 experimental hour represents about 1my in nature. The convergence velocity of 1 mm/h was scaled to represent the Arabia–Eurasia convergence velocity corresponding to about 2 cm/year in nature.

4. Results

4.1. InSAR maps and time series observations of surface displacements.

The present study demonstrates the capability of Interferometry SAR (InSAR) to monitor displacements of the ground surface on a regional scale. For InSAR, data obtained from the salt extrusions N and W of Garmsar were collected by the European Space Agency (ESA) Environmental Satellite (ENVISAT), which imaged the area between December 2003 and June 2005. We analyzed nine ASAR (Advanced Synthetic Aperture Radar) images spanning these 18 months to characterize the surface displacements for the area. Subsequently we used 22 interferograms for more detailed analyses of the deformation

over distinct time intervals, and finally we used time series data to calculate the rates of LOS surface deformation of localities representative for different geological units.

The surface displacement rate throughout the region ranges from subsidence of -40 to -50 mm/yr to uplift of 20 mm/yr. The most obvious seasonal effects are that the farmlands around the Eyvanekey plateau subside rapidly in spring and summer when they are irrigated by the extraction of groundwater that is not replenished at the same rate. The surface of the Eyvanekey plateau subsides at the beginning of each year and then recovers throughout the remainder of the year. We attribute this behavior to the water table falling as a result of extracting groundwater for irrigation.

The uplift rate is faster in the southern part of the Eyvanekey plateau than in more northern areas, whereas the steep margins of the Eyvanekey plateau subside rapidly. Subsidence increases locally along seismically active faults in the plains that are thought to control fluid flow in the region. Such fluid migration is compatible with fractional volume decrease in materials along the fault and subsidence along its surface trace. Our time series analyses indicate slow subsidence over the entire area with minor seasonal effects.

The maximum subsidence rates (40-50 mm/yr) occur E and W of the Eyvanekey plateau, where the agricultural lands are irrigated each spring and summer by wells extracting shallow groundwater. A steady increase of subsidence rate in the farmlands (outside of salt plateau) is recorded from 2003 to 2006.

InSAR maps like that of the present study should aid such management by distinguishing areas where current rates of pumping groundwater exceeds the natural recharge rates from those where the same density of wells appears to be sustainable.

4.2. The Garmsar Salt Nappe and seasonal inversions of surrounding faults on SAR Interferograms

The allochthonous Cenozoic salt of the Garmsar salt nappe extruded from where the most southerly point of the Alborz Mountains front is offset by the Zirab-Garmsar strike-slip fault. We used eleven descending Advanced Synthetic Aperture Radar (SAR) images, produced by the European Space Agency (ESA) Environmental Satellite (ENVISAT) from 2003 to 2006, to map surface displacement over 23 increments ranging in time from 30 to 2 months.

A 30 months SAR interferogram of the area shows that the regional folds and faults are active well S of the mountain front but are dampened by the allochthonous salt that is otherwise merely degrading at rates that vary with the season. Interferograms for shorter

epochs display different patterns of fault blocks in the country rocks that rose and fell with the seasons. By relating surface displacements mapped in these interferograms to the contemporaneous seismic record we find that seismic faults reactive repeatedly while their kinematics inverted on remarkably short time scales. Seismic disturbances propagate very slowly and faults are longer than expected for earthquakes with $ML < 3.5$ indicating that the regional strains are more aseismic than anticipated by earlier studies.

4.3. Analogue and geophysical modelling of the Garmsar Salt Nappe

To get more insights in the evolution of the Garmsar Salt Nappe, analogue modeling has been carried out using PDMS as salt analogue and sand as analogue for the brittle overburden. The structures produced consist of folds and thrusts which were formed, while the salt analogue PDMS was rising up. The modeling results are compatible with our interpretation that the deformation front of the Alborz Mountains advanced SSW when overridding a salt sequence in the Garmsar area.

The scaled analogue model was focusing on the extrusion of salt from under the advancing deformation front of the Alborz Mountains. The modelling has produced folds and thrusts which can be correlated with the structural inventory of the Alborz Mountain Range. The recent kinematics of the Alborz is controlled by N-S shortening between Arabia and Eurasia and by westward movement of the South Caspian domain relative to Iran. N-S shortening is compatible with dextral strike-slip along the NW trending faults of the western Alborz and sinistral strike-slip along the NE trending faults of the eastern Alborz. An equivalent slip system was active also in the analogue model, particularly at the interface between the rigid Styrofoam taper and the PDMS/sand model. The sections of deformed limbs of chevrons in the analogue models have revealed N and S dipping reverse faults and thrusts, which might correspond with folds and faults of the western Alborz. North dipping reverse faults, formed in the S of the model, have also been found in the SW part of the Alborz Mountains Range, such as the North Tehran fault. Moreover, steep reverse faults of the model are comparable with the Firouzkuh fault in the SE part of the Alborz Mountain Range.

The analogue model also shows two parallel faults in the northern part, which can be related to the North Alborz fault and the Khazar Fault, both of which are located in the northern part of the Alborz Range and in the southern part of the Caspian basin. Our model has shown a small amount of extruded PDMS, which correlates with rock salt that extruded at the taper of the wedge-shaped Alborz Mountains Range. In nature, the salt advanced

SSW and extruded on top of the plateau as the Garmsar salt nappe. Extrusion of salt in the hills N of Garmsar is controlled by faulting, as the Alborz deformation front is offset by ca. 9 km along the 130 km long SW-NE trending Zirab-Garmsar strike-slip fault.

The Bouguer gravity data in the study area show strong anomalies in the SW and weak anomalies in the NE. There are two highs in Bouguer gravity anomalies corresponding to the southern border of the work area, one of which is relatively strong. The strongest anomaly is situated furthest to the south of the work area. The anomaly values are less than in the northern weak anomaly belt, forming several local gravity lows.

There are negative anomalies in the N and NE of study area. Several local positive anomalies occur over relatively high anomalies toward S of the salt sheet of Garmsar, which related to the convergence of a series of volcanic rocks trending SW. Relatively low anomalies in the open toe of the salt sheet and a vast anomaly E of the salt sheet and N of Garmsar town indicate a negative anomaly zone.

In the study area, magnetic anomalies are divided into three zones, the latter trending E, SW and S, respectively. A positive magnetic anomaly in the S can be divided into two sub-zones trending S and W. A negative magnetic anomaly is presented in the N of the study area. A weakly positive magnetic anomaly zone is located in the SE.

Variation of magnetic data is mostly a reflection of volcanic rocks, a synthetic reflection of burial depth and composition. The negative anomaly in the N of the study area represents a large depression with thick sedimentary segments and its edges become gradually shallow. After extracting residual magnetic anomalies, and analysis of the geological bodies causing the magnetic anomaly, it is inferred that the locally residual magnetic anomaly with a strong positive value is a response of volcanic rocks.

Depth estimations using the gravity and magnetic fields suggest that the salt in the Garmsar salt nappe extruded from a depth of < 2000 m.

4.4. Pre-site study of the Garmsar Salt basin for Hazardous waste disposal.

The finding of a waste repository is an engineered structure that requires interdisciplinary cooperation. Geoscientific and technical studies are necessary to work out a concept in which site, deposition mode, properties of the host rock, and geological situation are coordinated in a way that natural and artificial barriers are available to protect man and environment.

The factors that determine whether or not a reservoir or salt cavern will act as a suitable storage facility are both geological and geographical. The first site selection is made on the

basis of geological maps, field studies and an evaluation of archival material, particularly seismic and other geophysical. Geographically, potential sites would be relatively close to the consuming regions or industry. They must also be close to transport infrastructure, including main and trunk pipelines and distribution systems.

Moreover, recommendations for geoscientific studies of the site are to be made on the basis of the available data. In the following investigation of the site, all parameters relevant to the project must be evaluated for the final assessment of the technical feasibility and long-term safety of the repository. The first task of the site study is to define the present situation:

Determination of the rock types, stratigraphy, structure, fissure systems, and faults by field and geophysical studies. Structural studies will focus on the stability and deformability of the repository. Seismic data will be used to determine the structural edifice at deeper structural levels as well as regional earthquake activity.

In the Garmsar Salt basin, deep geologic disposal provides the logical solution for waste with respect to near surface sites. Prior to selection of areas with favorable conditions for the disposal, at first areas with obviously unfavorable conditions shall be excluded by criteria.

In site selection process for potential host rocks for hazardous wastes in deep geological formations based on geoscientific exclusion criteria and minimum requirements, deep geologic repository is logical for hazardous wastes, also this study proves that it is impossible to safely and permanently dispose of chemical and industrial wastes in near surface sites.

5. Conclusions

The results of the present thesis suggest that the top of the salt is subsiding continuously at rates that depend on the seasons. The surface displacement rate throughout the region ranges from subsidence of - 40 to - 50 mm a⁻¹ to uplift of 20 mm a⁻¹. The agricultural lowlands, where groundwater extraction for irrigation exceeds recharge, are subsiding faster than the salt sheet. Correlation of surface displacements with active folds and seismic faults around the salt sheet also suggests that the study area is undergoing active deformation.

Furthermore the prepared interferograms indicate that most movement in the Garmsar area is mainly by folding offset along the Zirab Garmsar Fault and many minor range-perpendicular faults, for instance the Garmsar fault appears to have acted as a north dipping

thrust in the winter months and inverted to a normal fault in the summer months. The last of these inversions in our coverage may have been captured by the scissor-like motion along the Garmsar fault. Similarly, the main active fault trending SW-NE could be a sinistral transpressive fault in a period of time and a transtensional fault another time. This could indicate alternations between transpressive and transtensional stress fields.

The kinematics of some of the fault systems thus inverted 3 times in the 18 month epoch represented in our interferograms suggesting an inversion cycle ~6 months.

Some events like folding, the slow rates of seismic disturbances appear to have propagated between epicenters on the same day, active fault lengths longer than expected for such small earthquakes and displacements that vary in value along one or both sides of many faults, all indicate that aseismic deformation is significant in the area.

On the other hand a scaled sand-box model simulate the reverse faults and thrusts observed in the Alborz Mountains Range N of Garmsar including the folds and faults trending NW–SE in the western limb of the Alborz chevron and trending NE–SW in the eastern limb.

The gravity anomaly characteristics in the study area show strong anomalies in the SW and weak anomalies in the NE. A striking body of negative anomalies lies in the N, which basically represents the outline of the salt sheet of the study area.

Depth estimations based on gravity-magnetic data and Euler deconvolution algorithm indicate the salt on the surface rose from the depth of <2000 m. The upper part of the salt diapir with its very low magnetic property is located at a depth <2 km.

The selection process for potential host rocks for hazardous waste repositories in deep geological formations in the Garmsar salt basin was based on internationally recognized geoscientific exclusion criteria and minimum requirements, as well as other criteria considered from a geoscientific point of view.

Exclusion criteria with social background will be applied to the areas with favorable integral geological settings. Areas which do not satisfy these criteria are also excluded from the procedure. The near surface salt layers are out of the minimum requirements and it is impossible to safely and permanently dispose chemical and industrial waste in near surface host rocks.

The remaining possibilities such as deep geologic repositories imply favorable integral geological settings and are not excluded from planning for legal or socioeconomic reasons. In the next steps, regions within the remaining areas are identified. In order to do so, again a comprehensive set of geo-scientific and social-scientific criteria has to be developed. The significance of the geo-scientific and social scientific criteria must be evaluated so that a

ranking of the regions and sites can be performed. In this step, safety assessments have to be used to a larger extent, e.g., to be able to judge data uncertainties with regard to the isolation capability.

We look forward to future studies clarifying how far the active Alborz structures extend to the S of the mountain front. It would also be interesting to know the geography of the autochthonous salt layer signaled by the close spacing of folds and faults in the Zirab-Garmsar Fault and to the S and E. Of even greater interest would be the geography and timing of apparently episodic inversions of active faults and whether they only occur where autochthonous salt provides a shallow décollement. Continued monitoring using InSAR would be valuable, and a local array of GPS stations would be able to check changes in kinematics and a local array of seismometers should allow earthquake solutions to check the dynamics.

Subsurface studies are required to realize the structural and hydrological properties and dimension of the Salt basin for further applications.

6. References

- Alavi, M., 1996. Tectonostratigraphic synthesis and structural style of the Alborz mountain system in northern Iran. *Journal of Geodynamics* 21, 1–33.
- Allen, M.B., Ghassemi, M.R., Shahrabi, M., Qorashi, M., 2003. Accommodation of late Cenozoic oblique shortening in the Alborz range, northern Iran. *Journal of Structural Geology* 25, 659–672.
- Byerlee, J. D., 1978, Friction of rocks: *Pageoph*, v. 116, p. 615–626.
- Jackson, M.P.A., Cornelius, R.R., Craig, C.H., Gansser, A., Stocklin, J., Talbot, C.J., 1990. Salt Diapirs of the Great Kavir, Central Iran. Geological Society of America, Boulder 177.
- Massonnet, D., & Feigl, K. L. 1998 Radar interferometry and its application to changes in the Earth's surface. *Reviews of Geophysics*, 36: 441– 500.
- Ritz, J.-F., Nazari, H., Ghassemi, A., Salamati, R., Shafei, A., Solaymani, S., Vernant, P., Active transtention inside Central Alborz: A new insight into the Northern Iran-Southern Caspian geodynamics, *Geology*, 34 (6), 477-480, 2006.
- Safaei, H., 2001, Elastic diurnal movement of Masses of Tertiary salt extruded in north central Iran. *Journal of Sciences, Islamic Republic of Iran*. 12, No. 3, 241- 250.
- Talbot, C.J., 2000, Monitoring salt extrusions in Iran. *Unpublished Progress Report to Geol. Surv. Iran*.
- Weijermars, R. 1997: Principles of Rock Mechanics. *Alboran Science Publishing*. 359p.

7. Manuscripts are related to thesis

I. Baikpour, S., Zulauf, G., Dehghani, M. & Bahroudi, A., 2010, InSAR maps and time series observations of surface displacements of rock salt extruded near Garmsar, northern Iran, *Journal of the Geological Society, London*, 167, PP 171-181.

II. Baikpour, S., Talbot, C.J., 2010, The Garmsar salt nappe and seasonal inversions of surrounding faults imaged on SAR interferograms, northern Iran, In: Alsop, I. [ed.], *Salt Tectonics, Sediments and Prospective. Geological Society, London, Special publications (in press)*.

III. Baikpour, S., Zulauf, G., Sebti, A., Kheirolahi, H. and Dietl, C., 2010, Analogue and geophysical modeling of the Garmsar Salt Nappe, Iran: constraints on the evolution of the Alborz Mountains, *Geophysical Journal International*, 182, PP 599-612.

IV. Baikpour, S., Zulauf, G., Abdolahifard, I., 2010, Hazardous waste disposal in Iran: Results from a pre-site study of the Garmsar Salt basin. *Manuscript submitted to Journal of Sciences, Islamic Republic of Iran*.

InSAR maps and time series observations of
surface displacements of rock salt extruded
near Garmsar, northern Iran

InSAR maps and time series observations of surface displacements of rock salt extruded near Garmsar, northern Iran.

Shahram Baikpour⁽¹⁾ Gernold Zulauf⁽¹⁾ Maryam Dehghani⁽²⁾ Abbas Bahroudi⁽³⁾

⁽¹⁾ Department of Geosciences, Goethe University, Frankfurt a.M., Germany.

⁽²⁾ Department of Geomatics and Geodesy, K.N.Toosi University, Tehran, Iran.

⁽³⁾ Department of Mining engineering, Tehran University, Tehran, Iran.

Abstract

A large allochthonous sheet of Eocene rock salt is forming the Eyvanekey plateau west of Garmsar along the northern periphery of the Great Kavir basin. This salt extruded over the central plains of Iran, where the southward advancing front of the Alborz Mountain is offset by the NE-SW trending Zirab- Garmsar strike-slip fault.

Based on nine descending Advanced Synthetic Aperture Radar ASAR scenes, produced by the European Space Agency's ENVISAT satellite from 2003 to 2006, we used interferograms to map the displacement over 22 increments ranging in time from 2 to 18 months.

In order to study the surface deformation at high temporal and spatial resolution, a small subset of interferograms was used to map the mean velocity of surface deformation. The results suggest the top of the salt to be subsiding continuously at rates that depend on the season. The surface displacement rate throughout the region ranges from subsidence of -40 to -50 mm/yr to uplift of 20 mm/yr. The agricultural lowlands, where groundwater extraction for irrigation exceeds recharge, are subsiding faster than the salt sheet. Correlation of surface displacements with active folds and seismic faults around the salt sheet also suggest that the study area is undergoing active deformation.

Key words: InSAR, Garmsar, Interferogram, active deformation,

Introduction

The deserts of Iran are suitable natural laboratories for studying hundreds of subaerial salt extrusions that are usually submarine or subsurface elsewhere (*Talbot 1998*). The ca. 200 salt extrusions emergent in the Zagros Mountains are of Infracambrian to Cambrian age (Hormoz salt). The other extrusions of the central plateau of Iran in the fore-deep of the Alborz Mountains consist of Lower Oligocene to Miocene salt. Most Iranian salt extrusions, both Hormoz and Tertiary, can be considered as natural models of diapirs that extrude nappe piles consisting of normal upper crustal rocks. The shape of these diapirs is controlled by the rate of extrusion, lateral spreading, and rate of erosion.

Unlike most Iranian salt extrusions that probably gravity-spread for tens or hundreds of millennia from diapirs that reach the surface along faults (*Talbot et al., 2000*), the salt sheet that underlies the 20 x 10 x 0.32 km area of the Eyvanekey Plateau differs in having been squeezed to the surface as the Alborz mountain front advanced southward over the Garmsar Basin. In recent reviews this body of rock salt is referred to as the Garmsar salt nappe and quoted as an example of a sheet of allochthonous salt that extruded along a mountain front before undergoing open-toed advance. (*Hudec & Jackson 2006 and 2007*) The main aim of the present study was to check, whether this mountain front and its associated salt extrusions are still active.

Extrusion and dissolution rates of Hormoz salt have been constrained by analytical (*Wenkert, 1979, Talbot & Jarvis, 1984*) and numerical modeling (*Talbot et al., 2000*) and by repeated direct ground measurements of markers fixed on the salt (*Talbot & Rogers, 1980; Talbot et al., 2000, Bruthans et al., 2006, 2007*). Similar studies of extrusions of Tertiary salt are more limited. *Safaei (2001)* related large elastic strain, measured on southward facing salt faces in the Garmsar hills, to contemporaneous temperature changes via the thermal expansion of dry salt. *Talbot & Aftabi (2004)* investigated strain of an extrusion near the city of Qom, and *Talbot (2000, 2004)* and *Schleder & Urai (2006)* described some of the structures and microfabrics which help to explain strain softening of the salt in the Eyvanekey plateau. All of these ground measurements, however, only monitor surface strain at particular points on individual salt bodies.

Recent improvements in interferometry of synthetic aperture radar images have reached the stage where the surface strain over the entire bodies of the Iranian salt extrusions can be routinely and remotely mapped and monitored. *Weinberger et al (2006)* used time series interferograms, checked by precise ground leveling, to demonstrate that different

parts of the top of Mount Sedom in Israel rose at steady rates between 5 and 9 mm a⁻¹ since its top was truncated by a precursor to the Dead Sea at 14 ka.

InSAR (SAR interferometry) uses the phase difference between two SAR images of the same area acquired at different times to map either a digital elevation model (DEM) for the area or its surface displacement in the Line Of Sight (LOS) of the satellite. Data for this study of the salt extrusions north and west of Garmsar (Fig. 1) were collected by the European Space Agencies Environmental Satellite ENVISAT which imaged the area between December 2003 and June 2005.

We analyzed 9 ASAR (Advanced Synthetic Aperture Radar) scenes spanning these 18 months to characterize the surface displacements for the area indicated in Fig. 1 before using 22 interferograms for more detailed analyses of the deformation over distinct time intervals and finally using time series data to calculate the rates of LOS surface deformation of localities representative of different geological units.

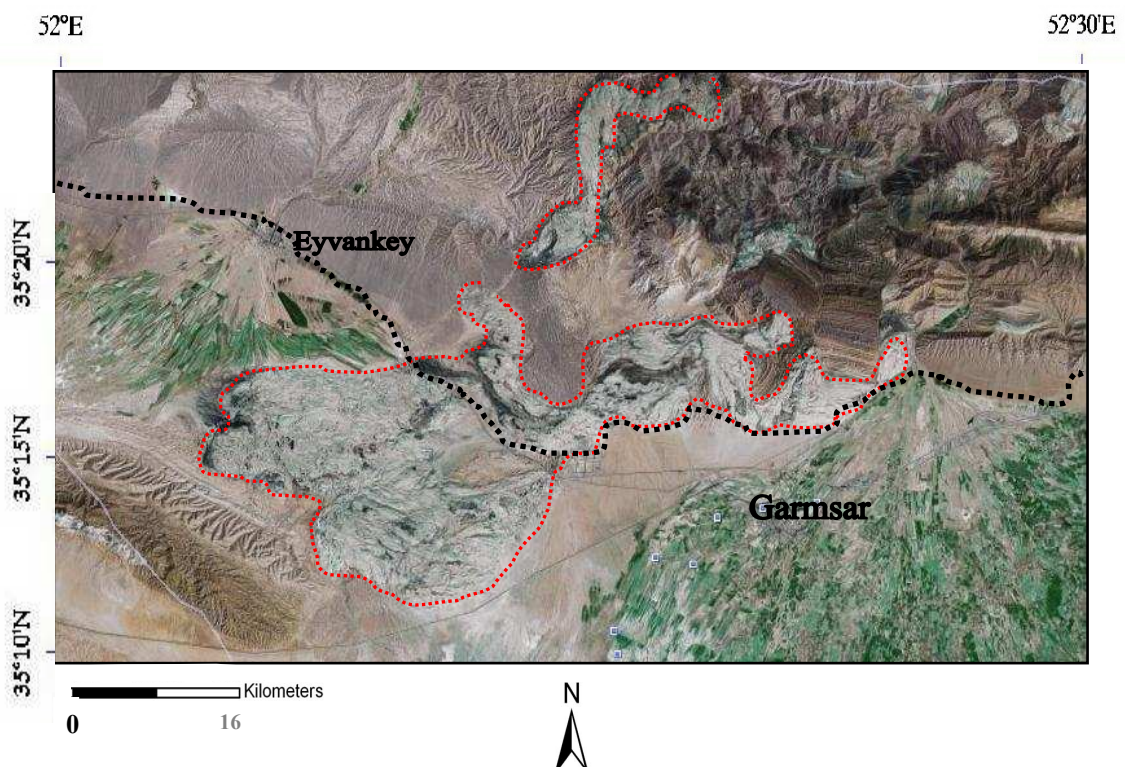


Fig.1. Eyvanekey plateau and hills north of Garmsar on Landsat satellite image (*source: Google earth*), with all major bodies of Tertiary salt outlined in red dots, the black dots show mountain front boundaries.

Geological Background

Diapirs of Tertiary salt are forming topographic highs in the Great Kavir basin and in several of its subbasins such as Qom, and Garmsar. Tertiary salt dissolved from these

topographic highs collect as brines in downslope topographic lows where it is often re-precipitated as modern salt.

The Garmsar basin (Fig. 1) is one of a series of basins in the foredeep of the Alborz Mountains forming an embayment in the northern periphery of the Great Kavir from which it is separated by the Kuh-e-Gachab and Dulasian swell (Fig. 3B). The oldest Tertiary strata in the region are marine Eocene sediments associated with volcanic rocks resting unconformably on top of folded Mesozoic strata. The initial thickness of the evaporite-bearing sequence is not clear due to its strong subsequent distortion but probably exceed 8000 m (*Jackson et al., 1990*). The age of the evaporitic sequence is unclear because of the lack of fossils. However lithological similarities with rocks from Qom Kuh and the diapirs in the Great Kavir (*Jackson et al., 1990*) suggest the Garmsar rocks to include evaporites of both upper Eocene and Oligocene age.

Some salt in the Garmsar basin could still be at place beneath the Mesozoic rocks in the deformation front of the Alborz Mountains. Other salt strata extruded to the surface in form of small diapirs along faults in the foothills without significant spreading over the surface (*Safaei, 2001 and Fig. 1*). However, it is likely that most of the salt overridden by the southward advance of the Alborz deformation front was expelled over recent sediments of the great Kavir (Figs. 1 and 3C) to the south and/or west. This salt is now present as the huge sheet of allochthonous salt that forms what we will call here the Eyvanekey Plateau (Figs. 1 and 3C). Smaller extrusions of salt in the hills north of Garmsar mark where the Alborz deformation front is offset about 9 km by the 130 km long SW-NE trending Zirab-Garmsar dextral fault. The latter is not a pure strike-slip but a transtensional fault.

The overridden salt is overlain by a mechanically significant roof, rafts of which are detached from the leading edge of the roof behind the extrusive toe.

Huge rafts of the Alborz mountains collapsed southward into the salt, while others were carried several kilometers southward along transfer strike-slip faults, or were rotated about steep axes. Given the salt in the Eyvanekey Plateau, situated west of Garmsar, was initially extruded southward from the line of diapirs emergent in the hills along the southern edge of the Alborz north of Garmsar, the Eyvanekey Plateau might have been dextrally displaced for ca. 9 km along the Zirab-Garmsar fault to its recent position (Fig.2). Whether the Zirab-Garmsar fault is still active will be constrained by future GPS studies.

The Eyvanekey plateau rises above the surrounding irrigated farm lands (Fig.3), and the smaller Garmsar salt extrusions fringing the Alborz front consist predominantly of salt and gypsum rock with subordinate marl, calcareous marl, shale and sandstone together with inclusions of mafic volcanic rocks.

The present surface of the plateau is barren and the salt is covered by several meters of residual insoluble soils after dissolution of the salt by rain (Talbot, 2004), most of these are light green to pale brown gypsum with subordinate marl and calcareous marl (Amini and Rashid, 2005).

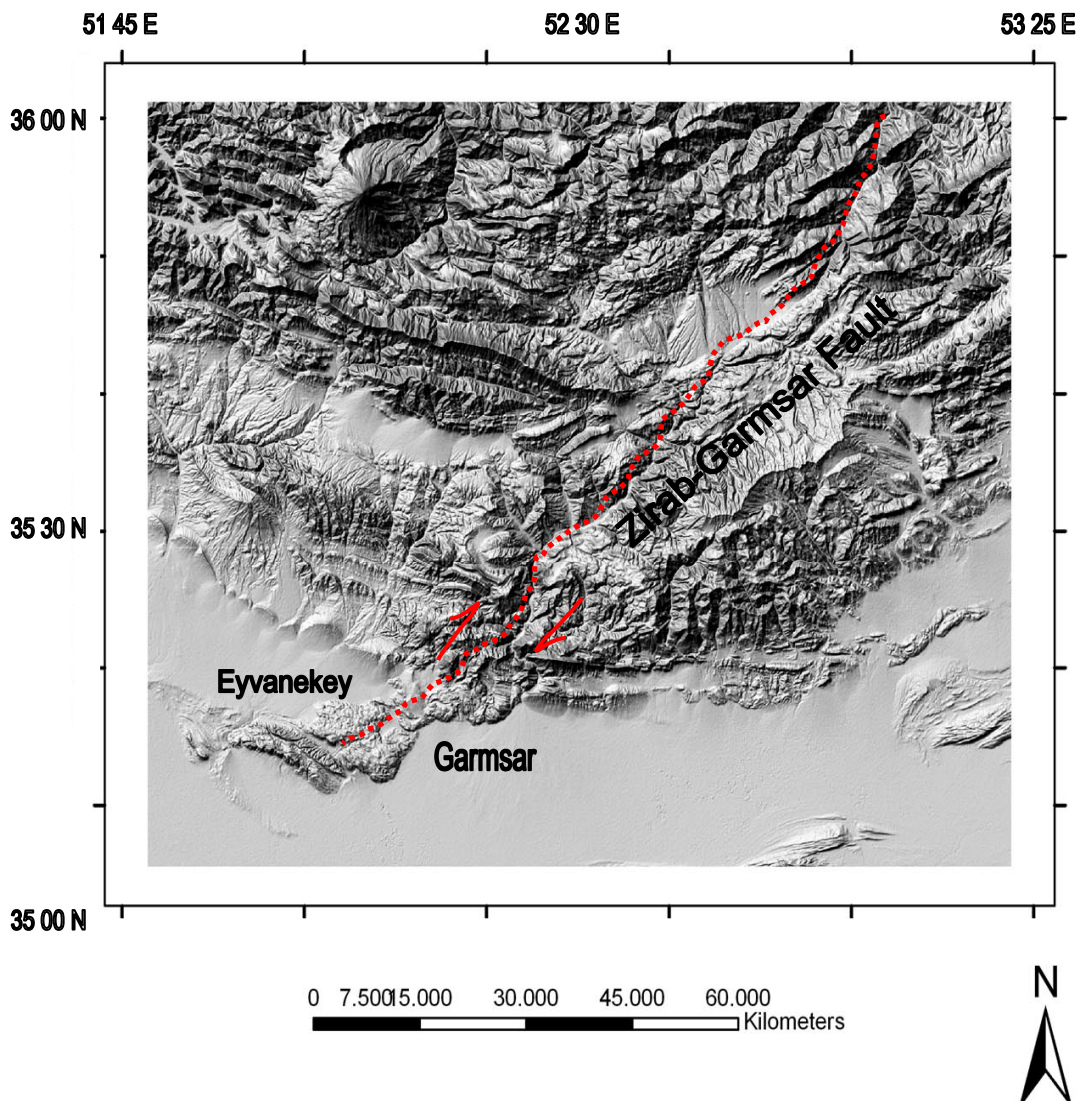


Fig. 2. The hill shaded Digital Elevation Model of Iran relates the Eyvanekey plateau with the southern end of the Zirab-Garmsar fault (red dots). Red arrows illustrate a key layer displaced 9 km dextrally. Mountain front outline is shown by yellow dots.

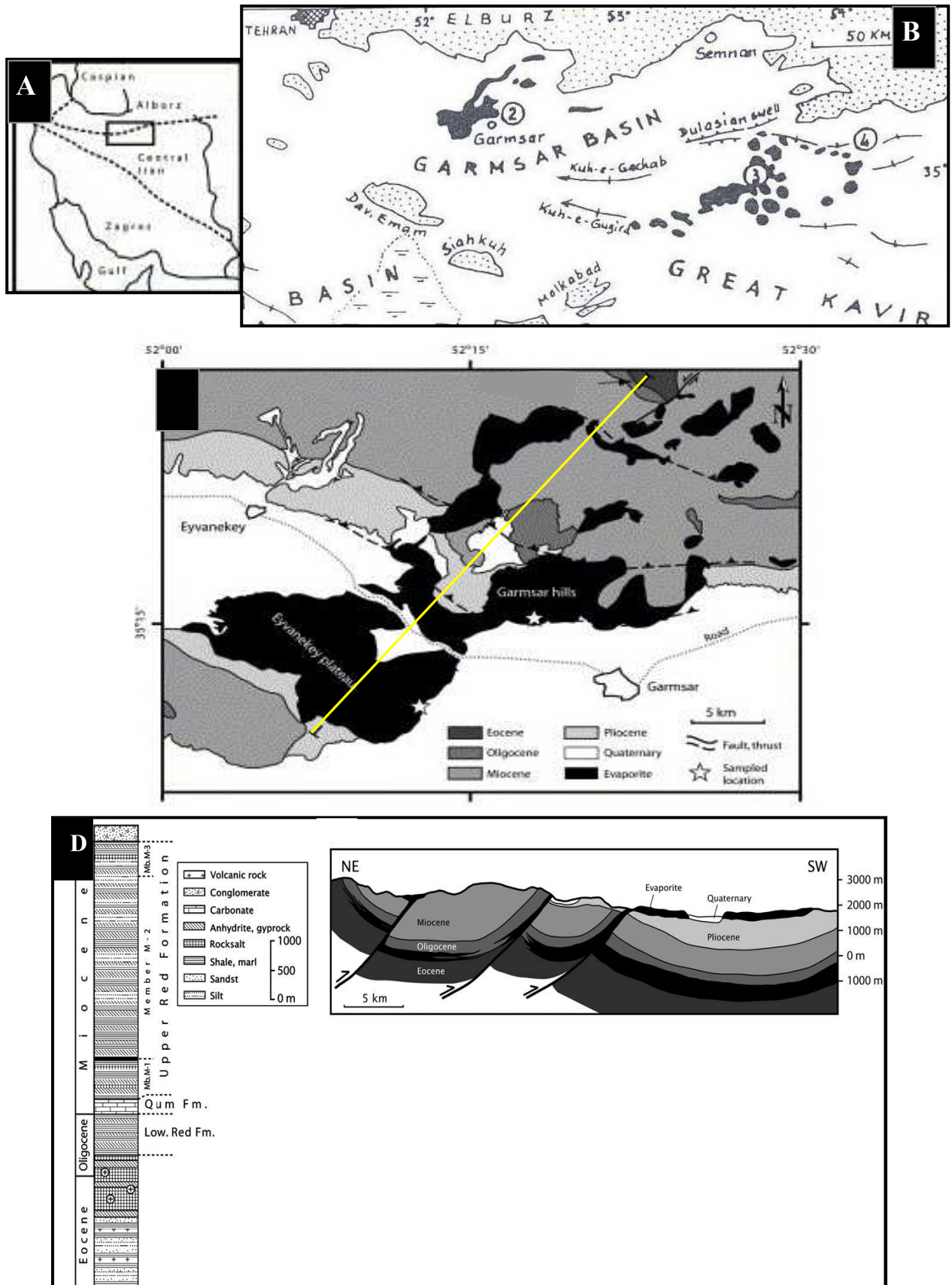


Fig. 3. Simplified regional setting of Garmsar hills, Eyvanekey plateau and surroundings. (A) Location of area in Iran shown in B. (B) Tertiary evaporites on the surface in the Garmsar, Qom and Great Kavir basins (Jackson *et al.*, 1990). (C) Simplified geological setting of Garmsar hills and Eyvanekey plateau after geological map of Amini and Rashid (2005). (D) Lithostratigraphic

column of the Garmsar basin after *Jackson et al. (1990)*. The Eocene-Oligocene rock salt is the main source for the extrusions of the Garmsar salt nappe and the diapirs in the hills to the north of Garmsar NE-SW cross-section. The latter cuts through the Garmsar salt nappe located on C (modified after *Amini and Rashid, 2005*).

Natural outcrops of salt are rare, but halite is accessible in many salt quarries and a few mines, most of which were opened in the last 10 years. Most of the salt is white and fine grained with a strong subhorizontal mylonitic foliation (*Schleder & Urai, 2006*) but some is red some has been subjected to what looks like static grain growth. The bedding in the salt sheets is generally subhorizontal but displays refolded recumbent folds exposed in steep N-S and W-E trending quarry faces (Figs.4A and 4B). The fine-grained salt is mechanically very weak (*Schleder & Urai, 2006*) but it is unknown *whether any of the salt in Garmsar is still moving today* (*Talbot, 2000.*).

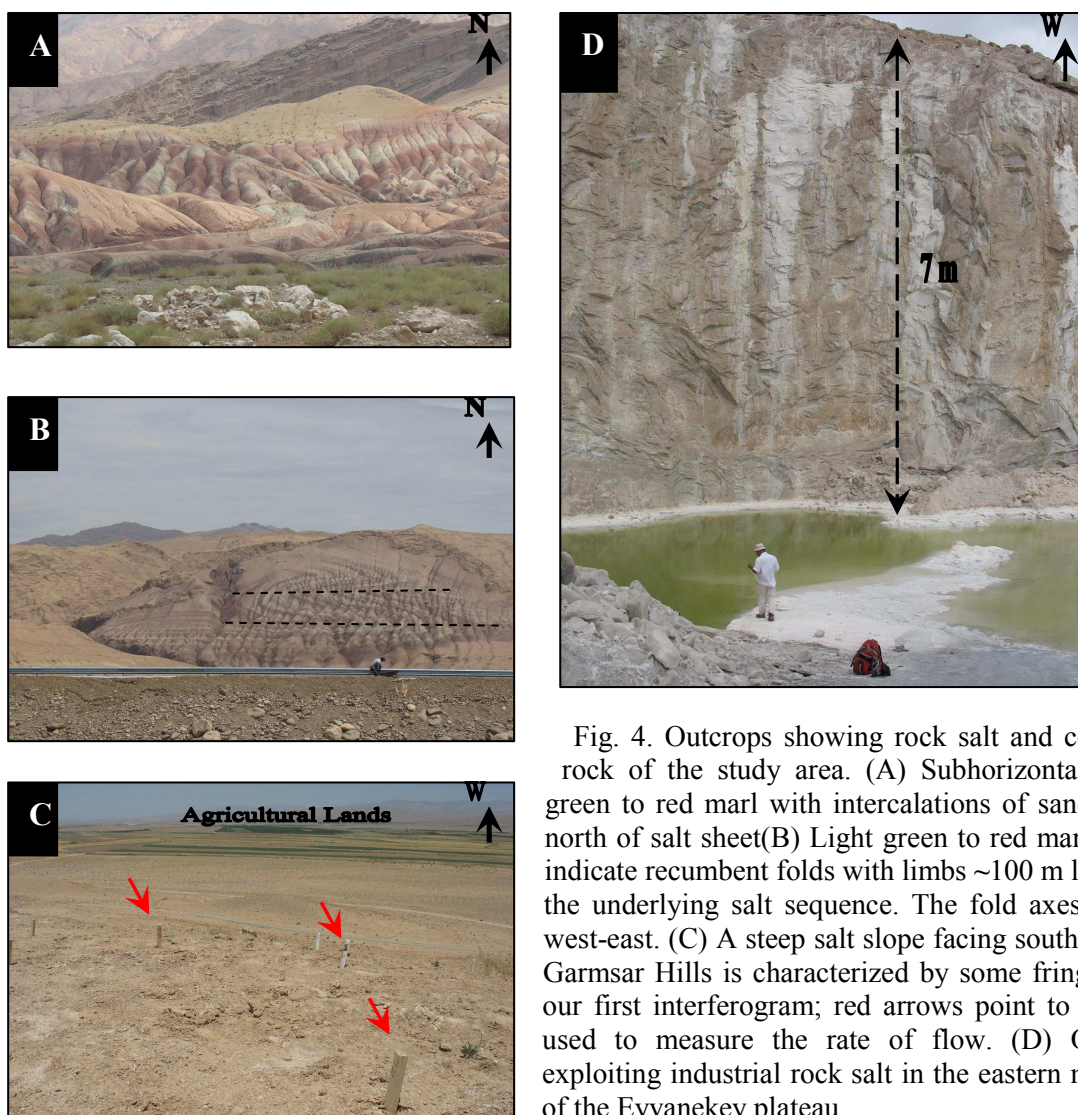


Fig. 4. Outcrops showing rock salt and country rock of the study area. (A) Subhorizontal light green to red marl with intercalations of sandstone north of salt sheet(B) Light green to red marl soils indicate recumbent folds with limbs ~100 m long in the underlying salt sequence. The fold axes trend west-east. (C) A steep salt slope facing south in the Garmsar Hills is characterized by some fringes on our first interferogram; red arrows point to stakes used to measure the rate of flow. (D) Quarry exploiting industrial rock salt in the eastern margin of the Eyvanekey plateau.

Methods of study

Interferometric analyses of SAR images have become a widespread, valuable technique to measure subtle displacements of the ground surface (*e.g.*, *Massonnet and Feigl, 1998*). When two radar scenes are made at different times from the same viewing angle, a small change in the position of the target (ground surface) may create a detectable change in the phase of the backscattered signals. The resulting difference of phase is expressed in an interference map (interferogram), which the resulting fringe pattern reflects the ground displacement that occurred between the two acquisitions, and the product is referred to as a ‘‘change interferogram’’. Rather than using the primary data to generate our own DEM, we used the DEM provided by the Shuttle Radar Topography Mission (SRTM) with the spatial resolution of 90 m.

In the case of the ENVISAT SAR satellite each fringe or colour cycle in a change interferogram corresponds to a map contour of displacement equivalent to half the radar wavelength. The mean incidence angle of this satellite is 23°. Thus, in the case of pure vertical movement, one fringe cycle represents 31 mm of displacement.

The phase change in the interferogram is the composite of topographic information, φ_{topo} , and surface displacement, between the two acquisitions, φ_{disp} , atmospheric delay, φ_{delay} , and noise, φ_{noise} . Successful InSAR generation requires the removal of the topographic phase contribution and so as to isolate the ground displacement component. The φ_{topo} can be simulated and eliminated by introducing DEM information.

$$\varphi = \varphi_{\text{topo}} + \varphi_{\text{disp}} + \varphi_{\text{delay}} + \varphi_{\text{noise}}$$

The atmospheric component, φ_{delay} , is primarily due to fluctuations of water content in the atmosphere between the satellite and the ground. The atmospheric delay can be identified using the fact that the fringe structure is independent over several interferograms; alternatively, it can be modelled by using data from a GPS network. It is also possible to reduce the atmospheric disturbance to the displacement phase term by using the ‘interferogram stacking technique’. The atmospheric effect can be estimated by plotting the phase against the height for each pixel; it is strong if there is a good correlation between height and phase. Maps displaying the mean displacement velocity were produced using MATLAB software.

Data

The data for the present study were collected by the European Space Agency (ESA) Environmental Satellite ENVISAT which imaged the study area between December 2003 and June 2005. The normal orbital cycle for this satellite is 35 days. To check if

any surface displacement is recognisable in the study area, we constructed a preliminary interferogram using two descending ENVISAT images acquired in August, 2003 and February, 2006. This interferogram shows large areas of coherent signal on the bedrock and salt and some fringes on the margins of the salt sheet, thus, encouraging further detailed investigations.

Subsequently we acquired 9 descending scenes from the European Space Agency ESA, (Table 1 and Fig. 5) and generated Change Interferograms for different periods that vary between 2 and 18 months between 2003 and 2005. As listed in Table 2, we generated 22 differential interferograms from the ESA data using GAMMA software (supplied in Remote Sensing group, Geological Survey of Iran GSI) and the two-pass method (Massonnet and Feigl 1998).

Satellite	Sensor	Date	Track	Orbit	Day	Baseline
ENVISAT	ASAR	2003 12 02	106	3507	245	364
ENVISAT	ASAR	2004 02 10	106	4509	315	318
ENVISAT	ASAR	2004 06 29	106	6513	455	-310
ENVISAT	ASAR	2004 08 03	106	7014	490	518
ENVISAT	ASAR	2004 11 16	106	8517	595	76
ENVISAT	ASAR	2004 12 21	106	9018	630	274
ENVISAT	ASAR	2005 03 01	106	10020	700	418
ENVISAT	ASAR	2005 04 05	106	10521	735	-15
ENVISAT	ASAR	2005 06 14	106	11523	805	413

Table 1. The 9 descending Radar images and details of them are acquired from ESA.

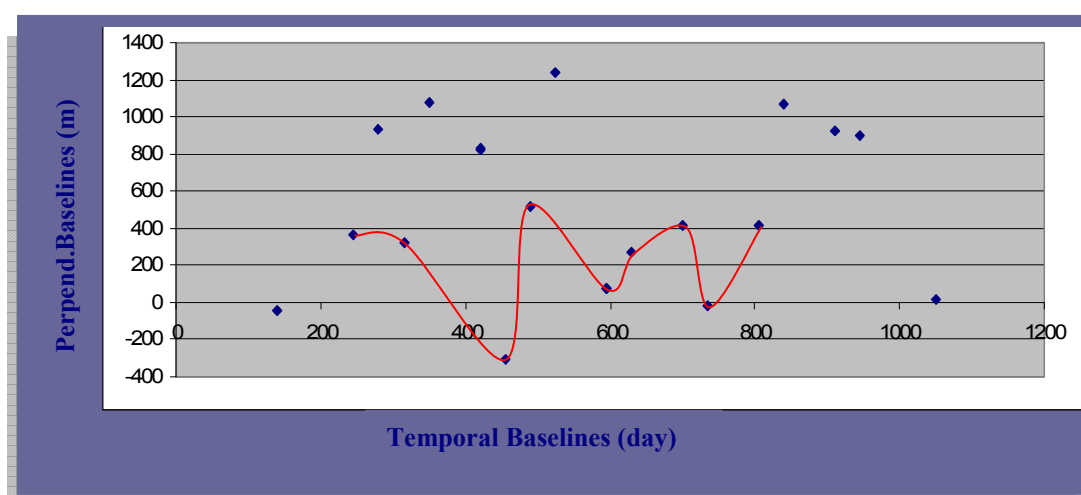


Fig. 5. 18 points (images) were acquired at first search for overlapped images for track (106) descending images, so 9 points (images) have a good relation in temporal and perpendicular baselines (red line shows relations of perpendicular and temporal baselines of nine descending Radar images).

Image sign	Epoch dates	Perpendicular Baselines(m)	Temporal Baselines (days)
A	2003 12 02 2004 02 10	46	70
B	2003 12 02 2004 06 29	674	210
C	2003 12 02 2004 08 03	154	245
D	2003 12 02 2004 11 16	288	350
E	2003 12 02 2004 12 21	90	385
F	2004 08 03 2004 06 29	828	35
G	2004 08 03 2004 11 16	442	105
H	2004 08 03 2004 12 21	244	140
I	2004 08 03 2005 03 01	100	210
J	2004 11 16 2004 12 21	198	35
K	2004 02 10 2004 12 21	44	315
L	2004 02 10 2005 03 01	100	385
M	2004 06 29 2004 11 16	290	140
N	2004 06 29 2004 12 21	584	175
O	2004 11 16 2005 04 05	91	140
P	2004 12 21 2005 06 14	135	175
Q	2005 03 01 2004 11 16	342	105
R	2005 03 01 2004 12 21	144	70
S	2005 03 01 2005 04 05	433	35
T	2005 03 01 2005 06 14	5	105
U	2005 04 05 2004 12 21	289	105
V	2005 04 05 2005 06 14	428	70

Table 2. Alphabetic signs of unwrapped and flattened images are prepared by the date of acquisitions of ENVISAT ASAR images and spatial and temporal baselines of the interferograms.

The effect of topography was removed from each interferogram using the Digital Elevation Model (DEM) with the spatial resolution of 90 m produced by the Shuttle Radar Topography Mission (SRTM). The InSAR technique maps surface deformation along the Line-Of-Sight (LOS) of the ENVISAT satellite.

Most of the surface displacement plotted in Fig. 8 can be assumed to be near vertical. Constructing interferograms for neighboring pairs in a series of acquisitions for the same area produces a time series of the surface deformation rate over the entire deformed area.

Results

One of our interferograms shows Colour fringes on the steep slopes of the margins of the small salt extrusion in the Garmsar hills and around the large salt sheet beneath the Eyvanekey Plateau (see figures in appendix). These fringes indicate a rate of surface displacement of the western margin of this salt body of ca. 1 cm/y. More detailed information on the displacement rate results from interferograms spanning shorter increments than 12 months. Twenty two interferograms were prepared and analyzed for

each pair of images for 22 epochs listed in Table 2 that ranged in length from 2 to 18 months.

Because the topographic phase has been removed from these flattened interferograms, the colors record mainly the surface deformation in the near-vertical satellite line of sight. Areas undergoing subsidence during this period are indicated by warmer colors.

Such type of sinking areas are present in all interferograms, but with different magnitudes of displacement. NE-SW and NW-SE trending profiles were prepared to show the rate of fluctuation of the surface displacement inside the extruded salt and its surroundings (Figs. 6 and 7).

To highlight the major deformation features and relate variations in the LOS surface displacement rates with seasonal parameters, such as temperature and amount of precipitation, as well as seismic data, maps of the mean displacement velocity (Fig. 8) were produced for four of the interferograms chosen from the 22 periods.

The mean displacement velocity is plotted against the distance along the NE-SW and NW-SE trending profiles, respectively (Fig. 9, for location of the profiles, see Fig. 8). Most of the time series data suggest subsidence to increase continuously from the top of the salt sheet downslope toward the agricultural lowlands. Most of this subsidence can probably be attributed to salt dissolution by the annual rainfall, the latter being in the range of ca. 100 mm/yr. The spatial changes in the magnitude of subsidence and subsidence rate might be controlled by the distribution of agricultural wells, the degree of mining activity in the margin of the salt glacier (Fig. 4C), as well as the presence of mechanical weak planes such as faults and fractures.

Discussion

InSAR provides continuous maps of the surface displacement rather than displacements at few discrete points that is usual for precise ground measurements.

The two orbital tracks of the satellite have to be within a few hundred meters for the signal to preserve coherence. This limits the number of interferograms that can be produced from satellite image pairs. Changes in the orbital geometry of the two acquisitions likely generally degrade the coherence in interferograms generated with longer baselines. In the present study only 22 interferograms are considered that have been processed from the 9 image pairs out of the potential 36 pairs generated by the ENVISAT satellite from 2003 to 2005 (Fig. 5). Local loss of coherence in the

interferograms might be related to vegetation, sudden changes in ground conditions such as those due to cultivation or changes in near-surface water, or slope instability.

Along the LOS surface displacement in each interferogram, shown in Fig. 6, ranges from several millimeters to centimeters. Below we discuss some of the factors that may control the surface deformation of the salt extrusion and the surroundings which include both barren and farm lands.

Local uplift rates of ca. 10 mm/yr are compatible with the rate of 10 mm/year measured for the uplift of the central Alborz Mountains using GPS studies (Masson et al., 2002). It has to be emphasized that Masson et al., (2002) expected this rise to occur along major faults, whereas our work indicates that movement in the Garmsar area is dispersed among many minor faults but is mainly related to folding. Rather than swelling by further extrusion of salt from deeper structural levels, or degrading by dissolution, the Garmsar salt nappe appears to be affected by folding, the latter related to N-S shortening. Given that shortening rates are between 1 and 11 mm/y, anticlines above a detachment should rise at rates of 10 mm/yr, whereas synclines should subside at rates $>$ ca. 3.3 mm/yr (Vita-Finzi, 1986, p. 139), These values are broadly consistent with the 8 ± 2 mm/yr N-S shortening rate across the central Alborz as indicated by GPS studies (Vernant et al., 2004). The GPS data further show that recent deformation seems to extend southwards beyond the piedmont area. SAR interferometry cannot be used to constrain the sinistral shear along the range parallel strike-slip faults inside the belt. The rate of this strike-slip has been determined at 4 ± 2 mm/year (Vernant et al., 2004).

Seasonal effects on surface displacement

Garmsar is the largest town in the study area. It is situated at ca. 825 m above sea level on the northern edge of Dasht-e Kavir, which is the largest desert on the central plateau of Iran. Garmsar means “hot place” in Farsi and the climate is characteristically dry and cloudless throughout the year with minimal rainfall (e.g. 100 mm/year) and temperatures ranging from -10 °C in winter to 40 °C in late summer. The farmlands on the plains overlooked by the Eyvanekey Plateau and to the south of Garmsar are cultivated by extraction of groundwater, particularly in spring and summer. Four change interferograms for periods between 2 and 18 months were chosen from the 22 interferograms to constrain the impact of seasonal parameters on the surface displacement rates. Surface LOS displacement rates on these 4 interferograms were

plotted along NE-SW and NW-SE profiles respectively along and across the likely transport direction of the salt in the Eyvanekey Plateau (Fig. 6).

It is obvious that in the period from 5th of March to 14th of June, the uplift rate was increased from the NE to SW along the extruded salt sheet of the profile (Fig. 7A).

However, although InSAR observations show that large sections of the salt in the NE Garmsar hills subsided (ca. -2 cm), the distal SW margin of the plateau, was lifted up as much as 2 cm.

The NE-SW trending profile *along* the Eyvanekey salt sheet indicates that the surface of its NE edge in the Garmsar hills subsided at -2 cm (Fig. 7A).

This subsidence in the salt extrusion zone diminishes to the SW where the salt surface increasingly rose reaching a value of ~1.5 cm at its distal southern edge.

The NW-SE trending profile across the Eyvanekey salt sheet shows a small rise (0.2 cm) in its centre that falls off to ca. -1 cm at its margins (Fig. 7B). This profile fits the dimensionless profile for a viscous droplet spreading under gravity seen in former salt fountains in the Zagros mountains (Figs.6 and 7; see also Fig. 3 of Talbot 1998) The agricultural lands adjoining the NW margin of the Eyvanekey plateau and south of Garmsar subsided as much as 3 cm. Putting these two profiles together suggests that salt may have risen into the head of the Eyvanekey salt sheet and flowed to the SW, and gravity spread away from a NE-SW axis.

The NW-SE profile across the salt sheet for 105 days, from 3rd of August to 16th of November, indicates that these trends are reversed (Fig. 7C). Both the salt sheet and farmlands subsided ca. 4 cm, whereas the top of the salt plateau subsided only ca. 0.5 cm.

The equivalent NE-SW profile (Fig.7D) for the period from 29th of June to 16th of November reveals changes in rise and sink form the highest part of salt sheet in the north toward middle parts of the salt sheet. Moreover it is showing a rising curve up to 2 cm in the steepest slopes above the southern margin. Meanwhile the surrounding agricultural lands subsided more than 5 cm. The NE-SW and NW-SE trending profiles shown on Fig. 7 have similar shapes but different ranges. The depth to the groundwater table is likely to be close to stable over the winter when the farmers have no need to extract ground water. On the other hand there was no subsidence in winter. The head of the salt sheet in the south-west subsided with respect to north-east of that (Fig.7E).

Structural effects on the deformation mechanisms

The southern prolongation of the Zirab-Garmsar strike-slip fault cuts through the Eyvanekey salt sheet extruded over the central Iranian plateau (Fig.2). The surface traces of many minor faults which are sub parallel to this major fault are shown on Fig. 8. The pattern suggest local disturbance along such minor faults which is obvious for example along the southeastern edge of the salt plateau (Figs. 8 and 9). The lineaments correlate well with active faults, the epicenters of earthquakes recorded from 2003 to 2006 (mb=2 & 3) are depicted also in Fig. 8.

These faults, however, may separate distinct units with different mechanical properties, so that the differential surface deformation (e.g. of the salt compared to the surrounding plain) may record differential dissolution, thermal expansion, gravity flow etc.

Some of the most obvious lineaments on the interferograms correlate well with the margins of the salt sheet beneath the Eyvanekey plateau. These lineaments may reflect localized dissolution or downslope flow of rock salt along the steep salt margins (Figs. 8 and 9).

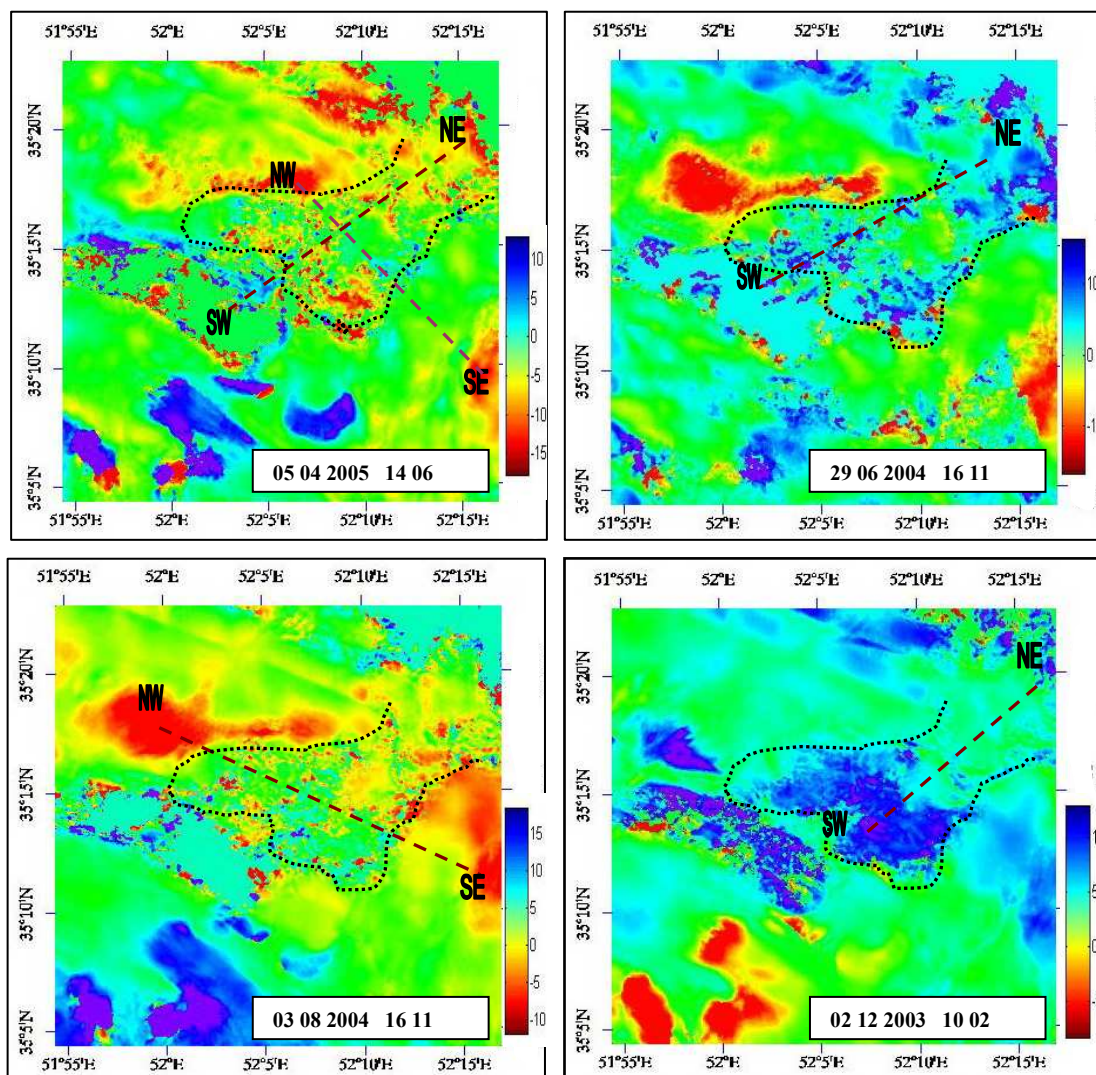


Fig.6. Four representative differential interferograms chosen from the 22 interferograms to show seasonal impacts on topography. .Date of each interferogram is labelled. Scaling of color bars is in cm.

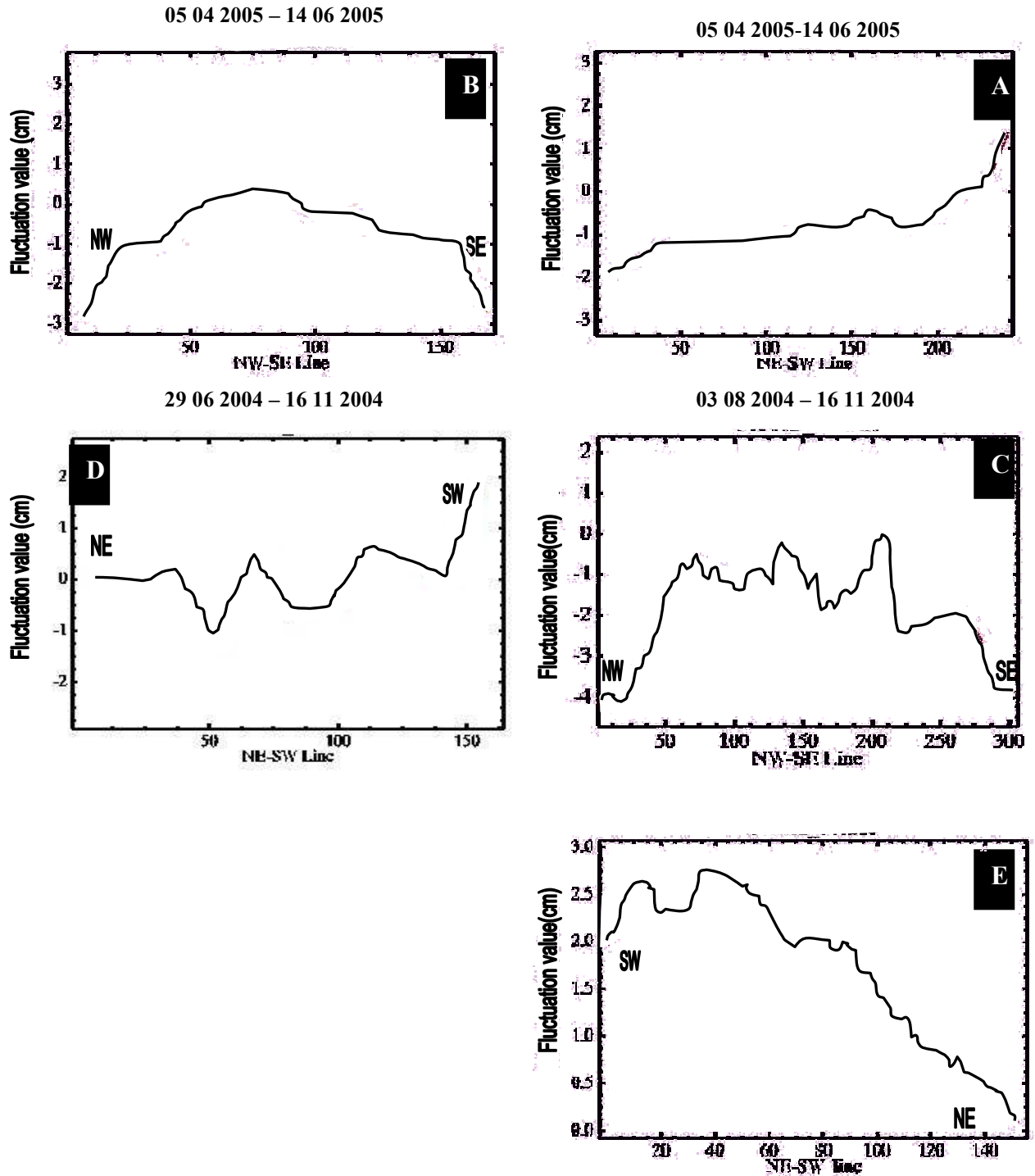


Fig.7. Fluctuation in vertical height along profiles indicated in the differential interferograms shown in Fig. 6.

InSAR time series observations

The individual interferograms record the incremental ground deformation between the acquisitions dates labelled. It is possible to produce a time series of the total surface displacement in the LOS between the starting time and each acquisition date.

As there are as many linearly independent interferograms as acquisition dates in an unbroken chain in our study, it is possible to use a least squares inversion to map/obtain the surface deformation for each time covered by the data [Biggs and Wright, 2004; Berardino, 2002]. The resulting mean displacement velocity map and plots (Figs .9 and 10) indicate that the surface of the Eyvanekey plateau and of the surrounding agricultural lowlands subsided continuously from 2003 to 2006. The maximum surface deformation rate is estimated to have been near 20 mm/yr in farmlands and 5 mm/yr in the centre of the sheet of allochthonous salt.

As shown by small dots in Fig. 8, a large number of water wells are used to irrigate the farmlands to the west and east of the Eyvanekey plateau, particularly in spring and summer time. We found 503 wells in the west and 181 wells in the east (some dots are out of the study area). There is an obvious correlation between these wells and the area of maximum subsidence near Garmsar east of the Plateau and some of the wells west of the plateau (Figs. 8 and 9) suggesting the surface to subside where the water table is significantly lowered by water extraction. Wells that cluster in areas of maximum subsidence appear to be over-exploiting the available groundwater. Wells in areas undergoing less subsidence may be fed more efficiently by water draining from the Alborz.

The graphs in Fig. 10 indicate that the subsidence rate is high along the eastern margin of the salt sheet. The subsidence rate increased continuously from 2003 to 2006. This observation could be related to downward flow of the salt along the steep eastern margin where it was undergoing dissolution. On the other hand brittle downslope sliding could be aided by daily elastic thermal strains and by the spoil heaps of the ca. 20 active quarries situated along this margin.

On the other hand, Fig. 10 shows unsteady surface displacement along the southern margin of the salt sheet. Two points underwent a sharp decrease in subsidence rate from the beginning to the middle of 2004 followed by a steady increase to the middle of 2005 after which it slowed down again.

We attribute this observation of enhanced subsidence to fluid-controlled strain softening of rock salt by increasing the rates of dissolution/reprecipitation in winter when the salt

is wet. The opposite case is given in summer when the salt is dry and thus much stronger.

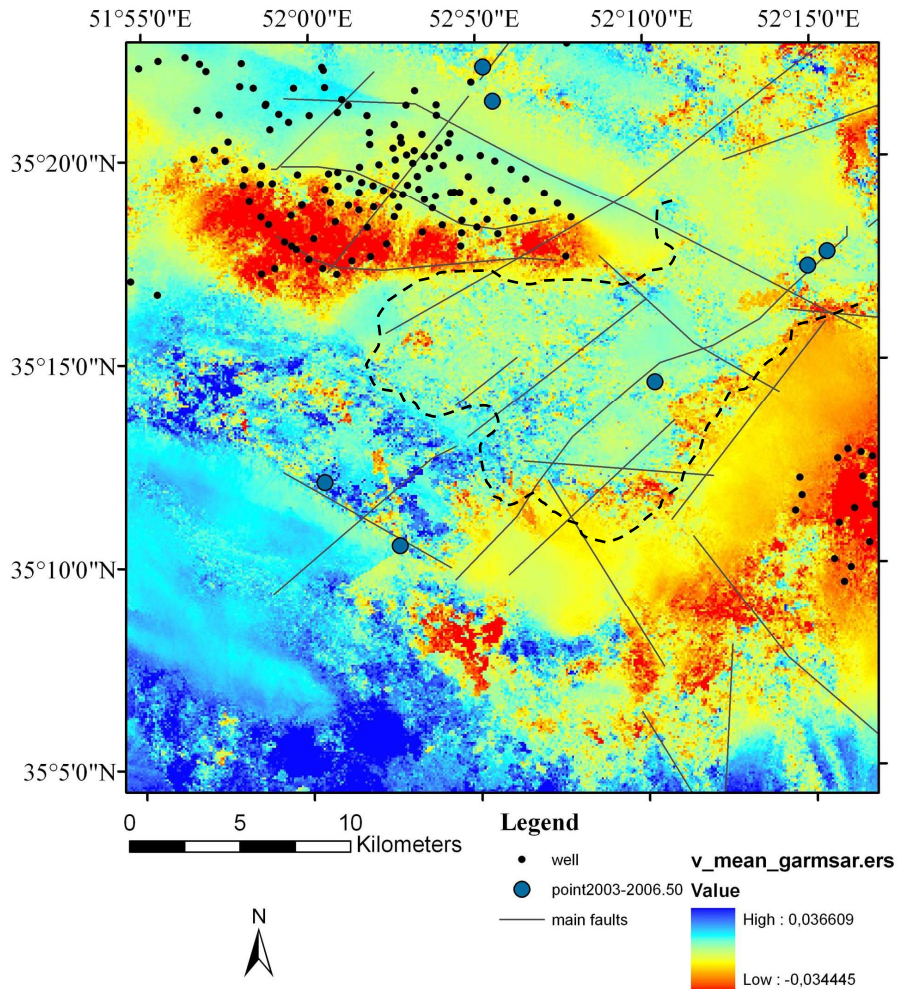


Fig.8. Mean displacement velocity map for the period 2003 12 02 - 2005 06 14. Velocity data have been calculated using MATLAB software. Blue filled circles indicate earthquake epicentres with magnitude ($m_b = 2$ and 3) from 2003-2006 (from the IIEES catalogue). Dashed line shows the outline of salt exposed at the surface. Scaling of velocity bar is in m/y.

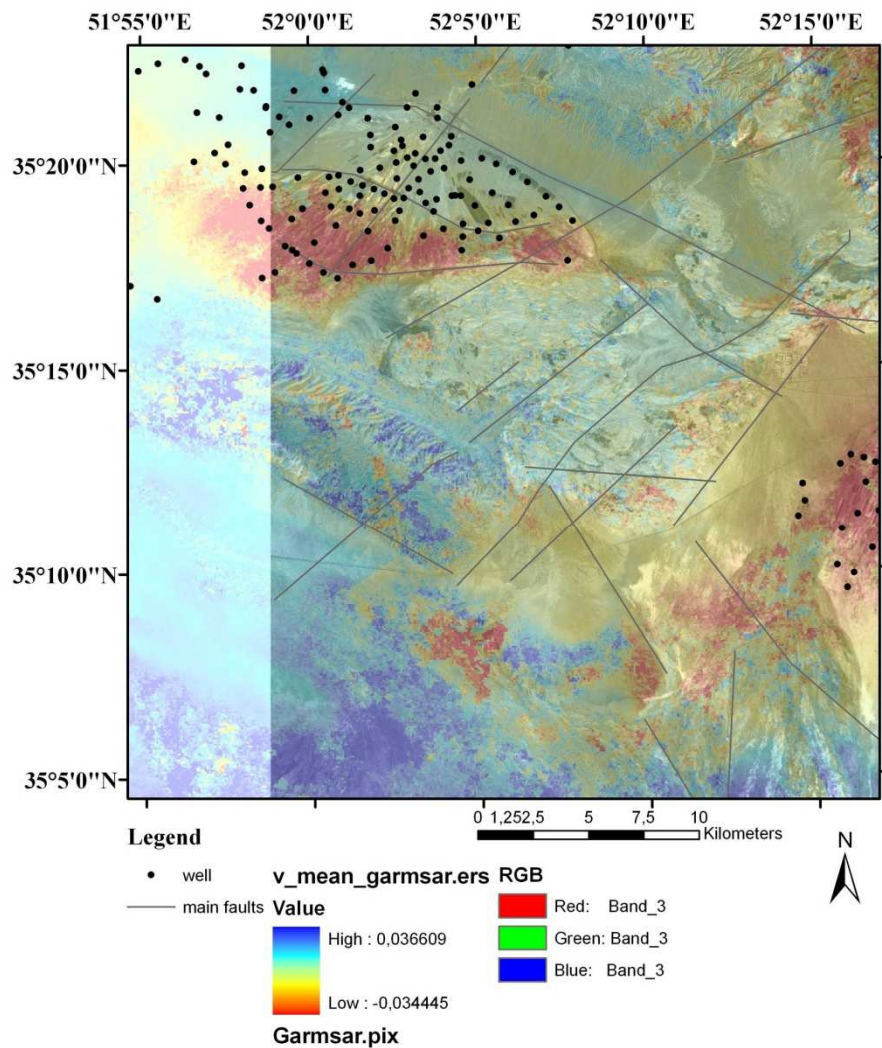


Fig. 9. Mean displacement velocity map superimposed on the Enhanced Thematic Mapper ETM image. For explanation, see legend in Fig. 8.

Conclusion

The results of the present study demonstrate the capability of SAR interferometry to monitor displacements of the ground surface on a regional scale. InSAR measurements were used to map (and calculate the rates of near-vertical displacement) in the Garmsar area. Nine Advanced Synthetic Aperture Radar ASAR scenes acquired during a period 2003–2005 were used to identify the main areas of subsidence and uplift in this area. These interferograms show organized phase differences as colour fringe patterns for epochs ranging in time from 2 to 18 months. The surface displacement rate throughout the region ranges from subsidence of -40 to -50 mm/yr to uplift of 20 mm/yr. The most obvious seasonal effects are that the farmlands around the Eyvanekey plateau subside rapidly in winter and spring when they are irrigated by the extraction of

groundwater that is not replenished at the same rate. The surface of the Eyvanekey plateau subsides at the beginning of each year and then recovers throughout the remainder of the year. We attribute this to the water table falling as a result of extracting groundwater for irrigation.

The uplift rate is faster in southern part of the Eyvanekey plateau than in more northern areas, whereas the steep margins of the Eyvanekey plateau subside rapidly.

Subsidence increases locally along seismically active faults in the plains that are thought to control fluid flow in the region. Such fluid migration is compatible with fractional volume decrease in materials along the fault and subsidence along its surface trace. Our time series analyses indicate slow subsidence over the entire area with minor seasonal effects.

The maximum subsidence rates (40-50 mm/yr) occur east and west of the Eyvanekey plateau, where the agricultural lands are irrigated each spring and summer by wells extracting shallow groundwater. A steady increase of subsidence rate in the farmlands (outside of salt plateau) is recorded from 2003 to 2006.

Recently the national government started controlling the rate of groundwater extraction in Iran, especially during the dry seasons. InSAR maps like that depicted in Fig. 10 should aid such management by distinguishing areas where current rates of pumping groundwater exceeds the natural recharge rates from those where the same density of wells appears to be sustainable.

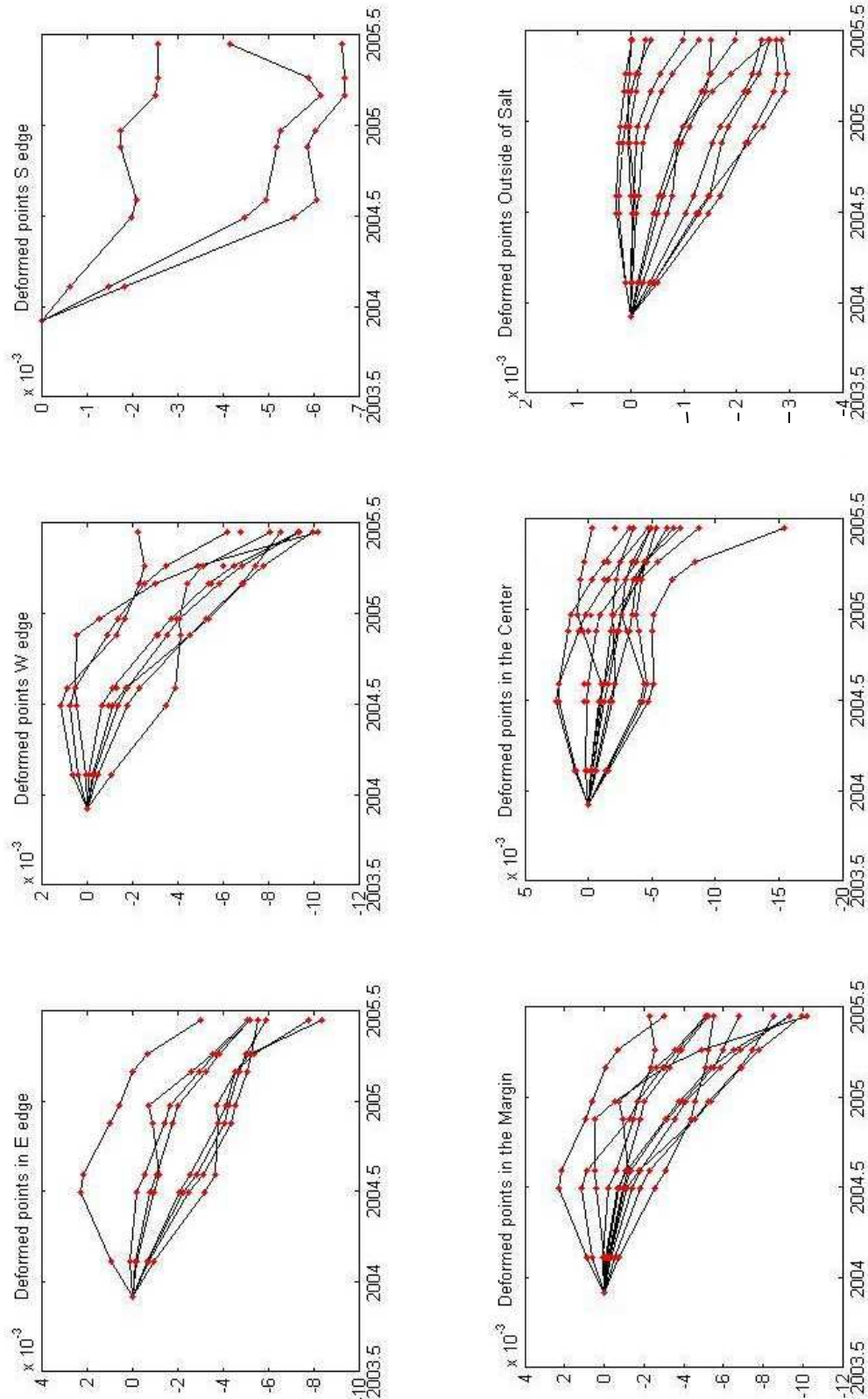


Fig. 10. Rate of deformation (in m/year) vs. time (in years) extracted from the Mean displacement velocity map for parts of salt sheet and surroundings outlined in Fig.9. Plots have been obtained using MATLAB software. Title of each plot showing the location of points selected on Mean Velocity Map of Fig. 9. All points were randomly selected outside or inside the salt sheet, Red dots represent 9 cumulated images.

Acknowledgements

We would like to thank European Space Agency ESA for supplying the ENVISAT data, the Geological Survey of Iran GSI for supplying the hard- and software and logistical support when we prepared and analysed the data. Special thanks go to the Department of Earth Science, Goethe University of Frankfurt. I would like to express my gratitude to Prof. Christopher j.Talbot for setting up the paper and giving me the possibility to work easily, he has always taken the time to explain and resolve my problems. We have also benefited greatly from the Semnan Regional Water Company who supplied well locations, special thanks to them.

References

- Amini, B., Rashid, H., 2005. Garmsar geological map 1:100000 in scale. Geological Survey of Iran, Tehran, Iran.
- Baer, G., Schattner, U., Wachs, D., (2002). The lowest place on Earth is subsiding—An InSAR (interferometric synthetic aperture radar) perspective.
- Bawden, G. W., Thatcher, W., Stein, R. S., Hudnut, K. W. and Peltzer, G. (2001). Tectonic contraction across Los Angeles after removal of groundwater pumping effects, *Nature*, 412: 812–815.
- Berardino, P., Fornaro, G., Lanari, R., and Sansosti, E. (2002). A New Algorithm for Surface Deformation Monitoring Based on Small Baseline Differential SAR Interferograms. *IEEE Trans. On Geoscience and Remote Sensing*, 40: 2375-2383.
- Biggs, J., Wright, T. (2004). Creating a time series of ground deformation using InSAR. Scientific report, Department of Earth Science, University of Oxford.
- Bruthans, J., Filippi, M., Gersl, M., Zare, M., Melkova, J., Pazdur, A., Bosak, P., 2006. Holocene marine terraces on two salt diapirs in Persian Gulf (Iran): age, depositional history and uplift rates. *Journal of Quaternary Science* 2, 843-857.
- Bruthans, J., Asadi, N., Filippi, M., Wilhelm, Z., Zare, M. 2007. A study of erosion 1430 rates on salt diapir surfaces in the Zagros Mountains, SE Iran. *Environmental Geology* 53, 1079-1089.
- Fielding, E., et al. (1998). ‘Rapid subsidence over oil fields measured by SAR interferometry’. *Geophys. R. L.* 25(17):3215–3218.
- Hudec, M.R., Jackson, M.P.A. 2006, Advance of allochthonous salt sheets in passive margins and orogens. *AAPG Bulletin* 90, 1535-1564.
- Hudec, M.R., Jackson, M.P.A. 2007. *Terra Infirma: understanding salt tectonics*. *Earth Science Reviews* 82, 1-28.
- Jackson, M.P.A., Cornelius, R.R., Craig, C.H., Gansser, A., Stocklin, J., Talbot, C.J., 1990. Salt Diapirs of the Great Kavir, Central Iran. *Geological Society of America, Boulder* 177.

- Masson, F.; Sedighi, M.; Hinderer, J.; Bayer, R.; Nilforoushan, F.; Luck, J.-M.; Vernant, P.; Chéry, J. 2002 Present-day Surface Deformation and Vertical Motion In The Central Alborz (Iran) From GPS and Absolute Gravity Measurements. EGS XXVII General Assembly, Nice, 21-26 April 2002, abstract #455.
- Massonnet, D., and Feigl, K. L. (1998). Radar interferometry and its application to changes in the Earth's surface. *Reviews of Geophysics*, 36: 441– 500.
- Motagh, M., et al. (2007). 'Land Subsidence in Mashhad Valley, northeast Iran: Results from InSAR, Leveling and GPS'. *Geophysical Journal International* 168:518–526.
- Raucoules, D., et al. (2007). 'Use of SAR interferometry for detecting and assessing ground subsidence'. *Geoscience*, doi:10.1016/j.crte.2007.02.002. .
- Safaei, H., 2001, Elastic diurnal movement of Masses of Tertiary salt extruded in north central Iran. *Journal of Sciences, Islamic Republic of Iran*. 12, No. 3, 241- 250.
- Schleder, Z., Urai, J.L. 2006. Deformation and recrystallization mechanisms in mylonitic shear zones in naturally deformed extrusive Eocene-Oligocene rock salt from Eyvanekey plateau and Garmsarhills (central Iran)
- Talbot, C.J., 2000, Monitoring salt extrusions in Iran. unpublished PR to Geol. Surv. Iran, March 2000.
- Talbot, C.J., 2004, Extensional evolution of the Gulf of Mexico basin and deposition of Tertiary evaporite: Discussion. *Journal of Petroleum Geology* 27, 95-104.
- Talbot, C.J., Jarvis, R. J., 1984: Age, budget and dynamics of an active salt 1812 extrusion in Iran. *Journal of Structural Geology* 6, 521-533.
- Talbot, C.J., Medvedev, S., Alavi, M., Shahrivar, H., Heidari, E., 2000. Salt extrusion rates at Kuh-e-Jahani, Iran: June 1994 to November 1997, *Geological Society London Special Publications* 174, 93-110.
- Talbot, C.J., 1998. Extrusions of Hormuz salt in Iran. In: Blundell, D.J., Scott, A.C. (Eds.), *Lyell; The Past is the Key to the Present*. Geological Society Special Publications, vol. 143, pp. 315-334.
- Talbot, C.J., in preparation. The Eyvanekey plateau, a 20 x 10 km sheet of allochthonous salt near Garmsar.
- Talbot, C.J., Aftabi, P., 2004. Geology and models of salt extrusion at Qom Kuh, central Iran. *Journal of the Geological Society* 161, 32-334.
- Talbot, C.J., Rogers, E.A., 1980. Seasonal movements in a salt glacier in Iran. *Science* 208, 395-397.
- Vernant, Ph., Nilforoushan, F., Chéry, J Bayer, R., Djamour, Y. Masson, F., Nankali, H., Ritz, J. -F., Sedighi, M., and Tavakoli, F. 2004. Deciphering oblique shortening of central Alborz in Iran using geodetic data. *Earth and Planetary Science Letters* Volume 223, Issues 1-2, 30 June 2004, Pages 177-185.

Vernant, P., Nilforoushan, F., Hatzfeld, D., Abbassi, M. R., Vigny, C., Masson, F., 2004. Present-day crustal deformation and plate kinematics in the Middle East constrained by GPS measurements in Iran and northern Oman, *Geophysical Journal International*, Volume 157, Issue 5, pp. 381-398.

Vita-Finzi, C., 1986. *Recent Earth Movements: An Introduction to Neotectonics*. Academic Press, ISBN 0127223703, 9780127223704, 226 pages.

Wenkert, D.D., 1979. The flow of salt glaciers, *Geophysical Research Letters* 6, 523-526.

Weinberger, R., Begin, Z.B., Waldman, N., Gardosh, M., Baer, G., Frumkin, A., Wdowinski, S., 2006. Quaternary rise of the Sedom diapir, Dead Sea basin, In Enzel, Y., Agnon, A., Stein, M., (Eds.) *New frontiers in Dead Sea paleoenvironmental research: Geological Society of America Special Paper 401*, 33-51.

Weinberger, R., et al. (2006). 'Mechanical modeling and InSAR measurements of Mount Sedom uplift, Dead Sea basin: Implications for effective viscosity of rock salt'. *Geochemistry Geophysics Geosystems*, Q05014, doi: 10.1029/2005GC001185. 7.

The Garmsar salt nappe and seasonal
inversions of surrounding faults imaged on
SAR Interferograms, Northern Iran

The Garmsar salt nappe and seasonal inversions of surrounding faults imaged on SAR interferograms, Northern Iran.

Shahram Baikpour¹, Christopher Talbot²

1) Department of Geology and Palaeontology, J. W. Goethe Universität, Frankfurt, Germany.

2) Hans Ramberg Tectonic Laboratory, Uppsala University, Sweden

Abstract

The allochthonous Tertiary salt of the Garmsar salt nappe extruded from where the most southerly point of the Alborz mountain front is offset by the Zirab-Garmsar strike-slip fault. We used eleven descending Advanced Synthetic Aperture Radar (SAR) images, produced by the European Space Agency's ENVISAT satellite from 2003 to 2006, to map surface displacement over 23 increments ranging in time from 30 to 2 months.

A 30-months SAR interferogram of the area shows that the regional folds and faults are active well south of the mountain front but are dampened by the allochthonous salt that is otherwise merely degrading at rates that vary with the season. Interferograms for shorter epochs display different patterns of fault blocks in the country rocks that rose and fell with the seasons. By relating surface displacements mapped in these interferograms to the contemporaneous seismic record we find that seismic faults reactive repeatedly while their kinematics inverted on remarkably short time scales. Seismic disturbances propagate very slowly and faults are longer than expected for earthquakes with $ML < 3.5$ indicating that the regional strains are more aseismic than anticipated by earlier studies.

Key words: InSAR, Garmsar salt nappe, active folds, fault inversions

Intrudocion

A V-shaped kink in the Alborz mountain chain points southward to the town of Garmsar 100 km SE of Tehran (Fig. 1A). The Eyvanekey plateau lies 10 km west of Garmsar on the northern periphery of the Great Kavir basin in central Iran (Fig. 1B). This plateau consists of a 20 x 10 x 0.3 km sheet of allochthonous Tertiary salt (NaCl) extruded from where the southward advancing Alborz Mountain front is offset ~9 km by the 200 km long NE-SW trending Zirab- Garmsar strike slip fault (Fig. 1A). In a recent review of the thousands of sheets of allochthonous salt now known in over 35 sedimentary basins worldwide, Hudec & Jackson, (2007) referred to this salt sheet as the Garmsar salt nappe. They used the Garmsar salt nappe to exemplify a sheet of allochthonous salt that extruded along frontal thrusts of the Alborz Mountains before undergoing open-toed advance as huge rafts of its dismembered roof collapsed forward into the salt (Fig. 1B).

An earlier Interferometric Synthetic Aperture Radar (InSAR) study (Baikpour et al., 2010) focused on interferograms and times series analyses of the same area for shorter epochs (<18 months). They established that the Garmsar salt nappe is now essentially wasting at rates that vary with the season. Here we start by using a 30-months interferogram (Fig. 2) to relate the Garmsar salt nappe to its former source diapirs and use the regional deformation structures to infer that the original source layer may still be autochthonous in large parts of the area. We then look again at the interferograms for shorter epochs and note that the kinematics of some of the faults appears to invert 3 times in 18 months.

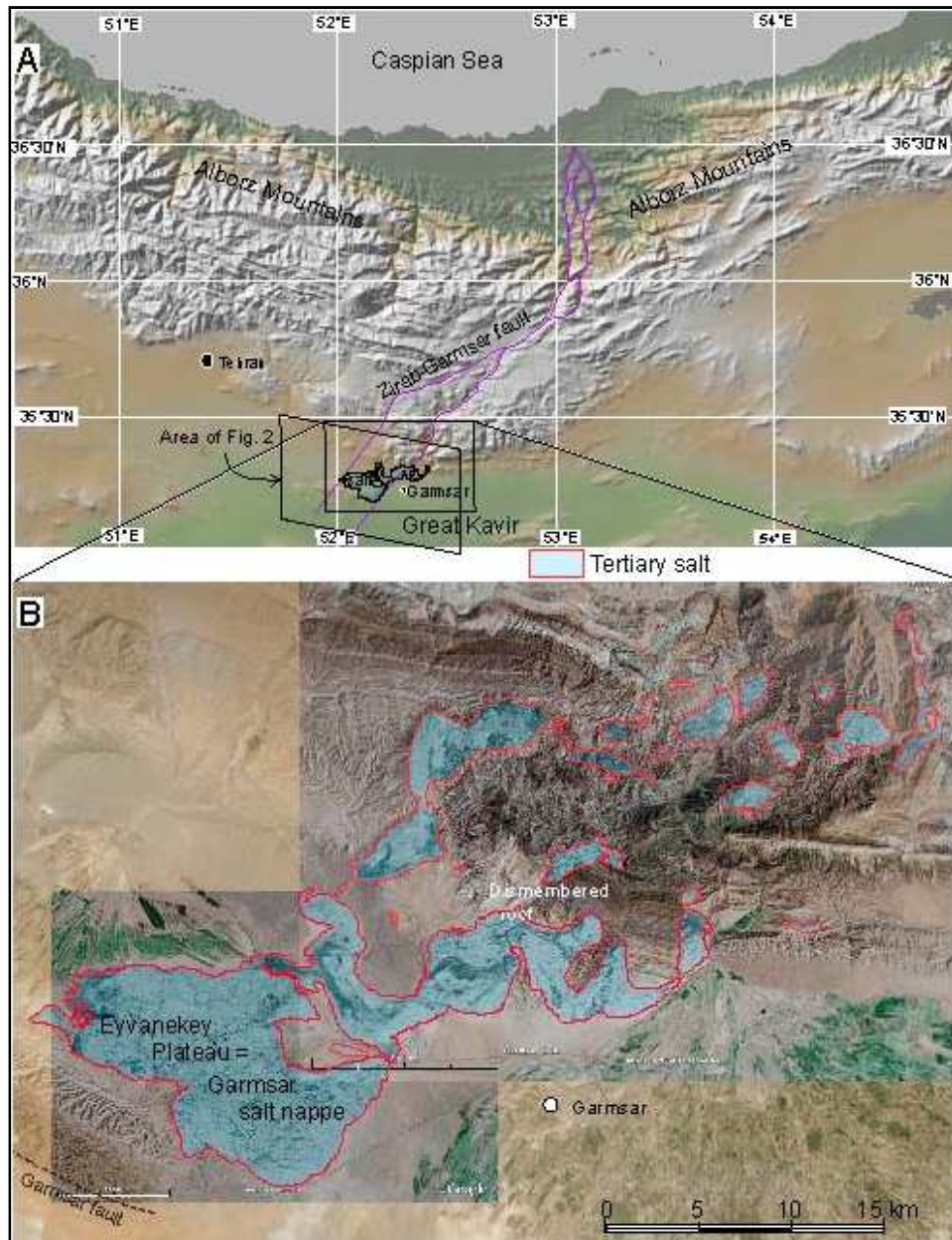


Fig. 1. Location of the Garmsar salt nappe where the Alborz mountain front is offset by the Zirab-Garmsar fault on a relief map by GeoApp.

InSAR Methodology and data

With its wide spatial coverage ($\sim 10^4$ km²), fine spatial resolution ($\sim 10^2$ m²), and high accuracy (~ 1 cm), Interferometric analysis of SAR (InSAR) images has become a widespread and valuable technique to map subtle displacements of the ground surface (e.g. Zebker and Goldstein 1986; Gabriel et al., 1989; Massonnet and Feigl, 1998, Fielding *et al.* 1998).

InSAR uses the phase differences between two SAR images of the same area acquired at different times to map surface displacement in the Line Of Sight (LOS) of the satellite to an accuracy of a few mm. The phase change in the interferogram is the composite of

topographic information, surface displacement between the two acquisitions, atmospheric delay, and noise. Successful InSAR generation requires the removal of the topographic phase contribution to isolate the component of ground displacement.

The atmospheric component is primarily due to fluctuations in water content of the atmosphere between the satellite and the ground. We have been unable to apply software (e.g. Zhenhong et al., 2006) for correcting known atmospheric humidity gradients because they are not known, a problem we address in detail.

Data for this study were collected by the European Space Agency (ESA) Environmental Satellite ENVISAT that has a normal orbital cycle of 35 days. This satellite imaged the study area (outlined in Fig. 1) with a spatial resolution of 100 m between December 2003 and February 2006.

Figure (2) is an interferogram using two descending ENVISAT images acquired on 2003.08.19 and 2006. 02.14. Figures 3 and 4 are based on the nine Track 106 descending Advanced Synthetic Aperture Radar (ASAR) scenes (Table 1) with baselines < 500 m produced by ENVISAT from August 2003 to February 2006. The resulting differential interferograms map surface displacement over 24 epochs ranging in length from 30 to 2 months. We also relate surface displacements mapped in these interferograms to reliable records of contemporaneous seismicity.

We used the two-pass method (Massonnet and Feigl 1998) and GAMMA software supplied by the Remote Sensing Group, Geological Survey of Iran to generate change interferograms for different time intervals (epochs) that varied between 35 to 385 days between December 2003 and June. Rather than using the primary data to generate our own Digital Elevation Model (DEM), we used the DEM provided by the NASA Shuttle Radar Topography Mission (SRTM) with a spatial resolution of 90 m (<http://srtm.usgs.gov>) to remove the topographic phase contribution and geocode the interferograms.

Each colour fringe maps contour of LOS surface displacement equivalent to half the radar wavelength that is 28 mm for the ENVISAT SAR satellite. As all our scenes are from descending satellite tracks we cannot distinguish the vertical and horizontal components separately and so report all the surface displacements as along the line-of-sight (LOS) of the ENVISAT satellite which, for descending satellite tracks is 23° from the vertical to the East so that, in the case of pure vertical movement, one fringe represents 31 mm of displacement.

MATLAB software was used to produce maps displaying the mean displacement *velocity* (here in mm a⁻¹ even for epochs as short as 35 days)

Date	Track	Orbit	Days	Baseline (m)
02 12 2003	106	3507	245	364
10 02 2004	106	4509	315	318
29 06 2004	106	6513	455	-310
03 08 2004	106	7014	490	518
16 11 2004	106	8517	595	76
21 12 2004	106	9018	630	274
01 03 2005	106	10020	700	418
05 04 2005	106	10521	735	-15
14 06 2005	106	11523	805	413

Table 1. Details of the nine descending ENVISAT ASAR images from ESA

Geological Setting

The Alborz and central plateau of Iran

Late Triassic extensional graben now in the southern-central Alborz inverted to thrusts when the closure of Neo-Tethys accreted the Iranian block to Eurasia in the Paleocene (Zanch et al., 2006). Such thrusts transported Precambrian to Tertiary rocks generally SSW in the rootless 3–5 km high, 3000 x 100 km Alborz Mountain belt across northern Iran (Alavi, 1996). E–W thrust faults and folds indicating Late Cenozoic transpression were followed by E–W right-lateral strike-slip faults associated with large ENE–WSW trending folds and ESE–WNW to SE–NW thrust faults and left-lateral strike-slip faults, some of which inverted some of the previous E–W right-lateral faults (Zanch et al., 2006).

The Alborz Mountains now accommodate the N-S convergence between central Iran and Eurasia and the NW motion of the South Caspian Basin with respect to Eurasia (Ritz et al., 2006). These motions have resulted in left-lateral shear to NNE–SSW transpression for the last 5 ± 2 Ma. This oblique shortening is partitioned along range-parallel left-lateral strike-slip and thrust faults that dip inwards from the range margins (Allen et al., 2003). Shortening across the range at the longitude of Tehran is ~30 km (25–30%) despite the crustal thickness of ~35 km, which is similar to adjacent basins. Guest et al., (2007) estimated that the central Iranian basin responded to Arabia–Eurasia collision by subsiding 3–6 km to its present elevation near 1 km above sea level since the middle Miocene.

Early GPS studies suggest that the central Alborz Mountains are rising at $\sim 10 \text{ mm a}^{-1}$ along major faults (Masson et al., 2005). Later GPS studies indicate approximately N-S shortening across the Alborz at $8 \pm 2 \text{ mm a}^{-1}$ (Vernant et al., 2004). Left-lateral shear occurs along E–W low-friction strike-slip faults within the belt at a rate of $4 \pm 2 \text{ mm a}^{-1}$ (Vernant et al., 2004). Deformation extends southwards beyond the mountain front but the crustal blocks of central Iranian are relatively aseismic and shorten N-S by $< 2 \text{ mm a}^{-1}$ (Vernant et al., 2004). The axes of the seismic strain-rate tensors in the Alborz are similar to those deduced from the GPS velocity field. The Alborz Mountains have been characterised by regular large historical earthquakes, and comparison of seismic and geodetic strain rates indicates that 30–100% of the total deformation is seismic in high strain zones of the Alborz (compared to $< 5\%$ in the Zagros Mountains where the earthquakes are smaller: Masson et al., 2005).

Results

Regional structures

Figure 2 is the flattened interferogram for the longest (30-month) epoch and was included as supplementary data with Baikpour et al., (2010). A disadvantage of such a long epoch is that signals are incoherent over large parts of the easily disturbed alluvial fans bordering the Alborz Mountains. Such loss of coherent signals is likely induced by vegetation and chaotic changes in ground conditions due to changes in near-surface water, cultivation, and slope instability. As the baseline for this interferogram was one of the shortest $< 10 \text{ m}$, this loss of coherence was mainly because this 30 month epoch was the longest.

The advantage such an interferogram is that the epoch was sufficiently long for signals recording differential surface displacements to accumulate coherently over large areas of bedrock and salt. The colour scale of Fig. 2A shows surface displacements over the 30 months in mm) and has been translated to mm a^{-1} in Fig 2B. We have overlain our interpretation of what we take as the most important deformation structures on Fig. 2B. These are active folds with axes that parallel the Alborz Mountain Front offset by faults with trends mainly near perpendicular to the front.

The general trend of the Alborz is WNW-ESE to the west of the Zirab-Garmsar Fault (ZGF, in purple on Figs. 1A & 2b) and SW-NE to the east. The two strands we interpret for the ZGF in Figure 2B differ from the interpretation shown in fig. 2 by Baikpour et al., (2010). The eastern and western strands of the ZGF border a SW-NE corridor across

Figure 2B that includes the Garmsar salt nappe and separates structures with different spacing to west and east. The axes of two major anticlines that rose at $>9 \text{ mm a}^{-1}$ alternate with synclines that sank at over $>3 \text{ mm a}^{-1}$ on either side of this corridor. These are offset dextrally by the same 9 km cited by Baikpour et al., (2010) but along the western strand of the ZGF shown here.

The wavelengths of the folds are near 20 km in the west but abruptly diminish to ~ 8 km across the western strand of the ZGF and the salt nappe corridor and are near 6 km to the east. The short wavelength folds (<10 km) in the country rocks probably indicate thin-skin buckles that are detached over shallow autochthonous salt west, south and east of the ZGF.

Similarly, the ~ 20 km spacing of faults to the west of the western strand of the ZGF decreases to nearer 6 km to the east. Some strands of the ZGF parallel or coincide with the margins of salt on the surface but in general, the colours on Fig. 2 bear remarkably little relationship to salt. Instead, they relate to the folds and faults that extend well south of the Alborz Mountain front (Vernant et al., 2004). Thus most of the northern edge of the Garmsar salt nappe sags into the incoherent signals of the Eyvanekey syncline and the eastern edge overlap with parts of two strike-slip duplexes along the eastern strand of the ZGF.

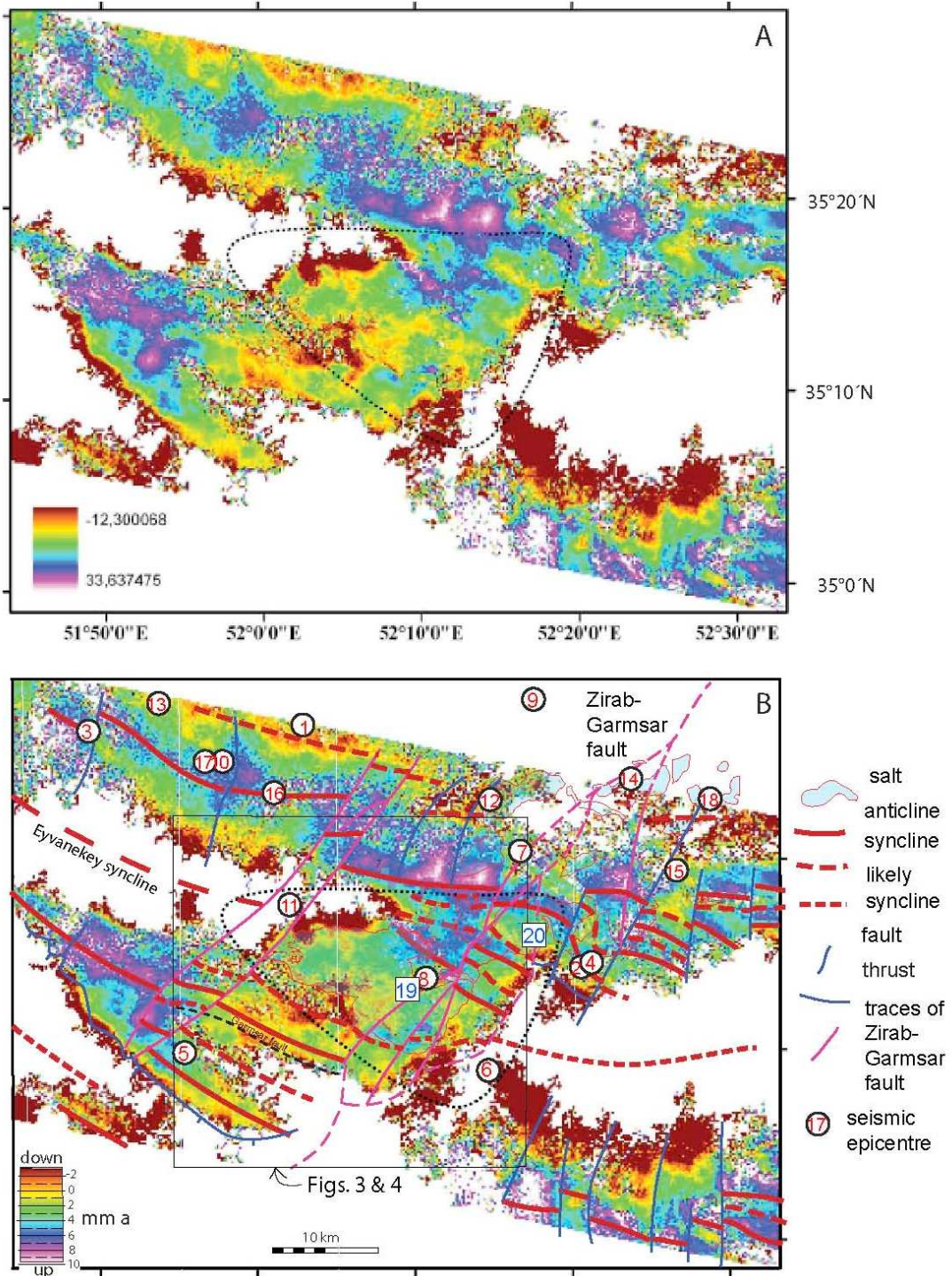


Fig. 2. A. Unwrapped or flattened interferogram for the 30-month epoch from 19.08.2003 to 13.02.2006 (From URL: [http:// www.geolsoc.org.uk/SUP18383](http://www.geolsoc.org.uk/SUP18383). White areas represent incoherent interference between equivalent pixels on image pair. The colours refer to surface displacement in the line of sight to the satellite. My blue and purple lines pick out traces of faults along abrupt colour differences and red lines indicate the axes of active folds with gentler colour gradients.

Some of the fastest rises in the country rocks occur behind a thrust in the SW corner and where the Alborz mountain front is riding up the back of the fragmented and displaced

former roof of the salt now in the Garmsar nappe. Diapirs still extruding along the Alborz mountain front probably supplied the Garmsar salt nappe in the past. However, a river has eroded a (post-emplacment?) gap between the salt in these diapirs and what is now essentially static allochthonous salt. This gap raises the possibility that the nappe extruded from the Zirab-Garmsar fault as well the mountain front.

There is very little evidence that might indicate that the GSN is still being supplied by new salt from depth. Plots of the rate of deformation against time for the 50 or so points with unspecified locations on the GSN (fig. 10, Baikpour et al., 2010) indicate 8 rising at up to 2.5 mm a^{-1} in the summer of 2004 and 6 rising almost as fast in the winter of 2005. However, it is striking on Figs. 6-9 that the proximal end of the salt nappe only ever rose in the 140 days from June to November 2004 when the distal allochthonous salt also rose (fig. 7D). Otherwise, significant parts of the GSN only ever rose (up to 2,5 cm in the 70 winter days from December 2003 to February 2004 (Baikpour et al., fig. 7e). These authors suggest that salt may have risen into the head of the Eyvanekey salt sheet and flowed to the SW, and spread under gravity away from a NE – SW axis. However, the same surface displacements could alternatively be attributed to the salt expanding when it was wet and shrinking when it was dry. In general, the top of the extruded salt subsided continuously at rates that broadly related to the rainfall (Baikpour et al., 2010, see also Aftabi et al., 2010).

Few faults in the country rocks extrapolate into the 300-200 m thick Garmsar salt nappe emphasising its ductile nature. By contrast, folds in the country rocks do extrapolate into the salt nappe but are notably more subdued (Fig. 2). An obvious interpretation is that the ductile allochthonous salt in the SW-NE corridor dampens regional folds active in the underlying bedrocks.

The relief map (Fig. 1) emphasises that the faulted anticlines to the W and SW of the Garmsar salt nappe are exposed in bedrock. However, the same major anticline that is folding as it faults to the southeast appears to affect the desert surface (probably in a manner too subtle to be recognisable in the field).

Interferograms for shorter epochs

Figure 3 repeats differential interferograms for 5 epochs of between 70 days and 18 months from (Baikpour et al., 2010). Be warned, the colour scales on Figures 3 and 4 and are almost inverted compared to those in Fig. 2. Baikpour et al., (2010) attributed the colour differences on Figs. 3B-E to seasonal effects and were undoubtedly correct where

they correlate with salt that expands on wetting (Figs. 3C, E) and shrinks on drying (Figs 3B, D). However, we take another approach here and explore the concept that the general patterns in each epoch are more likely to indicate active fault blocks than areas subject to different rainfall. Consequently, abrupt colour transitions are interpreted as the surface traces of active faults (black lines on Figs. 3 & 4).

The most significant characteristic of Fig. 3 is that different patterns of fault blocks rose and fell in the various epochs. The structural patterns apparent on the interferograms of Figs 2 to 4 noticeably change as the epochs shorten despite the same topography having been removed from all of them. In general, the emphasis changes from faulted folds that is clear over 30 months (Fig. 2) to different pattern of fault blocks as the epochs shorten to 18 months (Fig. 3A) and 70 days (Figs 3B & E). Figures 3 and 4 emphasise a common occurrence in continental rocks: rather than new faults developing, many old faults repeatedly reactivate.

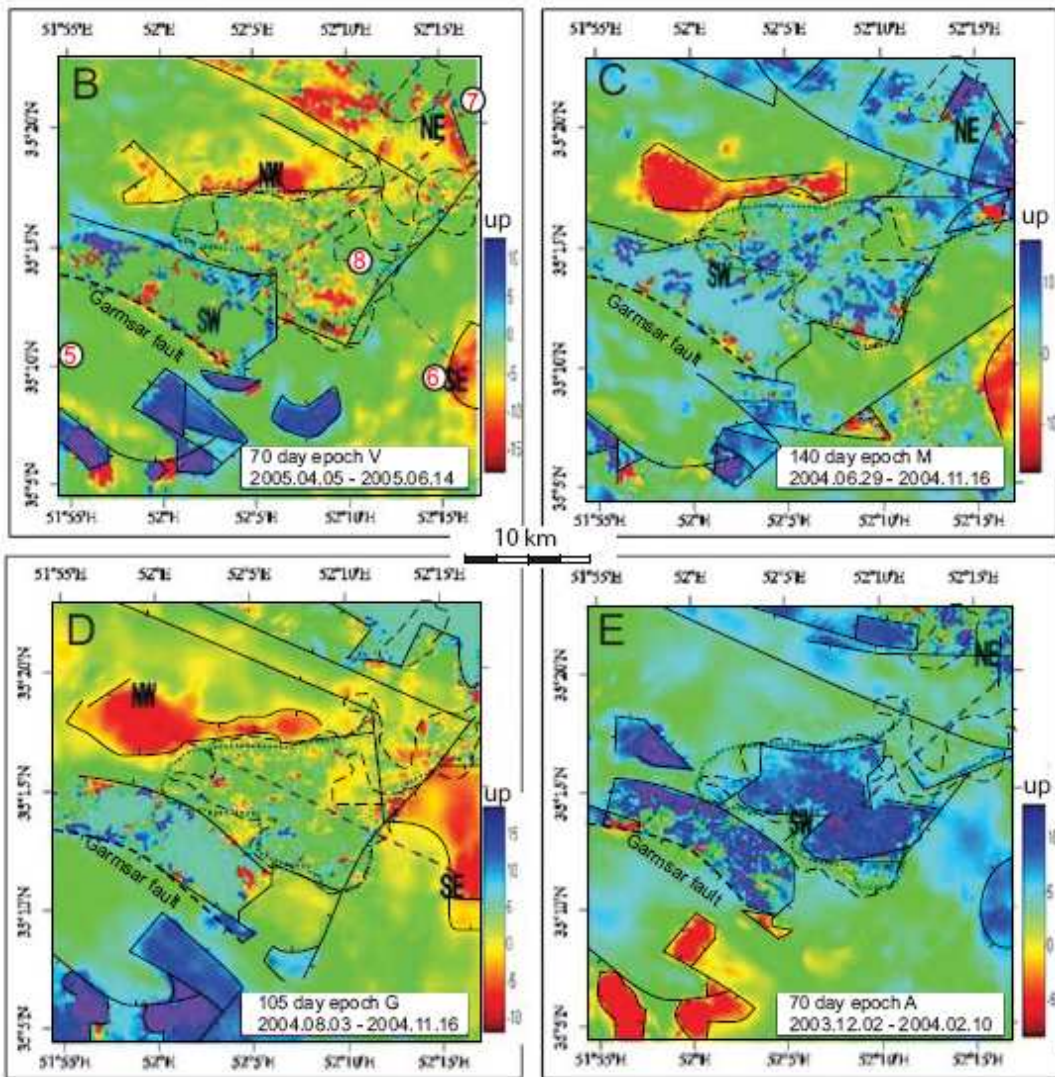
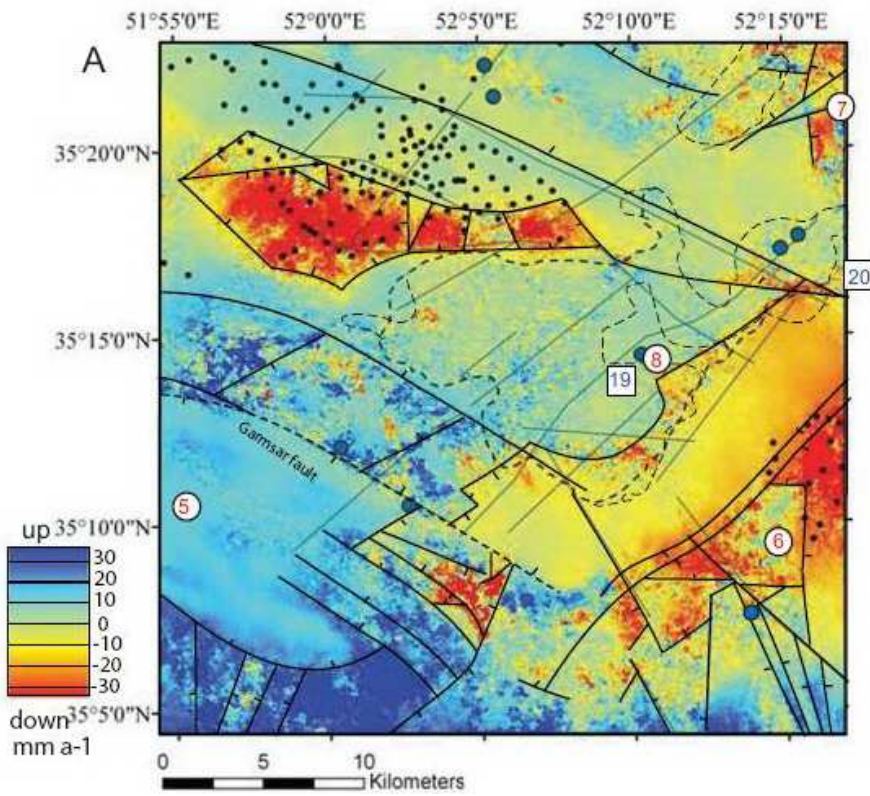


Fig. 3 A “Mean displacement velocity” map for the epoch 2 December 2003 to 14 June 2005 from fig. 8 of Baikpour et al., (2010). Be warned, the colour scales on Figs. 3 and are almost inverted compared to those in Fig. 2. Blue filled circles indicate earthquake epicentres with magnitude (mb) 2 and 3 from 2003 to 2006 (from the IIEES catalogue). I have added more dashed line to outline salt at the surface, re-scaled the velocity bar to mm a^{-1} , and interpreted faults active in each epoch as heavy black lines. (B-E) Four differential interferograms chosen to show seasonal effects by Baikpour et al., (2010) in their fig. 6. The length and dates of labelled epochs are indicated. Scaling of colour bars is in centimetres.

The colour scales for each epoch represented in Figs 3B-E (= fig. 6 in Baikpour et al., 2010) have been translated into cm a^{-1} despite the longest epoch being 140 days whereas the colour scale for Fig. 3A (= fig. 8 in Baikpour et al., 2010) is the mean displacement *rate* in mm a^{-1} . This difference intensifies the displacements shown in Fig. 3B-E compared to Fig. 3A. More faults appear in the interferogram for longest epoch (Fig 3A) than those for the shorter epochs (Figs. 3B-E).

The interferograms on Fig. 4 have been chosen to show fault displacements in particular epochs (Figure 5 relates the times and overlaps of the epochs). Figs. 4V and A show different expressions of the same data for the same epochs as shown in Figs. 3B and E. Their colour scales differ because those in Fig. 4A and V are the surface displacement in these two 70 day epochs whereas those in Fig. 3E show the same data translated into surface displacement *rates* in cm/yr .

The differential rates have shown in Figs. 3B and E greatly exaggerate the differential displacements shown in Figs. 4V and A.

Earthquakes and faults on Figs. 3 and 4

The bulletin compiled by the Iranian Seismological Center at the Institute of Geophysics, University of Tehran (irsc.ut.ac.ir/) was searched for seismic events of earthquakes that occurred in the study area and epoch. This search revealed 180 events recorded by the Tehran regional network of local short period seismic stations. However, most of these events have very uncertain location. Dr Mohammad Tartar of the International Institute of Earthquake Engineering and Seismology (IIEES) shortened the initial list to the 20 events with epicentres within the seismic network listed in Table 2, located on Fig. 2 and plotted on Fig. 5. Most of these events were recorded by at least 5 stations (including 4 P and 1 S reading), with horizontal and vertical uncertainty in location of <5 km, an azimuth gap in the received signals of $<180^\circ$, and average horizontal and vertical errors

for the epicentres of 0.8 and 2.4 km respectively. The depth errors for events 19 and 20 were 7.4 and 26.9 km respectively. Unfortunately all these reasonably well-located events followed a network upgrade so none occur in the first 8 epochs, A-H (Fig. 5).

The twenty epicentres of small (MN 1.1 to 2.6) earthquakes (Table 2) that occurred in the study area during the 30-month epoch plot near one or other of the faults on Fig. 2. Only six events fell within the area and epoch represented in Fig. 3A and only 4 in Fig. 3B. No kinematic solutions are available for any of these events.

Three pairs of earthquakes of similar magnitude occurred within a day of each other. Shocks 2 and 3 occurred 18 minutes and 51.5 km apart at depths of 25.65 and 15 km respectively along the strike of the Alborz Mountains. Any connecting disturbance travelled 51.5 km in 18 minutes = 2.86 km min^{-1}

Shocks 7 & 8 were of similar magnitude and depth and occurred 121 minutes 20 seconds and 15 km apart (perpendicular to the Alborz) implying that any connecting disturbance travelled 15 km in 7260 s = 21 cm s^{-1} .

Shocks 19 and 20 occurred 320 minutes and 13.4 km apart (also perpendicular to the Alborz) implying that any disturbance that travelled between them moved at $\sim 70 \text{ cm s}^{-1}$.

All three approximate disturbance velocities are very slow compared to brittle fractures that are expected to propagate at km s^{-1}

Event pair 7 and 8 were 19 and 21 km deep with epicentre just NW of strands of the ZGF. The depths of event pair 19 and 20 are poorly constrained but their epicentres are also close to the ZBF (Fig. 2) suggesting that the ZGF is sub-vertical and deep rooted.

The radii of seismic slip surfaces are expected to be about 10^4 times the displacements along them (Slunga 1991). The largest displacement along likely fault traces in the study area is $\sim 16 \text{ mm}$ (Fig. 4). This implies that the slip surfaces have radii near 160 m close to hypocenters at depths between 9 and 25 km. However, the active lineaments in the area are between 1 and 32 km long (Fig. 4). Many of the faults that appear to have moved are therefore much longer than expected from such small earthquakes.

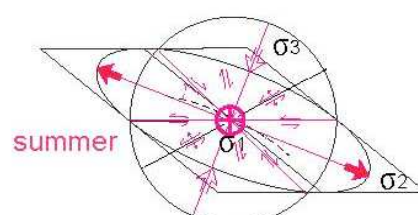
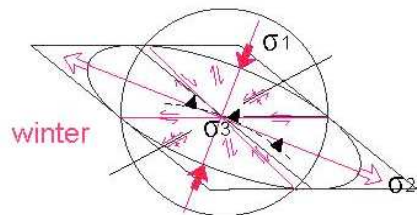
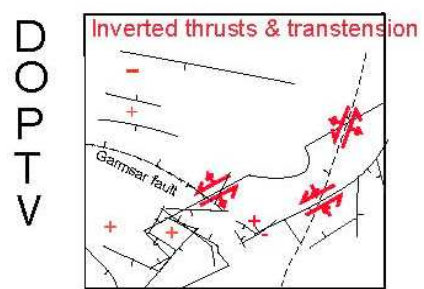
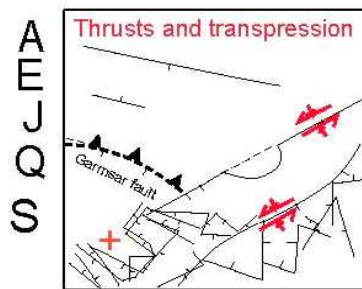
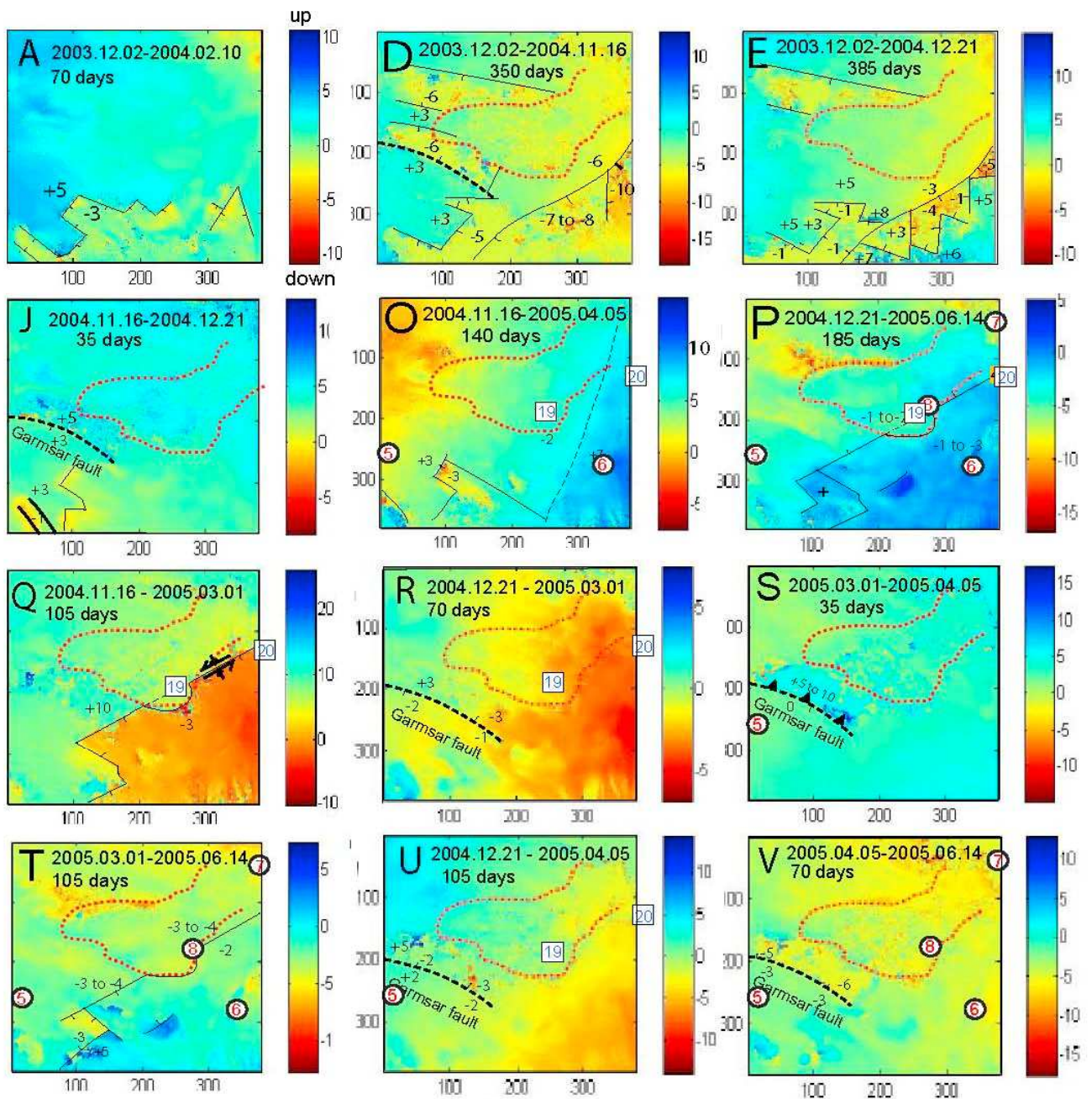


Fig.4. 12 unwrapped differential interferograms generated from the ESA data listed in Table 1. The labels correspond to those on Table 2 that lists dates, and perpendicular baselines of epochs that range in length from 35 to 385 days. The red dotted line outlines the Garmsar salt nappe. The colour bars are in units of mm during each epoch. Black lines indicate faults and white circles and squares represent the epicentres of earthquakes active in each epoch (and listed on Table 2).

Fault Inversions

Different patterns appear on the interferograms of Figure 4 even though the same topography has been removed from all of them.

There are elements in common in the different fault patterns recognisable on Fig 4. The two interferograms that look most likely to record the surface displacement of the same fault are those for Epochs P, and Q. Most of the main SW-NE lineament in Figs. 4P, and Q is straight and locally coincident with the eastern margin of the Garmsar salt nappe and extends further south. However, it makes a conspicuous bend around the SE corner of the nappe suggesting that fault displacement stopped at the base of the salt sheet. However, whereas the surface displacements on Fig. 4P suggest the hanging wall of this fault was to the NW, in marked contrast, those on Fig. 4Q suggest a hanging wall to the SE.

The NW-SE trending Garmsar fault (Amini & Rashid, 20005) also inverts. Shown as a heavy dashed line in all our Figures in which it appears the Garmsar fault is coincident with a local break in slope (Fig. 1). This fault is inconspicuous on Fig 2 but parallels a much more obvious un-named north dipping thrust 9 km further south. The hanging wall of the Garmsar fault is to the north in 7 epochs (A, F, J, N, Q, R, & S) but to the south in another 7 epochs (B, C, D, G, M, P, T, & V). Any movements of the same fault appear to have been insignificant in another 8 epochs (E, H, I, K, L, N, O & U). Either two faults with reverse kinematics have coincident traces or, more likely, the northern block rose relative to the southern block of the same fault from December 2003 to midsummer 2004 and from November 2004 until Spring 2005 but inverted in the intervening months (Fig. 5). The last of these three inversions appear to have been captured in interferograms for epochs R and U when the relative displacements across the Garmsar fault reversed along its strike and indicate different stages in a scissor-like movement (Figs. 4R and U and Fig.5). The northern block of the Garmsar fault is topographically higher than the southern block (Fig. 1B) implying that north-side up increments is generally larger than

south-side up increments so that block movements accumulate to render the Garmsar fault a long term thrust.

The folding, the slow rates at which seismic disturbances appear to have propagated between epicentres on the same day, active fault lengths longer than expected for such small earthquakes, and displacements that vary in value along one or both sides of many faults, all indicate that aseismic deformation is significant in the area. Despite being in a region subject to many small earthquakes these findings point to a much larger component of ductile strain than the 50 to 100% of the total deformation being seismic suggested as typical of the Alborz by Jackson and McKenzie (1988) or the 30 to 100% suggested by Masson et al. (2005).

Discussion

We are aware that interferograms for epochs as short as we show here are vulnerable to changes in humidity in the atmosphere (that are often taken as random). However, various relationships suggest that more fundamental effects are involved. The colour changes we interpret as faults are too abrupt to be due to atmospheric conditions and must record differences in ground movements. These may in turn reflect variations in ground conditions but the close association of many to seismically active faults (Fig. 2) suggest otherwise.

The lineament that coincides with the eastern margin of the GSN but takes a conspicuous bend around its SE corner (Figs. 4P, Q) suggests not only that the fault displacement stopped at the base of the salt sheet but also signals the effects of geological rather than atmospheric processes.

Most of these faults are clearer than most of those identified on interferograms of the subsiding floor of the Kasmar valley in NE Iran by Anderssohn et al., (2008). Furthermore, they are sufficiently systematic to speculate on the kinematics, even their dynamics.

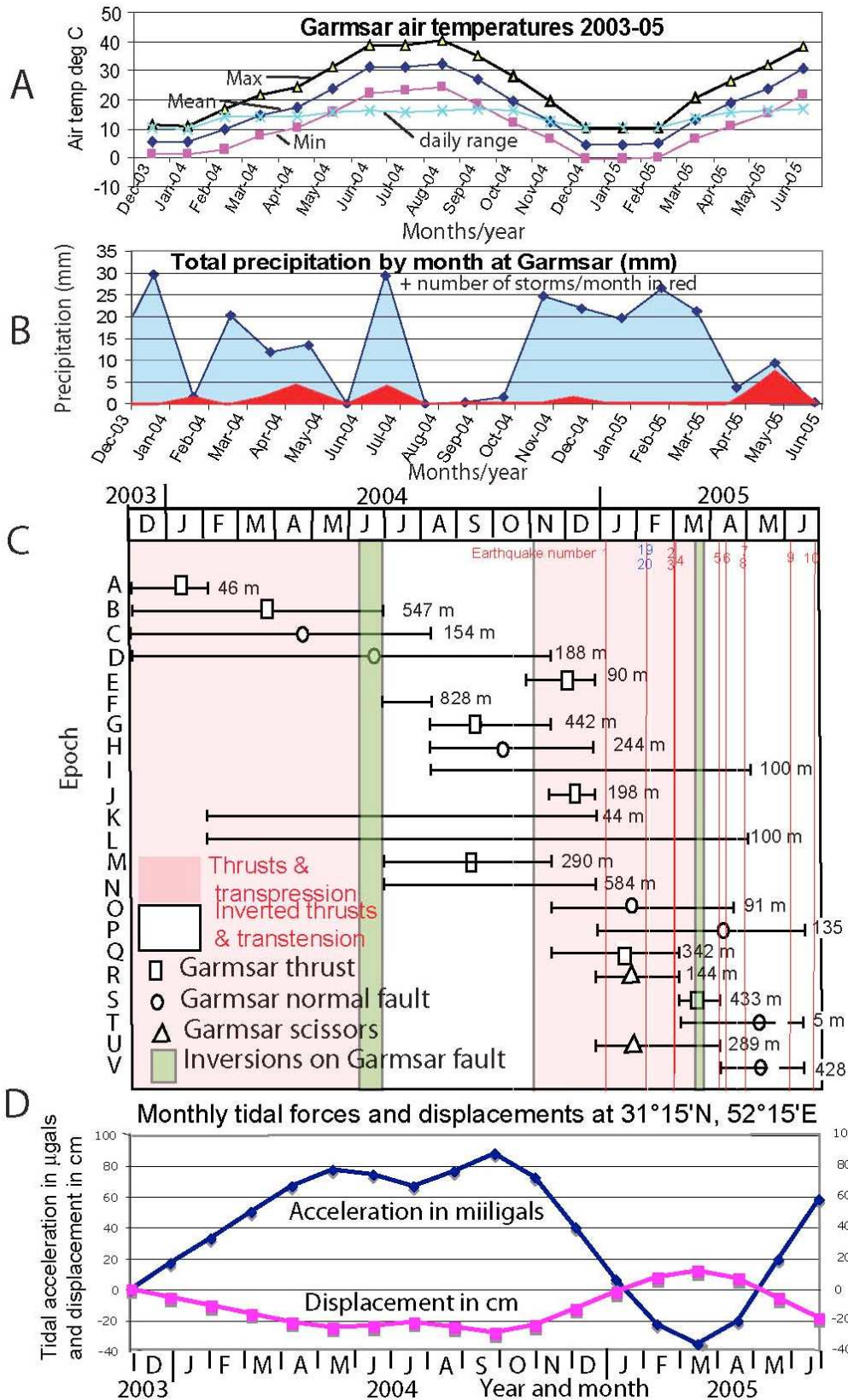


Fig. 5. Comparison of weather, earthquakes, tidal acceleration and displacement by month for the InSAR epoch of Fig. 3A. A. Maximum, minimum and mean temperatures with daily rang. B. Total precipitation (in blue) and number of storms per month (in red) (A & B: data for Garmsar station in Semnan Province from the Iran Meteorological Organization. C. Twenty-two InSAR

epochs (A-V) with baseline in metres. Earthquakes from Table 2 in thin vertical lines. Keyed symbols on epochs indicate interpretation shown on Fig. 4 leading to background shading for transpression or transtension fault displacements. D. Tidal forces (in milligal) and displacement (in cm) for the relevant time interval (From <http://www.taygeta.com/>)

Because of the potential atmospheric effects we pay little attention to the values of local offsets or their rates along faults (listed beside them in Figs. 3 and 4). However, we are impressed by their qualitative variations along faults, and in particular, their apparent inversions from epoch to epoch.

Faults often separate units with different mechanical properties so that the differential surface deformation across them may record different mechanical properties at superficial levels such as soil swelling, solubility, thermal expansively and compactability (etc). Rather than actual fault displacements, the colour patterns on Figure 4 could therefore represent different soils swelling or shrinking as they wet or dry. However, the relative areas of uplift and subsidence along the faults interpreted on Fig 4 are quite definite and cut across areas of low relief that are shown as having similar rock or soil types on the geological map (Amini & Rashid, 2005) and satellite images (Fig. 1B). Perhaps the most convincing fault pattern we interpret is that on (Fig. 2) but very few of those are on the geological map.

We therefore consider the colour patterns in Figure 4 more likely to record real inversions of fault movements associated with nearby earthquake epicentres.

Salt

Salt is still extruding from the Alborz mountain front and behind the fragmented and dispersed partial roof of the nappe (Figs. 1B and 2). Some of the salt diapirs in the Alborz front that probably supplied the Garmsar salt nappe are therefore still active (Fig. 2). Some of the many diapirs behind the front may also be active but are outside our SAR cover. However, post-emplacment river erosion has separated the nappe from its former sources north of the river. The data could be interpreted as indicating that the 200-300 m thick salt nappe appears to expand ~5 mm when it is wet and shrink as much as it dries. The Garmsar salt nappe is no longer supplied by new salt extruding from depth, instead it appears to be wasting, perhaps by gravity spreading, but certainly by dissolution.

Theory (Talbot and Jarvis, 1984) suggests that dissolution of exposed halite at 25°C could reach 17% of the annual rainfall. However, field measurements suggest that

dissolution of exposed salt can exceed this rate in natural conditions (Bruthans et al., 2007 and references therein), perhaps aided by micro organisms. Thus, salt exposed on the SE coast of Iran dissolves at 30-40 mm a⁻¹ in a mean annual rainfall over 5 years of 103 mm a⁻¹; this value fell to a mean of 3.5 mm a⁻¹ for salt beneath its own residual soils (Bruthans et al., 2007). These figures suggest that bare salt exposed near Garmsar may dissolve at nearly 29 to 39% of the decadal mean annual rainfall of 124 mm a⁻¹ (i.e., at 37 to 50 mm a⁻¹). However, a cover of residual soils protects most the Garmsar salt nappe and can be anticipated to limit its general dissolution rate to nearer 4 mm a⁻¹. Salt dissolution at this rate would be consistent with the time series analysis shown by Baikpour et al., 2010.

Folding

Local rise rates of ~9 mm a⁻¹ (Fig. 2) approach the 10 mm a⁻¹ measured for the uplift rate of the *central* Alborz Mountains by early GPS studies (Masson et al., 2002). A significant difference is that these authors expected differential rise along major range parallel faults whereas Figure 2 indicates that most movement in the Garmsar area is mainly by folding offset along the ZGF and many minor range-perpendicular faults. Seismic and GPS geodetic studies suggest that the 8±2 mm/yr S-N shortening across the Alborz is likely to be faster than the 4±2 mm/year left-lateral shear along the belt (Vernant et al., 2004).

Episodic fault inversions

Deformation within the Alborz Mountains is due to the N-S Arabia–Eurasia convergence (at ~3 cm a⁻¹: Masson et al., 2002), and westward motion of the South Caspian basin relative to Iran (Allen et al., 2003). Many workers have emphasized the complications of deformation within the Alborz Mountains. Thus Allen et al., (2003) recognized that range-parallel right-lateral strike-slip faulting reversed to left-lateral slip in Pliocene times (5 ± 2 Ma: Ritz et al., 2006) since when the oblique shortening has partitioned along range -parallel left-lateral strike-slip faults and thrust faults that dip inward from the range margins.

Ritz et al., (2006) claimed that parts of the central Alborz are not affected by the left-lateral shear due to NNE-SSW transpression general since middle Pleistocene; instead they display active transtension with a WNW-ESE extensional axis that developed after

the South Caspian Basin began subducting. Our data raises the possibility that both these stress fields alternate in the Garmsar area.

Two main types of inversions of tectonic forces are described in the literature:

1) Local stress fields that alternate either side of a critical value. Thus, phases of active lateral shortening that steepen the tapers of fold-thrust belts and accretionary prisms can alternate with phases when gravity spreading and/or sliding lowers their tapers (Platt, 1986). Applied to the Garmsar area, this picture suggests phases of lateral N-S shortening that steepen the Alborz Mountain front might alternate with phases when the slope decreases by gravity gliding over a basal detachment of subsurface salt.

2) Local stress fields that alternate between two far stress fields. Thus, two suites of regional joint sets superposed on the salt extrusion of Qom Kuh 168 km to the SW of Garmsar have been attributed to phases of N-S shortening alternating with phases of E-W shortening that drives the strike-slip faults of central Iran (Talbot and Aftabi, 2004). Applied to the Garmsar area, this picture suggests phases of N-S shortening with NNE-SSW transpression alternating with phases of N-S shortening accompanied by WNW-ESE transtension.

The Garmsar fault appears to have acted as a north dipping thrust in the winter months (Figs 4J & S) and inverted to a normal fault in the summer months (D & V). The last of these inversions in our coverage may have been captured by the scissor-like motion along the Garmsar fault (Fig. 4R, U) Similarly, the main active fault trending SW-NE could be a sinistral transpressive thrust in Figs. 4Q and a transtensional normal fault in Fig. 4P and T. This could indicate alternations between transpressive and transtensional stress fields. Using the kinematics of these two faults as guides suggests that the fault dynamics in epochs A, E, J, Q & S (Fig. 4) and the epochs G & M plus the 18 month epoch (Figs. 3A) can be attributed to left-lateral shear due to NNE-SSW transpression while those in epochs J, D, O, P, T & V (Fig. 4) can be attributed to transtension with an effective WNW-ESE extensional axis. The kinematics of some of the fault systems thus inverted 3 times in the 18-month epoch represented on Fig. 3A suggesting an inversion cycle near 6 months (Fig. 5).

Plate movement rates are often thought of as steady because measurements averaged over millions of years are reported in mm a^{-1} . However earthquakes, ground measurements, GPS surveys, and InSAR, all demonstrate that fault movements become increasingly irregular as the time window they are observed in shortens. Fault inversions in the geological literature (e.g. Allen et al., 2003; Zanchi et al., 2006) occur over

millions of years because the data they are based on can only resolve inversions over millions of years. In effect, we are arguing here that the short time span of InSAR allows the distinction of similar tectonic inversions seen in the geology but over much shorter time intervals. Indeed, the most convincing fault pattern is on the 30-month interferogram (Fig. 2) and very few of those are on the geological map.

The strain ellipses shown at the bottom of Fig 4 summarise the distortion of a 100 km square of the Alborz over 5 million years at the measure rates of 4 mm a^{-1} left lateral shear and 6 mm a^{-1} N-S shortening (Vernant et al., 2004) across the Alborz which is consistent with the 30 km shortening at the longitude of Tehran (Allen et al., 2003).

The *stress* fields that could be responsible for the inverted fault movements shown for each of the two groups of epochs indicated have their principal axes labelled at the bottom of Fig. 4. Epochs during which particular faults act as thrusts and transpressive faults are shown as having a SSW-NNE maximum horizontal axis (δ_1), a WNW-ESE intermediate axis (δ_2), with gravity being the smallest principal stress (δ_3).

Tension is unlikely as any principal tectonic stress, even when former thrusts and transpressive faults invert to normal and transtensional faults. However, the WNW-ESE horizontal principal stress (δ_2) exceeds the SSW-NNE horizontal principal stress (δ_3), if gravity acts as the maximum stress (δ_1) as shown for the second group of epochs. This interpretation implies that both the models accounting for tectonic inversions above can be involved in the Garmsar area. Local stress fields could be said to alternate either side of a critical value (Platt 1984) *and* between two far stress fields (Allen et al., 2003; Ritz et al., 2006).

N-S shortening between Arabia and Asia steepens the taper of the Alborz mountain front by thrusts (and folds) with transpression along SW-NE trending strike-slip faults mainly in winter. Gravity acting as δ_1 exceeds the lateral stresses and the WNW-ESE compressive stress exceeds the SSW-ENE compressive force leading to inversion of the thrusts and SW-NE strike-slip faults mainly in summer, the taper of the Alborz mountain front decreases by gravity gliding over a basal detachment of subsurface salt (where it is still present). The left-lateral transtension along the Alborz allows westward motion of the South Caspian relative to Iran so that the southern Caspian basin can subduct.

Figure 5 relates the epoch shown in interferograms on Figs. 3 and 4 to the monthly record of temperature, precipitation and tidal acceleration and displacement. The 4 rainstorms in July 2004 and Epoch F were the first significant summer rainfall for at least a decade. Close inspection shows little correlation between the displacements on

the interferograms and the temperatures but some agreement with both the rainfall and the maximum and minimum solid earth tides.

The rainfall in the Alborz Mountains must be higher than in the Great Kavir suggesting that the level of the water table in the Garmsar area is subject to comparatively large seasonal fluctuations. Such large seasonal changes in groundwater pressures might, together with tidal maxima and minima, somehow trigger switching from one stress field to the other and account for the kinematic Inversions along many faults in the Garmsar region.

Conclusions

In summary, our InSAR results generally match previous studies of Alborz deformation but add interesting details.

As the Alborz Mountain Front advanced SSW in the last ~ 5 Ma, it overrode a salt sequence buried in the Garmsar basin and extruded some of it over the surface of the Great Kavir as the Garmsar salt nappe from where the Zirab-Garmsar Fault offsets the mountain front by ~ 9 km (Baikpour et al., 2010). The shorter wavelengths of both faults and folds in and east of the ZGF suggest that salt is still autochthonous at depth in a 10 km wide fringe to the west of the nappe and to unknown distances to the south and east.

The slow transmission of disturbance between earthquakes, active faults that are longer than expected of such small earthquakes and clear folding points to tectonic strain with a larger than anticipated proportion of aseismic strain.

Rather than swelling by extrusion of salt from underground, the Garmsar salt nappe now appears to be essentially inactive and degrading either by dissipation due to continued gravity spreading or, more likely, its general dissolution. Too ductile to fault, the salt sheet dampens the regional folding due to N-S shortening.

We look forward to future studies clarifying how far the active Alborz structures extend to the south of the mountain front. It would also be interesting to know the geography of the autochthonous salt layer signalled by the close spacing of folds and faults in the ZGF and to the south and east. Of even greater interest would be the geography and timing of apparently episodic inversions of active faults and whether they only occur where autochthonous salt provides a shallow décollement. Continued monitoring using InSAR would be valuable, and a local array of GPS stations would be able to check changes in kinematics and a local array of seismometers should allow earthquake solutions to check the dynamics.

Acknowledgments

We thank the Geological Survey of Iran GSI for supplying the hard- and software as well as logistical support when we prepared and analyzed the data. We also express our gratitude to Dr. Maryam Dehghani, who has always taken the time to try and explain and resolve our problems.

References

- AFTABI, P., ROUSTAIE, M., ALSOP, G.I. & TALBOT, C.J. 2010. InSAR mapping and modelling of an active Iranian salt extrusion. *Journal of the Geological Society, London*, 167, 155-170.
- ALAVI, M., 1996, Tectonostratigraphic synthesis and structural style of the alborz mountain system in Northern Iran *Journal of Geodynamics*, 21, 1-33.
- ALLEN, M. B., GHASSEMI, M. R., SHAHRABI, M., & QORASHI M., 2003. Accommodation of late Cenozoic oblique shortening in the Alborz range, northern Iran. *Journal of Structural Geology*, 25, 659-672.
- AMINI, B. & RASHID, H. 2005. *Garmsar geological map, 1:100 000 scale*. Geological Survey of Iran, Tehran.
- BAIKPOUR, S., ZULAUF, G., DEHGHANI M. & BAHROUDI, A., 2010, InSAR maps and time series observations of surface displacements of rock salt extruded near Garmsar, northern Iran, *Journal of the Geological Society, London*, 167, 171-181.
- BRUTHANS, J., ASADI, N., FILIPPI, M., WILHELM, Z., & ZARE, M., 2007, A study of erosion rates on salt diapir surfaces in the Zagros Mountains, SE Iran. *Environmental Geology*, 53, 1079–1089.
- FIELDING, E. J., BLOM, R. G. & GOLDSTEIN, R. M. 1998. Rapid subsidence over oil fields measured by SAR interferometry. *Geophysical Research Letters*, 25, 3215-3218.
- GABRIEL, A. K., GOLDSTEIN, R. M. & ZEBKER, H. A. 1989. Mapping small elevation changes over large areas: Differential radar interferometry. *Journal of Geophysical Research*, 94, 9183-9191.
- GUEST, B., GUEST, A., & AXEN, G., 2007. Late Tertiary tectonic evolution of northern Iran: A case for simple crustal folding, *Global and Planetary Change*, 58, 435-453.
- HUDEC, M.R., & JACKSON, M.P.A., 2007. Terra Infirma: understanding salt tectonics. *Earth Science Reviews*, 82, 1–28.
- JACKSON, J. & MCKENZIE, D., 1988, The relationship between plate motions and seismic moment tensors, and the rates of active deformation in the Mediterranean and Middle East, *Geophysical Journal* 93, 45-73.

- MASSON, F.; SEDIGHI, M.; HINDERER, J.; BAYER, R.; NILFOROUSHAN, F.; LUCK, J.-M.; VERNANT, P.; CHÉRY, J. 2002. Present-day Surface Deformation and Vertical Motion In The Central Alborz (iran) From GPS and Absolute Gravity Measurements. EGS XXVII General Assembly, Nice, 21-26 April 2002, abstract #455.
- MASSON, F., CHÉRY, J., HATZFELD, D., MARTINOD, J., VERNANT, P., TAVAKOLL, F. & GHAFORY-ASHTIANI, M. 2005, Seismic versus aseismic deformation in Iran inferred from earthquakes and geodetic data. *Geophysical Journal International*, 160, 217-226.
- MASSONNET, D. & FEIGL, K.L. 1998. Radar interferometry and its application to changes in the Earth's surface. *Reviews of Geophysics*, 36, 441 - 500.
- PLATT, J. P., 1986. Dynamics of orogenic wedges and the uplift of high-pressure metamorphic rocks. *Geological Society of America Bulletin*, 97: 1037 - 1053.
- RITZ, J.-F., NAZARI, H., GHASSEMI, A., SALAMATI, R., SHAFEI, A., SOLAYMANI, S., & VERNANT, P., 2006. Active transtension inside central Alborz: A new insight into northern Iran–southern Caspian geodynamics. *Geology*, 34; 477-480.
- SLUNGA, R.S., 1991: The Baltic Shield earthquakes. *Tectonophysics*, 189, 323–331.
- TALBOT, C. J. & JARVIS, R. J. 1984. Age, budget and dynamics of an active salt extrusion in Iran. *Journal of Structural Geology*, 6, 521-533.
- VERNANT, PH., NILFOROUSHAN, F., CHÉRY., J BAYER, R., DJAMOUR, Y. MASSON, F., NANKALI, H., RITZ, J. –F., SEDIGHI, M., & TAVAKOLI, F. 2004. Deciphering oblique shortening of central Alborz in Iran using geodetic data. *Earth and Planetary Science Letters*, 223 , 177-185.
- VERNANT, P., NILFOROUSHAN, F., HATZFELD, D., ABBASSI, M. R., VIGNY, C. & MASSON, F. 2004b. Present-day crustal deformation and plate kinematics in the Middle East constrained by GPS measurements in Iran and northern Oman. *Geophysical Journal International*, 157, 381 – 398.
- ZANCHI, A., BERRA, F., MASSIMO MATTEI, M., GHASSEMI, M.R., & SABOURI, J., 2006. Inversion tectonics in central Alborz, Iran. *Journal of Structural Geology*, 28, 2023-2037.
- ZEBKER, H. A. & GOLDSTEIN, R. M. 1986. Topographic Mapping from Interferometric Synthetic Aperture Radar Observations. *Journal of Geophysical Research*, 91, B5, 4993-4999.
- ZHENHONG, L., FIELDING, E.J., CROSS, P., & MULLER, J-P., 2006, Interferometric synthetic aperture radar atmospheric correction: Medium Resolution Imaging Spectrometer and Advanced Synthetic Aperture Radar integration, *Geophysical Research Letters*, 33, L06816, doi:10.1029/2005GL025299, 2006.

#	DATE	ORIGIN TIME	LAT N	LONG E	DEPTH	MN	NO	Az.GAP	DMIN	RMS
<u>ERH</u>										
1	50105	05:16:21.23	35.46317	52.04233	17.67	1.4	5	136 12.7	.00	.0 .0
2	50301	00:17:19.26	35.24967	52.33900	25.65	1.3	8	144 45.8	.04	.2 1.1
3	50301	00:35:59.03	35.45750	51.81250	15.00	2.1	12	86 23.9	.15	.6 2.3
4	50302	05:10:59.66	35.25517	52.35400	10.23	2.5	7	105 46.2	.07	.5 1.8
5	50408	18:23:09.62	35.17533	51.90933	9.74	1.1	5	164 26.0	.01	.1 .1
6	50414	07:14:45.80	35.15850	52.24033	9.28	2.1	7	172 50.2	.03	.3 .7
7	50428	16:12:53.97	35.35067	52.27500	19.00	1.8	8	145 33.4	.08	.7 2.5
8	50428	17:33:48.00	35.24233	52.17017	21.00	1.7	8	155 39.2	.04	.3 1.3
9	50605	09:04:36.94	35.48517	52.28667	10.96	1.3	6	155 25.2	.22	2.3 4.4
10	50626	08:02:05.30	35.43217	51.95450	15.00	1.3	5	131 17.6	.16	2.6 4.9
11	50922	23:31:44.34	35.30717	52.02517	15.00	1.9	8	157 30.0	.07	.5 2.3
12	51018	12:28:36.36	35.39583	52.24267	21.09	1.5	7	167 27.7	.24	2.3 4.9
13	51108	03:10:22.70	35.48450	51.88800	10.60	2.2	7	144 16.6	.14	1.1 2.0
14	51110	22:17:01.40	35.41400	52.39767	8.85	1.7	7	135 37.8	.06	.5 1.4
15	51203	13:33:43.45	35.33583	52.44633	20.67	2.1	9	150 43.9	.11	.7 3.0
16	51207	03:23:43.50	35.40367	52.00867	15.00	1.6	8	157 19.4	.17	2.0 4.3
17	51220	20:21:16.88	35.43267	51.93600	12.25	1.7	8	135 18.3	.19	1.1 3.2
18	60206	00:31:27.69	35.39567	52.47783	9.55	.00	12	145 37.0	.18	.7 2.0
19	50208	18:30:22.74	35.23200	52.15533	22.86	2.2	8	186 39.9	.35	2.6 7.4
20	50208	21:50:12.40	35.27833	52.28900	15.00	2.6	6	192 40.5	.33	3.9 26.9

Table 2. List of reliably located events from Iranian Seismological Institute Earthquakes Bulletin for 30-month epoch from 19.08.2003 to 13.02.2006 between latitudes 34.90° and 35.50° and longitudes 51.34° and 52.53°. The events listed as 19 and 20 are less well located than the others.

Analogue and geophysical modeling of the
Garmsar Salt Nappe, Iran: constraints on the
evolution of the Alborz Mountains

Analogue and geophysical modelling of the Garmsar salt nappe, Iran: constraints on the evolution of the Alborz Mountains.

Shahram Baikpour ⁽¹⁾ Gernold Zulauf ⁽¹⁾ Iraj Abdolahifard ⁽²⁾ Gholamreza Peyrovian ⁽²⁾
Carlo Dietl ⁽¹⁾

⁽¹⁾ Department of Geology and Palaeontology, Goethe Universität, Frankfurt a.M., Germany.

⁽²⁾ Department of Geophysics, National Iranian Oil Company (NIOC), Tehran, Iran.

Abstract

The Alborz Mountains are forming a ~100 km wide east-west trending orogenic belt that stretches 2000 m across northern Iran south of the Caspian Sea. The Alborz Mountains consist of salt-bearing Neogene sediments which are folded and cut by faults. Global Positioning System (GPS) studies indicate N-S directed shortening across the Alborz range which is accommodated by right and left-lateral strike-slip along ESE-WNW and ENE-WSW trending faults, respectively. A 20 km x 10 km x 03 km sheet of salt extruded over the central plateau of Iran arising at the front of the advancing Alborz Mountains. The extruded salt forms the Eyvanekey plateau between Eyvanekey and Garmsar which is now known as the Garmsar salt nappe.

To get more insights in the evolution of the Garmsar salt nappe, analogue modeling has been carried out using PDMS as salt analogue and sand as analogue for the brittle overburden. The structures produced consist of bivergent folds and thrusts which were formed while the salt analogue PDMS was rising up. The modeling results are compatible with our interpretation that the deformation front of the Alborz Mountains advanced SSW when overriding a salt sequence in the Garmsar area.

Depth estimation by Euler deconvolution of gravity and magnetic data indicate that salt was extruded from depths less than 2000 m.

Key words: Alborz, Garmsar, analogue modeling, rock salt

Introduction

The Alborz Mountains Range (Fig.1) results from different tectonic events which occurred during different orogenic cycles: (1) the Late Triassic (Cimmerian) collision of the Iranian block and Eurasia, and (2) the present day intra-plate deformation related to the convergence between the Arabian and the Eurasian plates (*Zanchi et al 2006*).

The central part of the Alborz Mountain Range (between longitudes 50°E and 54°E) shows a map-scale wedge shape which is related to folds and faults trending NW-SE in the western Alborz and NE-SW in the eastern Alborz (Fig.1). A recent Global Positioning System (GPS) study has shown that N-S shortening across the Alborz occurs at 5 ± 2 mm/yr and that left-lateral shear across the overall belt occurs at a rate of 4 ± 2 mm/yr (*Vernant et al., 2004*). Seismological data recorded in the Alborz Mountains and around the South Caspian Basin indicate the South Caspian Basin to move NW with a maximum velocity of 5–6 mm/yr (*Jackson et al., 2002*).

The right-lateral ESE-WNW trending strike-slip faults are related to Miocene N-S directed shortening (*Allen et al., 2003*). Dextral transpression is also suggested by the en-echelon arrangement of the main fold trains that consist of large ENE-WSW trending open anticlines which are trending oblique to the main faults.

Some salt in the Garmsar basin could still be at place beneath the Mesozoic rocks which are forming the nappes of the Alborz Mountains. Other salt strata became mobile and extruded to the surface in form of small diapirs along faults in the foothills without significant lateral spreading over the surface (*Safaei, 2001*). However, it is likely that most of the salt overridden by the southward advancing Alborz deformation front was expelled over recent sediments of the great Kavir to the south and west (Figs. 2 and 3 A). This salt is now present as the huge sheet of allochthonous salt that forms what we will call here the Eyvanekey Plateau (Fig.3B). Smaller salt extrusions in the hills north of Garmsar indicate where the Alborz deformation front is offset ca. 9 km by the 130 km long dextral SW-NE trending Zirab-Garmsar fault (Fig. 5).

The aim of the present study is to reconstruct the development of tectonic structures in a wedge-shaped fold and thrust belt that is strongly controlled by mobile rock salt. Result of analogue modelling show how the extrusion of rock salt is related to an advancing mountain chain. To realize the relationship between surface and sub-surface structures geophysical data will be considered.

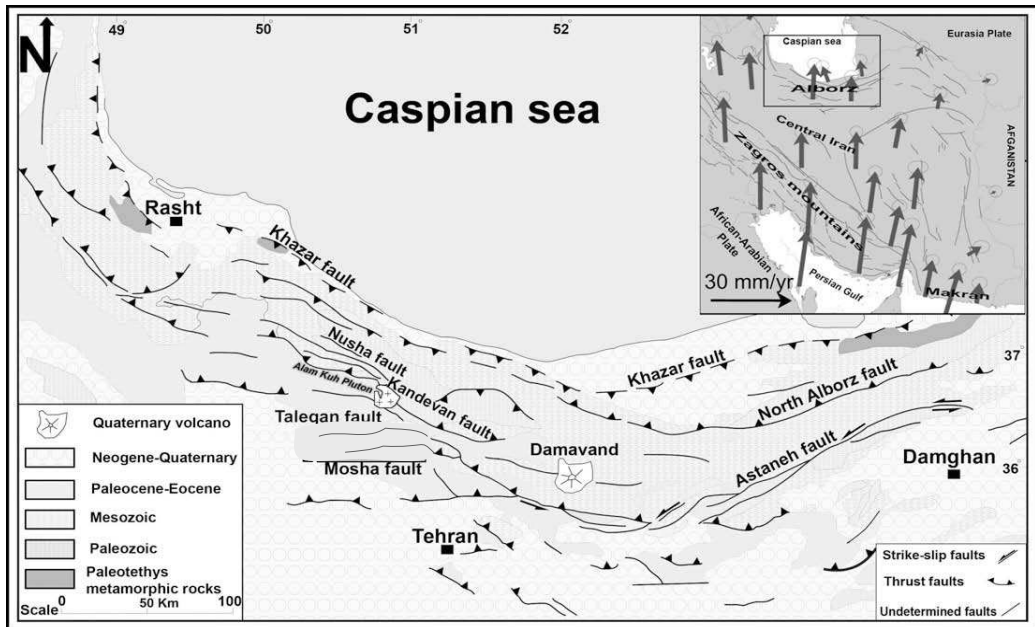


Fig. 1. Structural map of the Alborz Range (after Yassaghi and Madanipour's, 2008). The inset is a fault map of Iran (after Berberian and Yeats, 1999); arrows show GPS derived direction and velocities of plate movement in Iran relative to stable Eurasia (after Vernant et al., 2004).

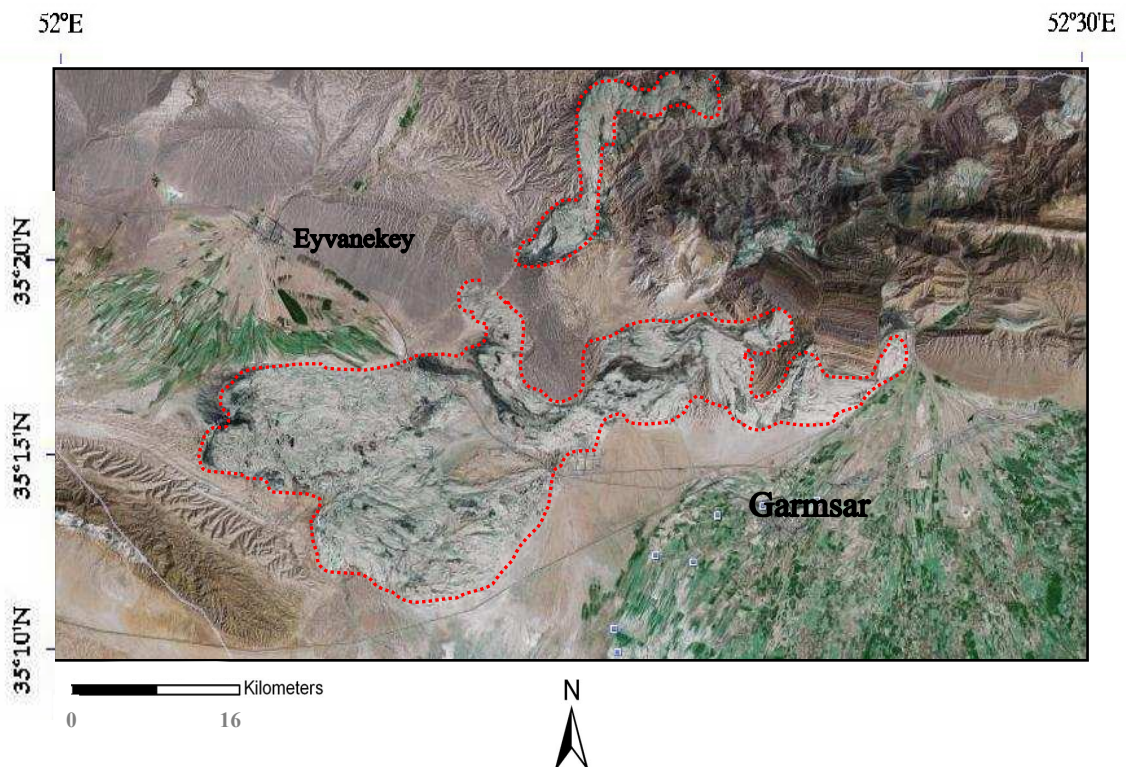


Fig. 2. Eyvanekey plateau and hills north of Garmsar. Major bodies of Tertiary salt are marked by red dotted line. Landsat satellite image, source: Google earth.

Geological setting

The Alborz Mountains represent a composite orogenic belt consisting of salt-bearing Neogen sediments that underwent shortening and uplift during the Cenozoic (*Alavi, 1996*). Sediments older than Miocene are not exposed at Garmsar. Exploration drilling may have touched the top of the Eocene sediments. The stratigraphy of the Great Kavir Basin is interpreted from outcrops rimming the Kavir. The lower part of the Eocene rocks consists of a variegated sequence made of sandstone, shale, marl and volcanics. The upper part consists of rock salt and anhydrite/gyprock which reflects regression (Fig 4 A&B). This evaporate sequence continues into the Oligocene (Fig. 4A). In the Eyvanekey-Garmsar hills, the upper Eocene and lower Oligocene evaporites cannot be distinguished. These hills consist of large diapiric bodies of salt and gyprock with inclusions of mafic volcanic rocks. Diapiric distortion and glacial extrusion have obscured stratigraphic order, and fossils are lacking. Major parts of the rock salt are white and fine grained with a tight subhorizontal mylonitic foliation (*Schleder & Urai, 2006*). Thin (<2 m) beds of red, yellow, brown or black salt provide useful strain markers. Blue halite crystals are found outside the entrance of a mine in the Garmsar hills.

The upper part of the Oligocene sequence, the Lower Red Formation, is made of gyprock, sandy shale and some volcanics. A similar sequence, referred to as Upper Red Formation, was deposited in the Miocene. Between the Lower and Upper Red Formation there is a sequence of limestone, marl, shale and sandstone which is called the Qom Formation (Fig 4 A&B). The age of the latter is upper Oligocene to lower Miocene.

The present surface of the Garmsar salt nappe is covered by several meters of barren residual insoluble soils after dissolution of the salt by rain (*Talbot, 2004*). Most of these soils are light green to pale brown gypsite with subordinate marl and calcareous marl (*Amini and Rashid, 2005*).

Almost all of the shortening was accommodated by movement along north and south dipping reverse faults, which are the main structures within the Alborz Mountains. The reverse faults are largely north dipping in the southern part of the range, and steeply south dipping in the northern part. From north to south these faults of the central area are the Khazar, North Alborz, Nusha, Kandevar, Mosha, and North Tehran faults (Fig.1; *Yassaghi and Madanipour's 2008*).

While the deformation front of the Alborz Mountains advanced towards SSW during the last 5 m.y, it was overriding a salt sequence in the Garmsar Basin. This movement of the

Alborz Mountain front squeezed most of the mobile evaporites to the SSW, where rock salt extruded in the Great Kavir forming the Garmsar salt nappe below the Eyvanekey Plateau (Fig. 2 and 3 A&B).

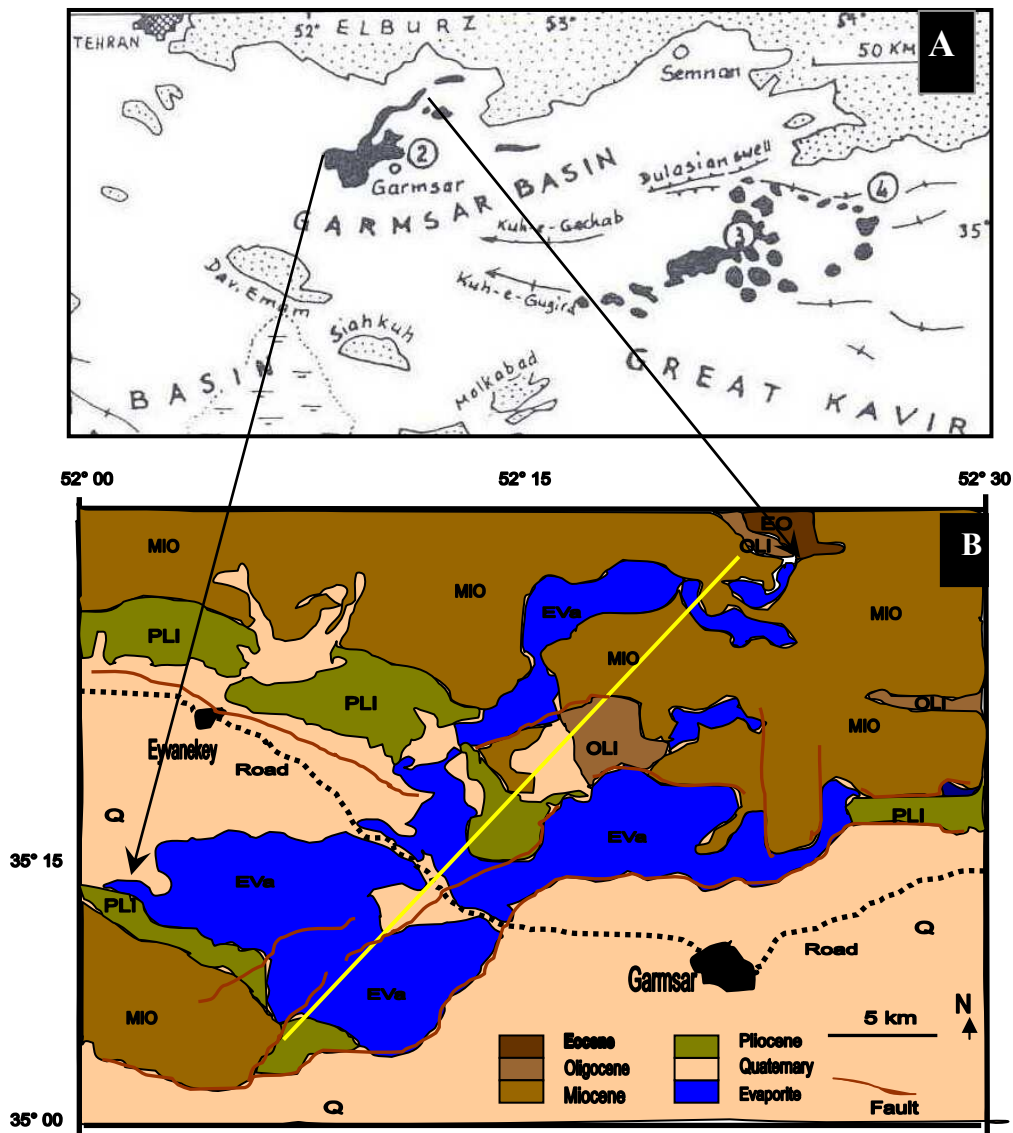


Fig. 3. Simplified geological setting of Garmsar hills, Eyvanekey plateau and surroundings. (A) Cenozoic evaporites at surface in the Garmsar and Great Kavir basins (Jackson et al. 1990). (B) Geological map of Garmsar hills and Eyvanekey plateau (after Amini & Rashid, 2005). The yellow line indicates cross section shown in Fig.4

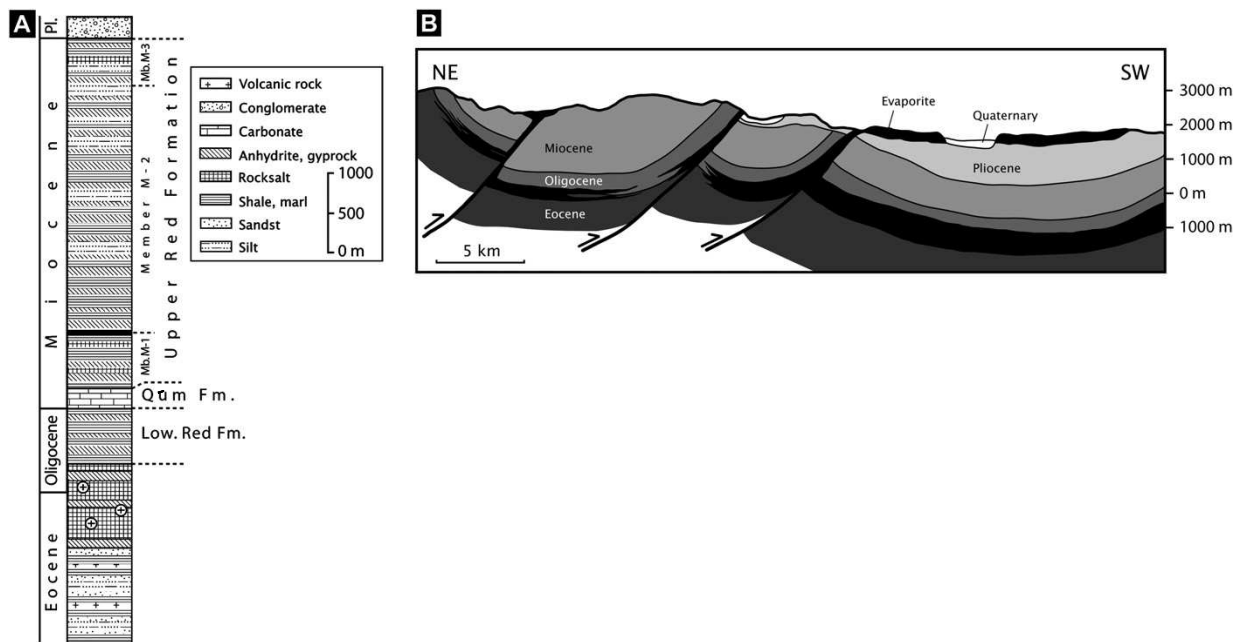


Fig. 4. (A) Stratigraphy of the rocks of the Garmsar basin (after Jackson et al., 1990). The Eocene to Oligocene rocksalt is the main source for the extrusions of Garmsar hills and Eyvanekey plateau. (B) Cross section through the Garmsar hills and Eyvanekey plateau (modified after Amini and Rashid, 2005). For location of cross section, see Fig. 3.B

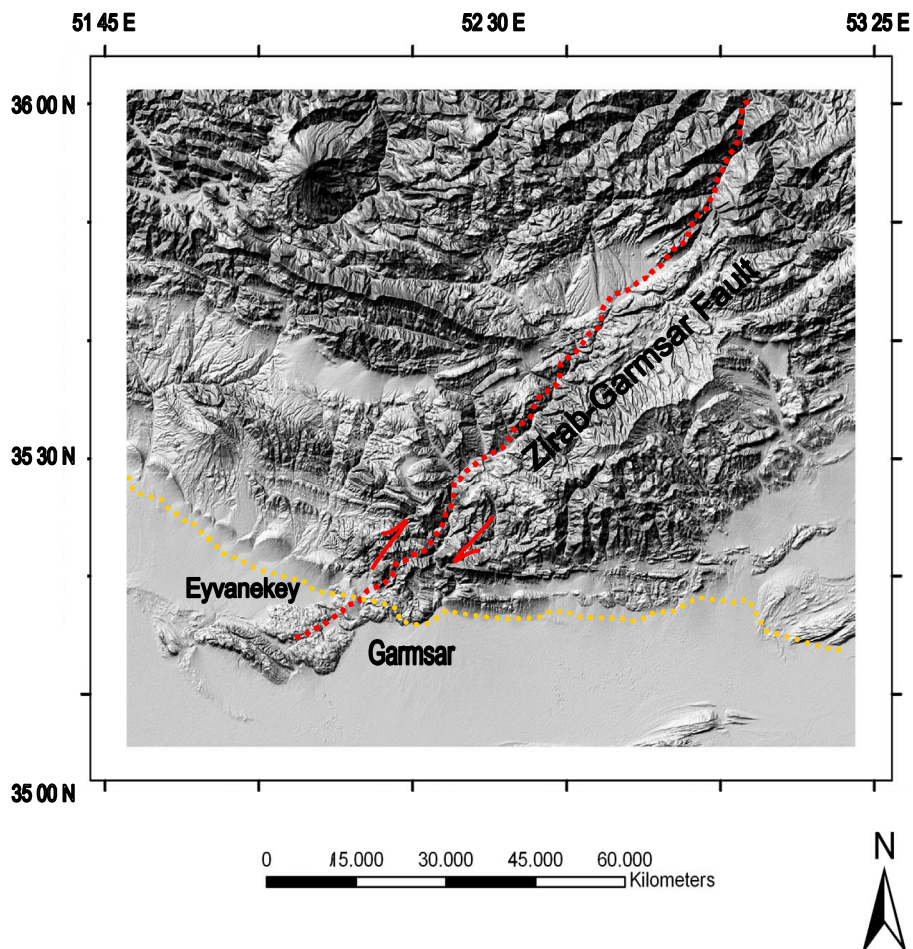


Fig. 5. Directionally shaded digital elevation model (DEM) of the study area in northern Iran showing the relation of the Eyvanekey plateau to the southern end of the Zirab– Garmsar fault (Red dotted line). The arrows relate to a key layer which shows a dextral offset of 9 km. The mountain front outline is shown by the fine yellow dotted line.

Methods

Analogue modelling

Model design and deformation apparatus

Analogue modelling is focusing on shortening of a brittle sedimentary overburden, with laterally varying thickness, resting on top of a weak viscous layer of rock salt. We used Polydimethylsiloxane (PDMS) to model the viscous rock salt. PDMS is a transparent Newtonian viscous fluid with a viscosity of 2.3×10^4 Pa s and a density of 0.964 g/cm^3 at a temperature of 20°C . Given that the flow of Garmsar rock salt was dominated by fluid-assisted solution-precipitation creep (Schléder and Urai, 2006), its rheology should have been almost linear viscous (Newtonian). Dry quartz sand with a grain size of 0.5 mm was used to simulate the brittle overburden. The sand has negligible cohesion, an angle of internal friction of ca. 30° , and a density of 1.4 g/cm^3 . Sand is a good analogue for most sedimentary rocks of the upper continental crust, which show Mohr-Coulomb behaviour (Byerlee, 1978; Weijermars *et al.*, 1993). The sand chosen exhibits Mohr-Coulomb behaviour by developing narrow ($<3 \text{ mm}$) shear zones which mimic fault zones.

The dimensions of the model are 34 cm x 25 cm x 2.5 cm. The map-scale chevron shape of the Alborz Mountains Range was initially simulated by casting a taper made of Styrofoam (Fig 6). The limbs of the taper were 20 cm long and the hinge began 13 cm wide (Figs. 6 and 8 A1& A2).

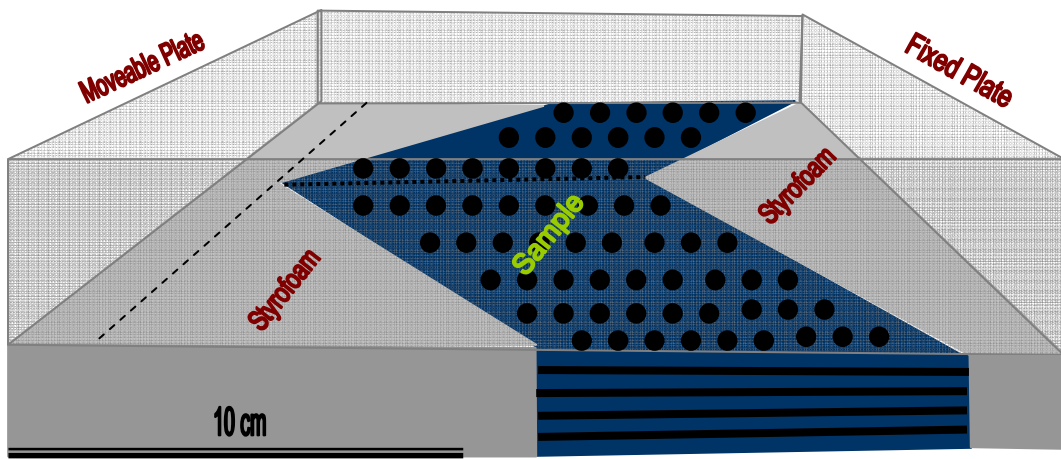


Fig.6. Schematic drawing of model before deformation; the V shape structure of the sample within the Styrofoam shows a view of Alborz mountain range before and during shortening. PDMS as rock salt analogue is present in the apex and inside of the V shaped body.

Dry sand was deposited to a depth of 2.5 cm around the Styrofoam taper and then removed. In the open space left by the Styrofoam, sand of different colour was deposited to simulate the stratigraphy of the rocks of the Alborz Range. In order to model the evolution of a salt sheet in front of the advancing Alborz Mountains, a tiny triangular layer (1 cm x 1 cm x 0.5 cm) of PDMS was placed below the apex of the taper. This PDMS layer was covered with sand.

The model was placed into a thermo-mechanical apparatus designed and built at the Department of Earth Sciences, Frankfurt University and shortened between two movable plates [x] and [y], the latter driven by a step motor via four spindles (Fig.7). In the present case only plate [x] was pushed. The model was subjected to 25 % horizontal shortening at a rate of 1mm/hr. For geometrical analysis, the deformed model was cut into slices (Figs. 9-11).

The model of the present study is scaled geometrically, kinematically, and dynamically to the Alborz region. Several models with the same composition were deformed to show the effect of shortening in the Alborz Mountain emphasizing the process of salt extrusion at the mountain front. Scaling was chosen that 1 cm in the experiment represents 10 km in nature, and 1 hour of the experiment represents 1m.y. in nature. The convergence velocity of 1mm/hr was scaled to represent the Arabia–Eurasia convergence velocity corresponding to about 2 cm/year in nature. Dynamic similarity is given because the analogue materials used have similar rheological properties like the natural counterparts (see above).

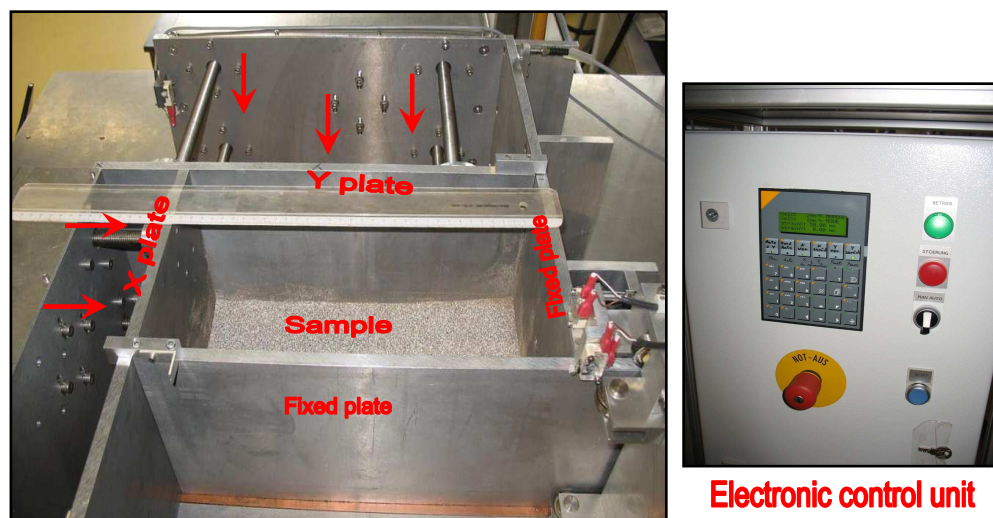


Fig.7. Deformation apparatus (A) and electronic control unit (B).

Basin reconstruction using geophysical data

In the present study we used processed gravity and magnetic data collected by the National Iranian Oil Company (NIOC). Their workload was ca. 4674 km² and a total of 13270 G/M stations had been acquired.

In order to estimate the depth of the Garmsar salt basin from magnetic and gravity data, we used the Euler deconvolution method implemented in the Geosoft software of the Geological Survey of Iran. The Euler deconvolution method is useful for rapid interpretation of potential field data, such as gravity and magnetic maps. It is particularly helpful when delineating contacts and providing rapid depth estimates. This technique can be treated as an automatic black box to estimate depths and is designed to provide computer-assisted analysis on large volumes of magnetic and gravity data. Euler's equation has been used widely for analyzing both gravity and magnetic anomalies.

The advantages of this technique over more conventional depth interpretation methods (i.e. characteristic curves, inverse curve matching, etc.) are that no particular geological model is assumed and the deconvolution can be directly applied and interpreted even when a particular model, such as prism or dyke, cannot properly represent the geological situation.

For an anomalous field caused by elementary sources, Euler's differential equation has the form

$$(x - x_0) \frac{\partial T}{\partial x} + (y - y_0) \frac{\partial T}{\partial y} + (z - z_0) \frac{\partial T}{\partial z} = -N(T - B) \quad (1)$$

where T is the amount of total field, B is the regional field strength, $(x_0; y_0; z_0)$ and (x, y, z) are the anomaly source coordinates and N is the source structural index, that represents the rate of decrease of the field strength with distance.

Results of analogue modelling

Shortening of the analogue model resulted in weak folding of the axial plane of the taper and led to folding and to oblique thrusting of the layers. At the front of the taper PDMS extruded to the surface of the model as is shown in top view (Figs. 8B1& B2 ,C1&C2). As the model is characterized by strong heterogeneous strain, the geometry of folds and thrusts can be revealed only in three dimensions. For this reason the deformed sample

was cut along both E-W and N-S trending sections. All of the reverse faults and thrusts are related to folding.

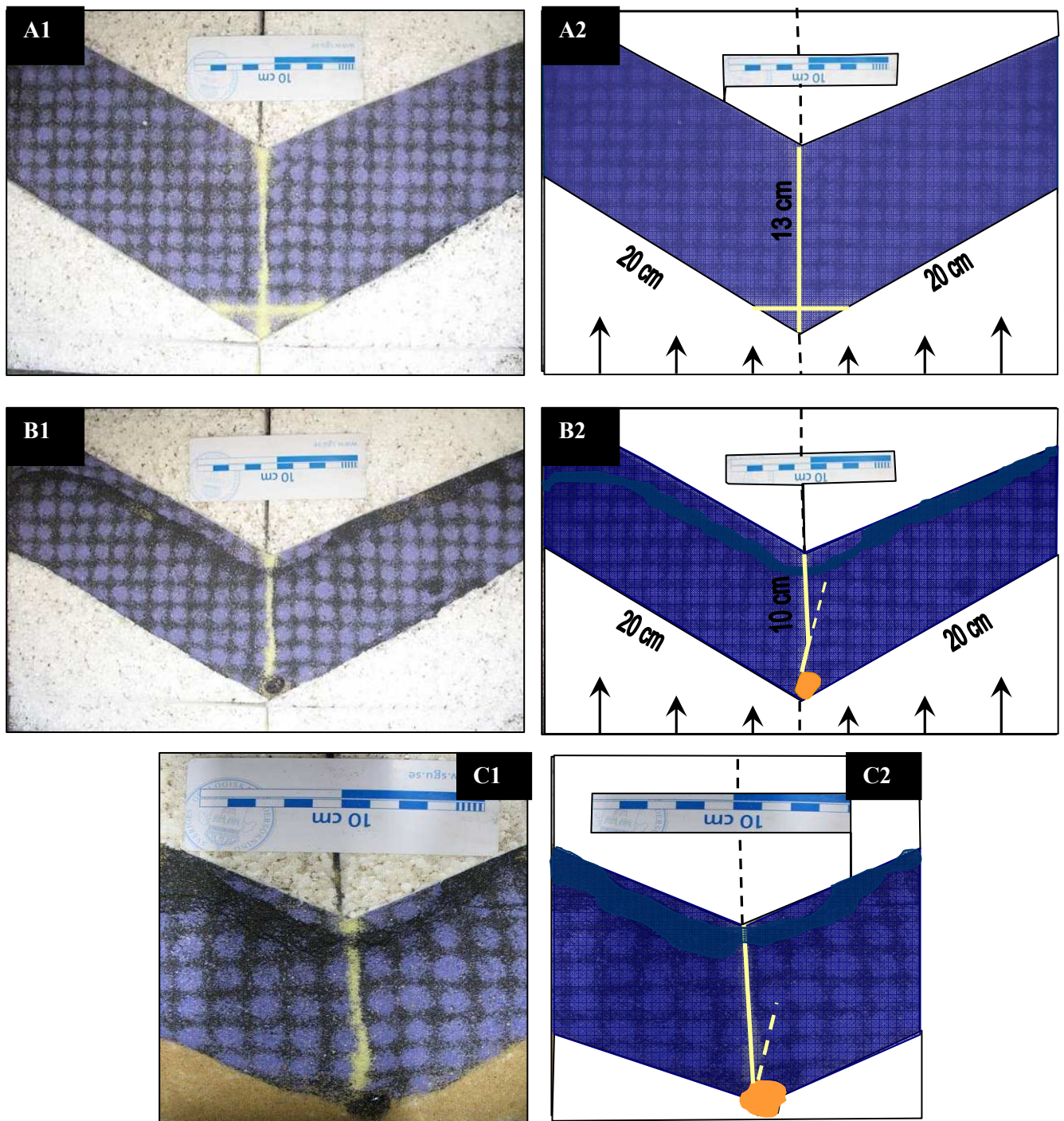


Fig.8. Undeformed (A1 and A2) and deformed (B1 and B2) analogue models. Black arrows show direction of shortening. Yellow dashed lines in B2 indicate the bent hinge of the taper which could correspond to the Zirab-Garmsar fault in the prototype. A small bulb of PDMS extruded at the apex of the taper simulating the Garmsar salt nappe. C1 and C2 are close-up views of B1 and B2, respectively.

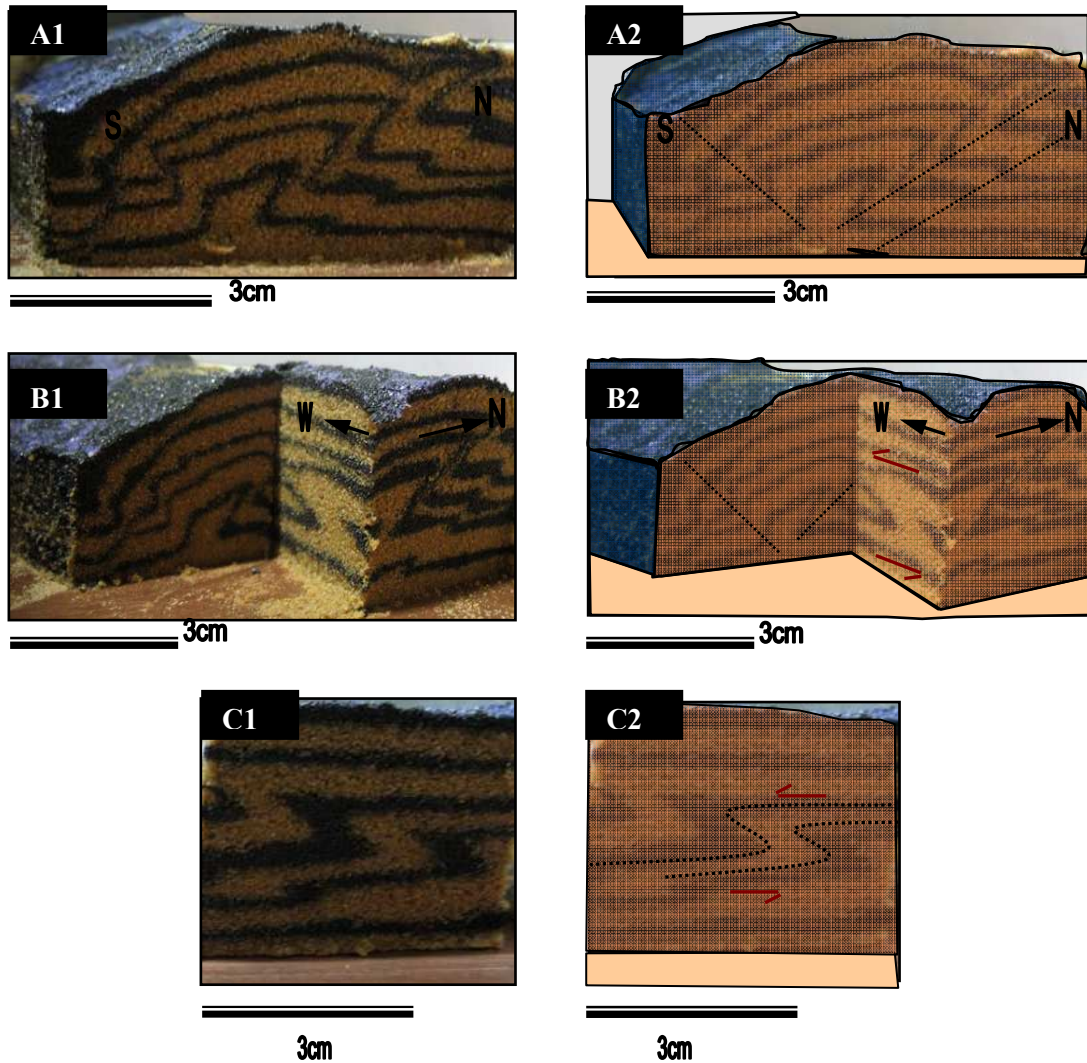


Fig .9. Sections of deformed limbs of chevrons. (A1, A2) 2D view after cutting across eastern limb of chevron. Initially horizontal black markers exhibit different patterns of reverse faults in the left (“S”) and right (“N”) sides of sample. Reverse faults and thrusts to the left (indicated by dotted black lines), are comparable to the Firouzkuh Fault in the S of Alborz Range. Reverse faults and thrusts to the right could be equivalents of the North Alborz and Khazar fault in the N of the Alborz Range. (B1, B2) Partial N-S and E-W sections of the deformed model show reverse faulting in both sections. In the E-W section the initially horizontal layers are deformed to an S-shape due to left-lateral movement corresponding to left-lateral faults in the eastern limb of the Alborz chevron. (C1, C2) are close-up views of S-shaped folds in E-W sections.

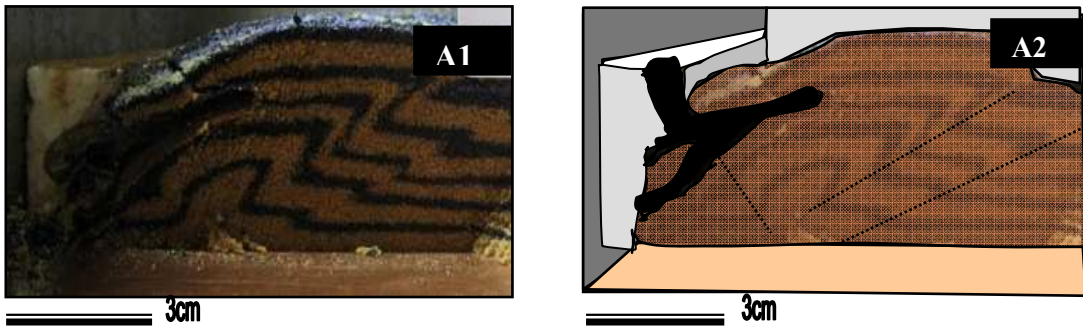


Fig .10. Section of deformed model cut along N-S axis of the taper. Black dotted lines show reverse faults and thrusts. The black mass consists of PDMS that extruded from the southern fault as shown in A2. A similar amount of PDMS is missing from A1 because it was dislodged during the cutting.

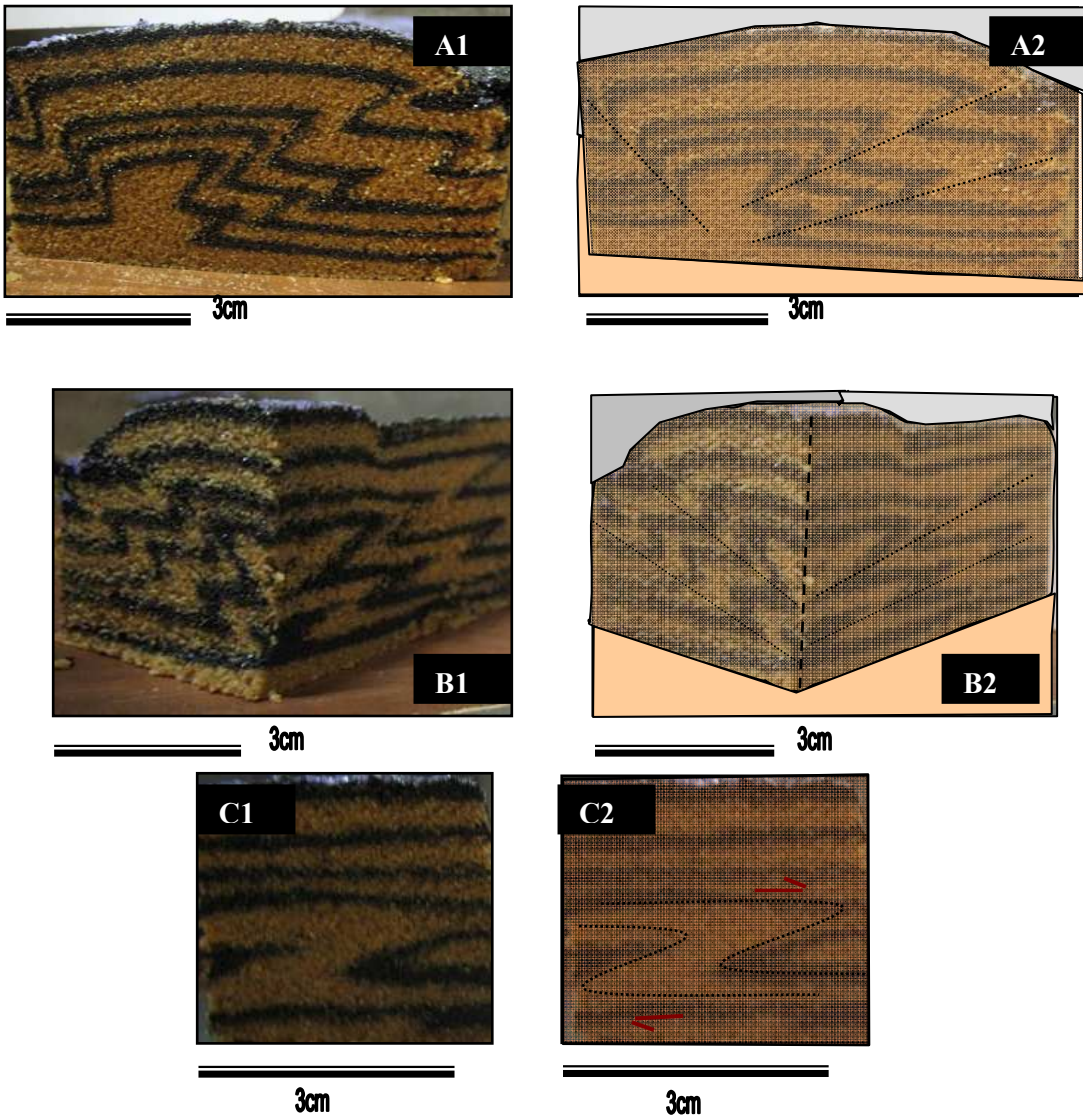


Fig.11. Sections of deformed sandy sample shown in Figure 7. (A1, A2) Western part of V shaped sample. The folded layers show geometrical differences in the S and N. There are two kinds of faults which are comparable to those shown in Fig.16. Reverse faults and thrusts could form equivalents of the North Tehran Fault, the North Alborz fault and the Khazar Fault. (B1,

B2) 3D view showing equal reverse faults both in N-S and E-W sections (C1, C2) Close-up views of sections trending E-W showing Z shaped fold.

Results of Geophysical modelling

The Bouguer Anomaly Gravity map reflects the relative density distribution of rocks below the Earth's surface in and around the Garmsar salt nappe (Fig. 12). Similarly, the magnetic anomaly map presents the magnetic properties of the rocks in the same area (Fig. 13).

The colours of the gravity map range from red through yellow and green to blue. Red colours represent areas of the Earth's crust which contain rocks of high density. The blue colours show those areas consisting of rocks with a lower density.

The densities of rocks are measured in g/cm^3 , with the the crust of the earth having an average background value of ca. 2.67 g/cm^3 . Sedimentary deposits like sand and evaporites are generally less dense than igneous rocks like granite and basalt. Within the area of interest it is primarily the distribution of different rock types resulting in highs and lows shown on Fig. 12.

Igneous rocks generally have very high magnetic strengths compared to sedimentary rocks. Evaporitic rocks (like the Garmsar salt nappe), on the other hand, have very low magnetic strengths. The warm colors in Fig. 13 indicate the more magnetic rocks and the cold colors indicate rocks with lower magnetic strengths.

As shown in figures (12 & 13) and gravity and magnetic anomaly maps, red disks indicate anomalies situated at depth $> 5000 \text{ m}$. Green and yellow disks show anomalies at depths of 2000 to 3000 m , and blue circles disks indicate anomalies $< 2000 \text{ m}$. White line indicates outline of Garmsar salt nappe that is also shown on geological map at the left-hand lower corner of the figure

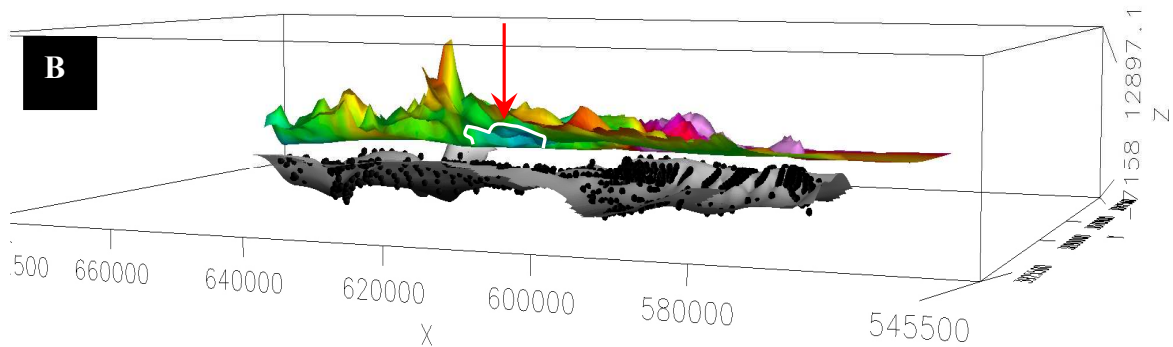
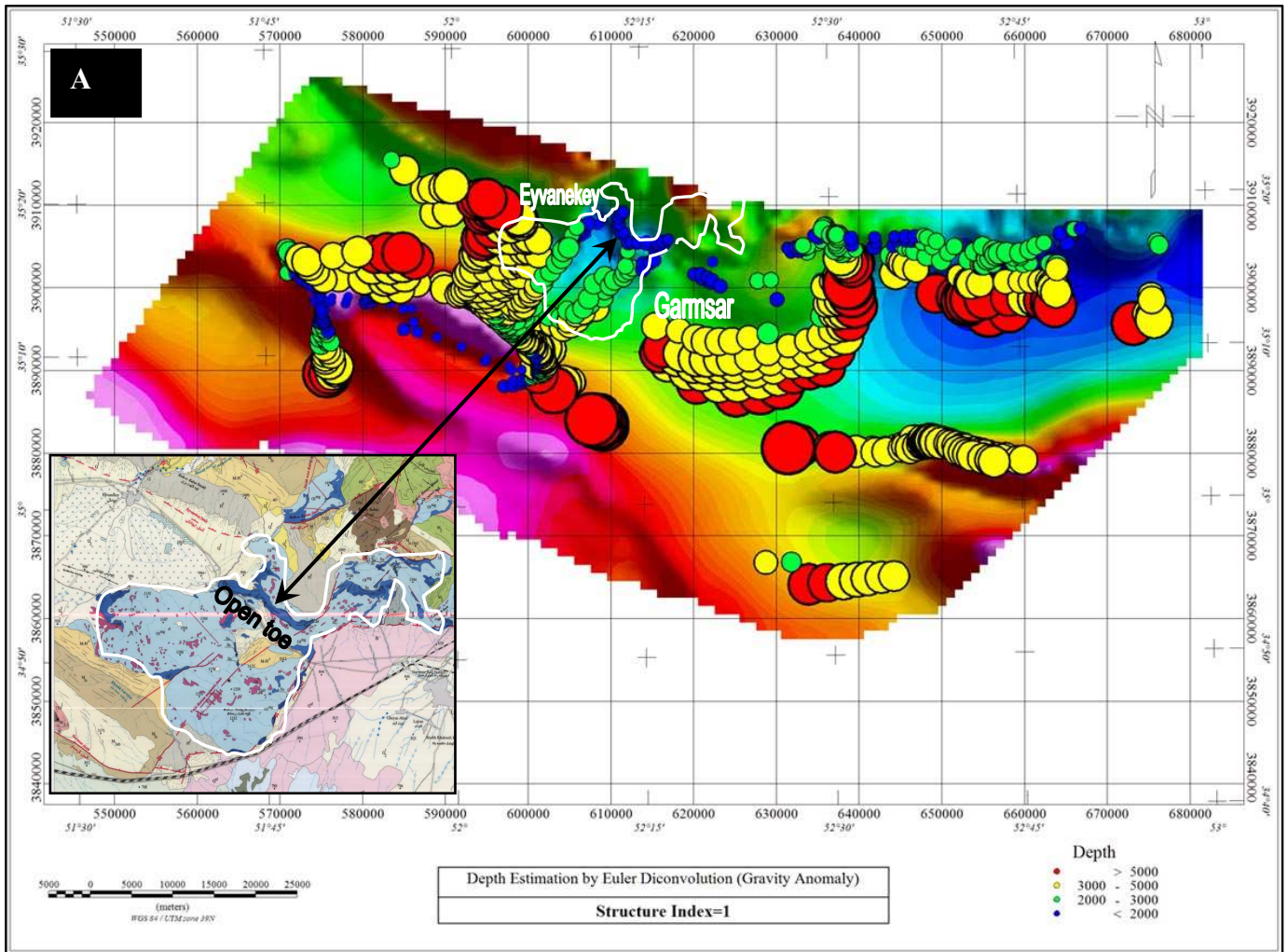


Fig. 12. (A) Iranian national Bouguer Anomaly Gravity map of the Garmsar area superposed by depth-estimates (marked with disks with sizes proportional to the depth) from the Euler deconvolution algorithm. Steep density gradient > 5000 m is shown by red circles; green and yellow disks represent anomalies at depths of 2000 to 3000 m, and blue disks indicate contacts < 2000 m. White line indicates outline of Garmsar salt nappe that is also shown on geological map at the left-hand lower corner of the figure. (B) Oblique view of 3D block diagram (x,y,z) of depth estimates. Top surface reflects topography with map colours. Grey surface indicates steepest density gradient at depth and black dots locate local density anomalies. Outline of Garmsar salt nappe is shown by white line.

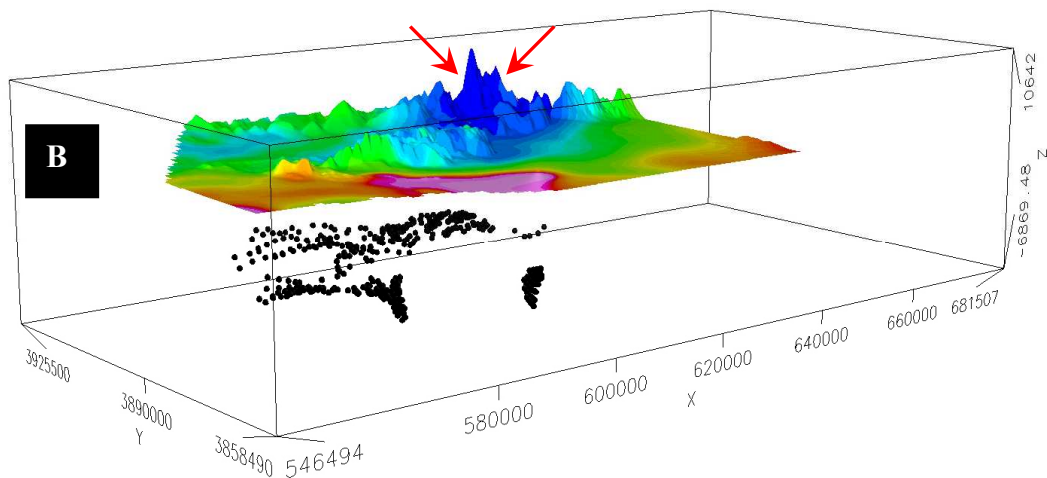
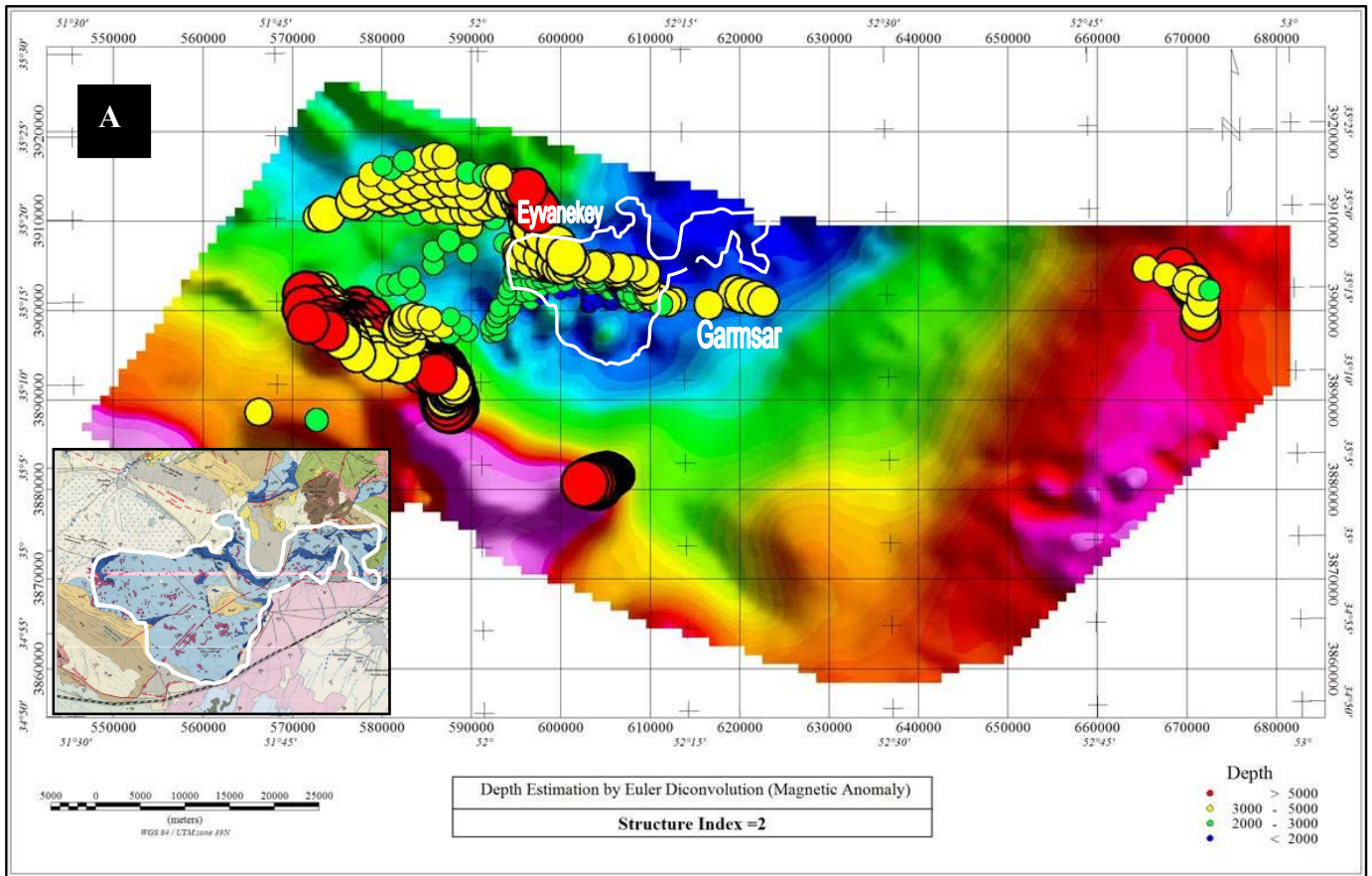


Fig. 13. (A) Depth-estimation (marked with disks with sizes proportional to the depth) based on Euler deconvolution algorithm using magnetic filed map. Red disks indicate anomalies situated at depth > 5000 m. Green and yellow disks show anomalies at depths of 2000 to 3000 m, and blue circles disks indicate anomalies deeper 2000 m. White line indicates outline of Garmsar salt nappe that is also shown on geological map at the left-hand lower corner of the figure. (B) Oblique view of 3D block diagram (x, y, z) of depth estimates. Top surface reflects topography with map colours. Black dots locate magnetic point anomalies at depth. Outline of Garmsar salt nappe is shown by white line.

Discussion

Interpretation of the experimental results and application to natural examples

Our scaled analogue model was focusing on the extrusion of salt from under the advancing deformation front of the Alborz Mountains. The modelling has produced bivergent folds and thrusts which can be correlated with the structural inventory of the Alborz range. The recent kinematics of the Alborz is controlled by N-S shortening (Fig.15) between Arabia and Eurasia and by westward movement of the south Caspian domain relative to Iran. N-S shortening is compatible with dextral slip along the NW trending faults of the western Alborz and sinistral slip along the NE trending faults of the eastern Alborz (Fig. 14). This slip system was active in the analogue model, particularly at the interface between Styrofoam taper and the PDMS/sand model. The sections of deformed limbs of chevrons in the analogue models (Figs. 9 - 11) have revealed N and S dipping reverse faults and thrusts which might correspond with folds and faults of the western Alborz. North dipping reverse faults formed in the south of the model (Fig. 11) have also been found in the southwestern part of the Alborz range as the North Tehran fault (Fig. 16). Moreover steep reverse faults of the model are comparable with the Firouzkuh fault in the southeastern part of the Alborz Range (Figs. 9 and 16).

The analogue model also shows two parallel faults in the northern part which can be related to the North Alborz fault and the Khazar Fault, both of which are located in the northern part of the Alborz range and in the southern part of the Caspian basin (Figs. 9, 10 and 16).

While the deformation front of the Alborz Mountains advanced SSW during the last 5 m.y. it overrode a salt sequence in the Garmsar basin.

Our model has shown a small amount of extruded PDMS which correlates with rock salt that extruded at the taper of the wedge-shaped Alborz range. In nature, the salt advanced SSW and extruded on top of the plateau as the Garmsar salt nappe (Fig. 8). Some salt may remain at place beneath the deformation front of the Alborz and its foreland and several small diapirs are rising up along faults in the foothills (*Safaei, 2001*). Extrusion of salt in the hills north of Garmsar is controlled by faulting, as the Alborz deformation front is offset by ca. 9 km along the 130 km long SW-NE trending Zirab-Garmsar strike-slip fault (Fig. 5). This fault has shown in the model by the dashed yellow line (Fig. 8B&C).

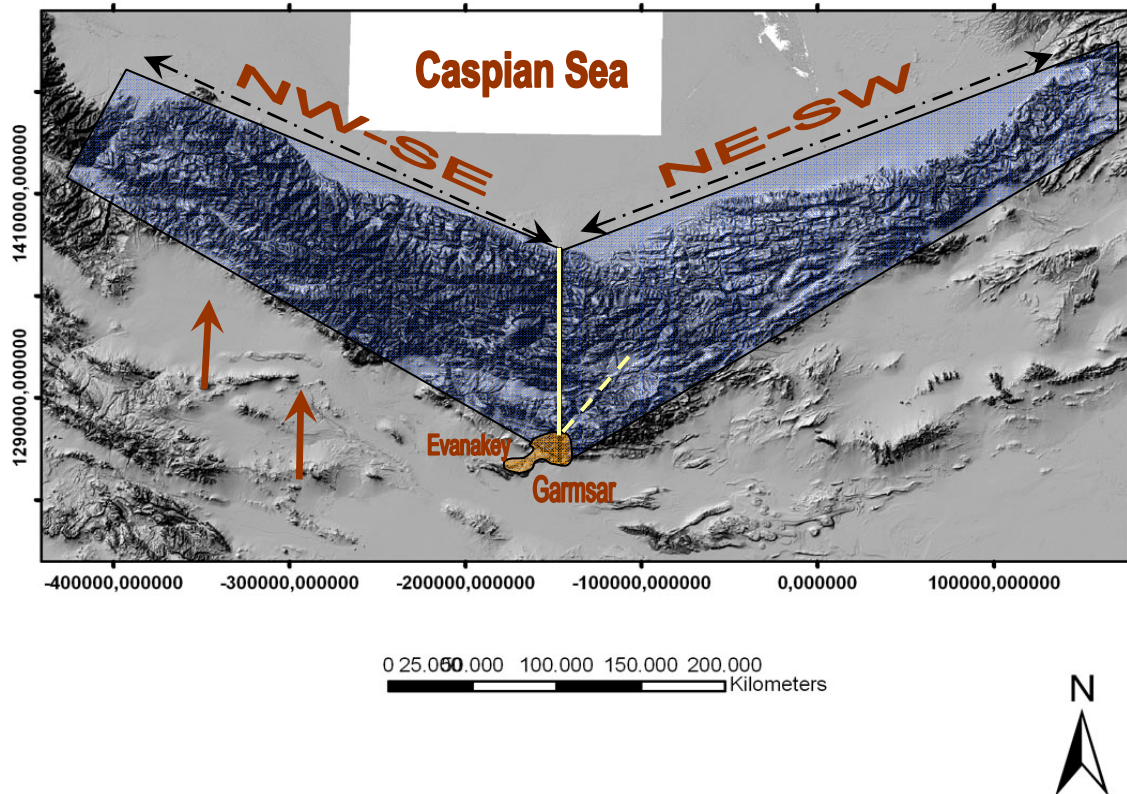


Fig. 14. Shaded Digital Elevation Model (DEM) of central Alborz Range. NW-SE limb is wider than NE-SW limb. Solid yellow line approximates the median line of the V. Dashed yellow line shows the Zirab-Garmsar fault. The Garmsar salt nappe extruded at the apex of the V, where the Zirab –Garmsar fault offsets the Alborz mountain front by about 9 km. A close up view of the Garmsar salt nappe and the southern termination of the Zirab-Garmsar fault is shown in Fig. 5

GPS data indicate N-S shortening across the Alborz to be twice as fast as the left-lateral shear along the belt (Fig. 15; *Vernant et al., 2004*). However the right-lateral strike-slip movements along ESE-WNW faults have been related to a N-S compression during the Miocene (*Allen et al., 2003*). Figure (11) shows a partial E-W profile across the western part of model in which Z shape in an initially horizontal black marker simulates a left-lateral movement along strike-slip faults in nature. The S shape structure in E-W direction in the model (Fig.9) shows a left-lateral movement. It is comparable with the left lateral movements along strike slip faults in eastern Alborz.

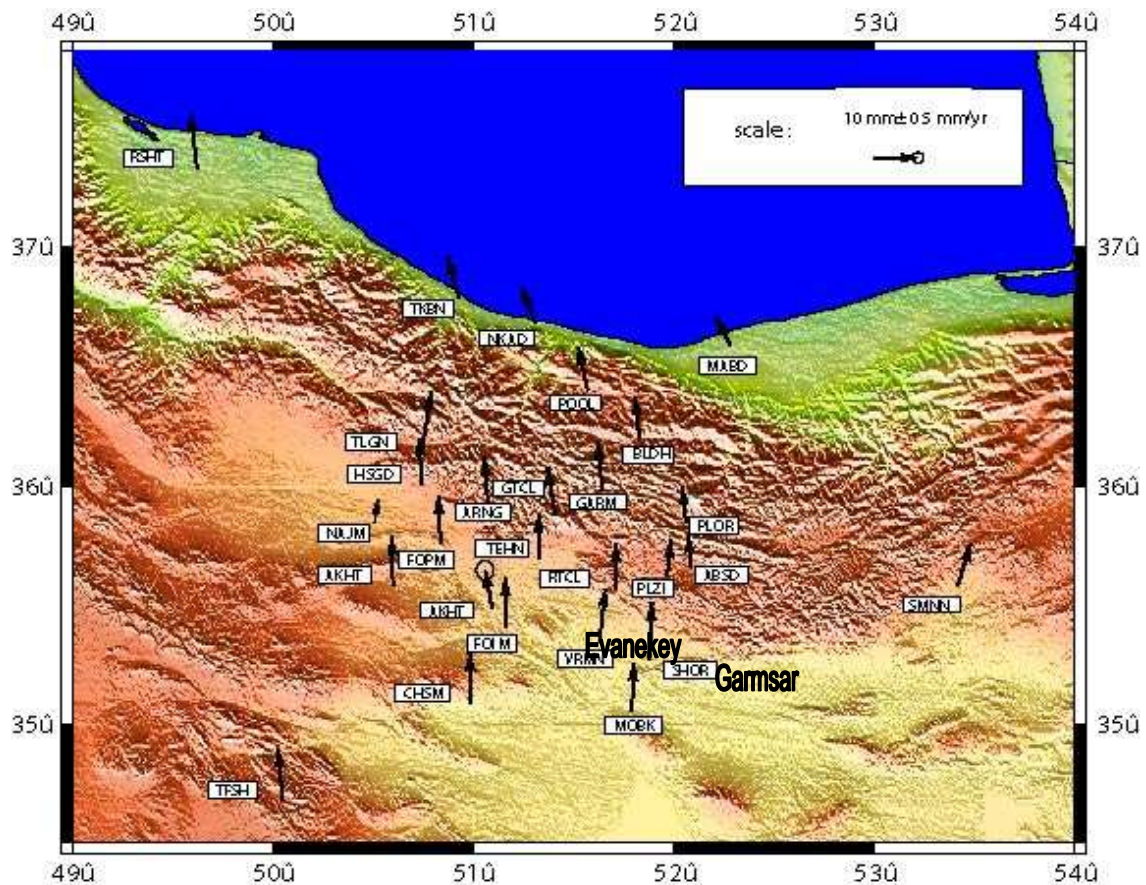


Fig.15 . Velocity field (black arrows) of Central Alborz based on recent GPS surveys (National cartography centre NCC); SHOR Station is located between Eyvanekey and Garmsar.

Interpretation of the Geophysical results and application to natural examples:

The Bouguer gravity anomaly characteristics in the study area show strong anomalies in the SW and weak anomalies in the NE (Fig.12). There are two uplifts in Bouguer gravity anomalies corresponding to the southern border of the work area, one of which is relatively strong. The strongest anomaly is at the furthest south of the work area. Anomaly values are less than in northern weak anomaly belt, forming several local gravity low (Fig.12).

There are negative anomalies in the N and NE of work area. Several local positive anomalies occur over relatively high anomalies toward south of the salt sheet of the Garmsar, which related to the convergence of a series of volcanic rocks trending SW, Relatively low anomalies in the open toe of the salt sheet and a vast anomaly east of salt sheet and north of the Garmsar town indicate a negative anomalies zone (Fig.12).

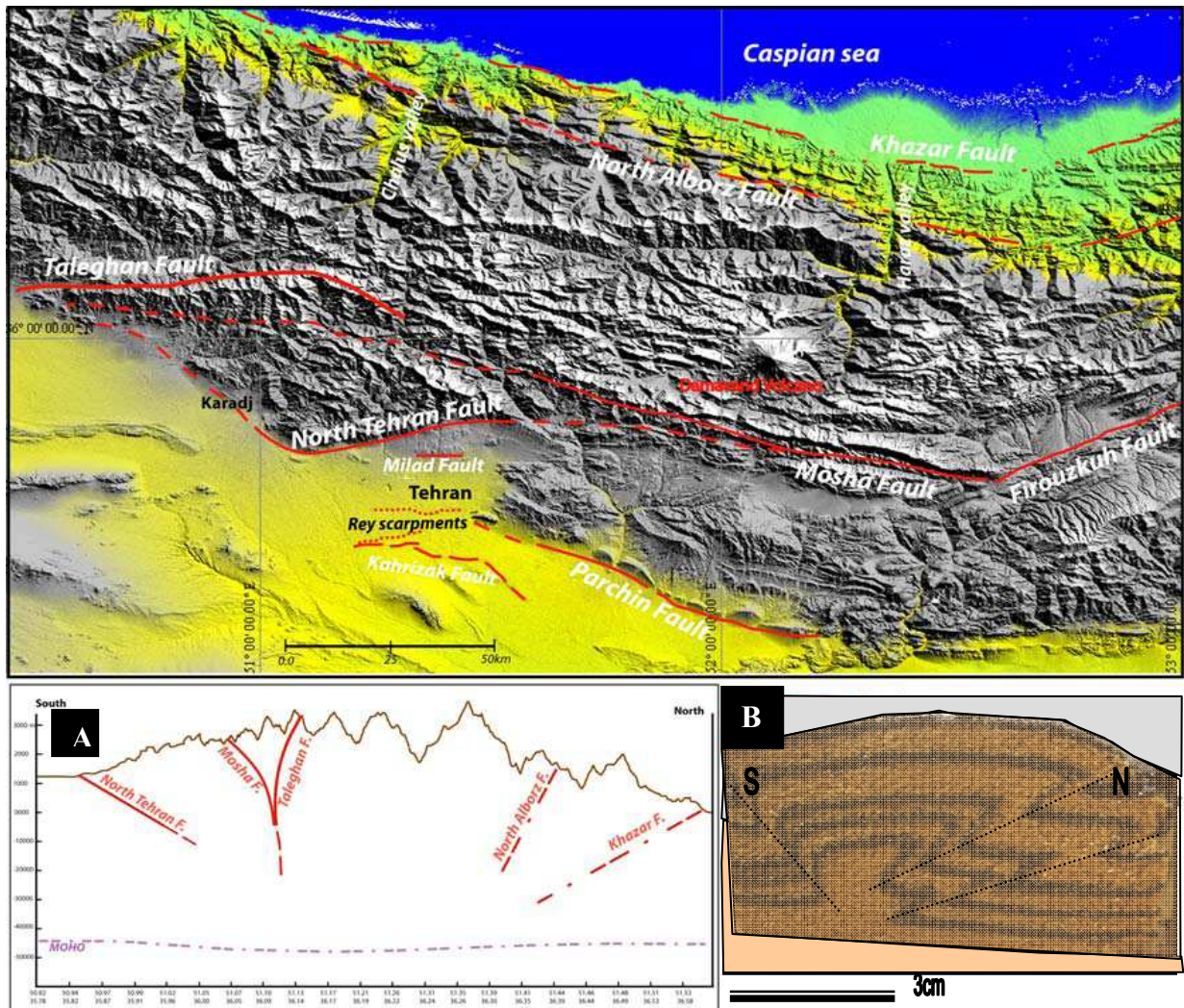


Fig.16. Fault map of central Alborz (after Nazari et al., 2007). (A) Cross section of western part of Alborz Range; fault pattern is comparable with that shown in section of the analogue model (B).

Anomaly characteristics present high in SW, low in NE and slightly lift in north of map, and main body of negative anomalies lies in the north with easting of work area, it is to say, the north part sunken while its south sides asymmetrically uplift. This basically represents the outline of salt sheet of work area.

In the study area, magnetic anomalies are divided into three zones, the latter trending E, SW and S, respectively. A positive magnetic anomaly in the south can be divided into 2 sub-zones trending south and west direction. A negative magnetic anomaly is presented in the north of study area. A weakly positive magnetic anomaly zone is located in the SE.

Variation of magnetic anomaly is mostly a reflection of igneous rocks, a synthetic reflection of burial depth and composition. The negative anomaly in the north of the work area represents a large depression with thick sedimentary segments and its edges become shallow gradually. Anomaly distribution along the strike of structures is a direct reflection of the distribution of igneous rocks.

After extracting residual magnetic anomalies (Fig.13), and analysis of the geological bodies causing the magnetic anomaly, we infer that the locally residual magnetic anomaly with a strong positive value is a response of volcanic rock.

Depth estimations using the gravity and magnetic fields suggest that the salt in the Garmsar salt nappe (Figs. 12 & 13) suggest that the salt extruded from a depth of 2000 m, The blue circles on Figure 12 correlated with a line of salt diapirs extruding in the low magnetic bodies (cold colors) on Figure 12 indicate that the salt of the Garmsar salt nappe with its very low magnetic strength are <2 km thick.

Conclusion

- Our scaled sand-box model shows that while the deformation front of the Alborz Mountains advanced SSW in the last ~5 M.y, it overrode a salt sheet in the Garmsar Basin. Our model has shown a small dimension of PDMS was evidenced as salt basin under the Alborz mountain front, it was affected by the Alborz Mountain front squeezing, also most of the salt has flowed toward the SSW so it extruded over the surface of the Great Kavir as the Garmsar Salt Nappe.
- Analogue models simulate the reverse faults and thrusts observed in the Alborz Range N of Garmsar including the folds and faults trending NW-SE in the western limb of the Alborz chevron and trending NE-SW in the eastern limb.
- The gravity anomaly characteristics in the study area show strong anomalies in the SW and weak anomalies in the NE. A striking body of negative anomalies lies in the N, indicate the N part sunken while its S sides asymmetrically uplift. This basically represents the outline of the salt sheet of the study area.
- In Garmsar area, magnetic anomalies are divided into three zones, the latter trending E, SW and S, respectively. A positive magnetic anomaly in the S can be divided into 2 sub-zones trending S and W direction. A negative magnetic anomaly is presented in the N of study area. A weakly positive magnetic anomaly zone is located in the SE.

- Depth-estimates from the Euler deconvolution algorithm applied to the gravity filed indicate that the salt on the surface rose from the depth of < 2000 m.

Acknowledgements

We thank the National Iranian Oil Company for supplying Geophysical data, and the Geological Survey of Iran GSI for supplying the hard- and software as well as logistical support when we prepared and analyzed the data. We also thank Hassan Kheirolahi and Arash Sebti(from GSI) for processing the Geophysical data.

We also thank laboratory staffs for advice during our modeling at the Department of Earth Science, University of Frankfurt. We also express our gratitude to Prof. Christopher Talbot, who has always taken the time to try and explain and resolve our problems by e-mail.

References

- Alavi, M., 1996. Tectonostratigraphic synthesis and structural style of the Alborz mountain system in northern Iran. *Journal of Geodynamics* 21, 1–33.
- Allen, M.B., Ghassemi, M.R., Shahrabi, M.Qorashi, M., 2003. Accommodation of late Cenozoic oblique shortening in the Alborz range, northern Iran. *Journal of Structural Geology* 25, 659–672.
- Amini, B., Rashid, H., 2005. Garmsar geological map 1:100000 in scale. Geological Survey of Iran, Tehran, Iran.
- Berberian, M., Yeats, R.S., 1999. Patterns of historical earthquake rupture in the Iranian plateau. *Bulletin of the Seismological Society of America* 89, 120–139.
- Byerlee, J. D., 1978, Friction of rocks: *Pageoph*, v. 116, p. 615–626.
- Jackson, M.P.A., Cornelius, R.R., Craig, C.H., Gansser, A., Stocklin, J., Talbot, C.J., 1990. Salt Diapirs of the Great Kavir, Central Iran. Geological Society of America, Boulder 177.
- Jackson, J., Priestley, K., Allen, M., Berberian, M., Active tectonics of the South caspian Basin, *Geophys. J. Int.*, 148, 214-245, 2002.
- Mandal, N. and Karmakar, S. 1989 Boudinage in homogeneous foliated rocks. *Tectonophysics* 170, 151 – 158.
- Nazari H., Ritz J-F., Salamati R., Solaymani S., Balescu S., Michelot J-L. Ghassemi A., Talebian M., Lamothe M. and Massault M. Paleoseismological analysis in Central Alborz, Iran 50th

Anniversary earthquake conference commemorating the 1957 Gobi-Altay earthquake (July-August 2007- Ulaanbaatar-Mongolia)

Safaei, H., 2001, Elastic diurnal movement of Masses of Tertiary salt extruded in north central Iran. *Journal of Sciences, Islamic Republic of Iran*. 12, No. 3, 241- 250.

Schleder, Z., Urai, J.L. 2006. Deformation and recrystallization mechanisms in mylonitic shear zones in naturally deformed extrusive Eocene-Oligocene rock salt from Eyvanekey plateau and Garmsarhills (central Iran). *Journal of Structural Geology*,1-15.

Talbot, C.J., Aftabi, P., 2004. Geology and models of salt extrusion at Qom Kuh, central Iran. *Journal of the Geological Society* 161, 32-334.

Vernant, P., Nilforoushan, F., Chery, J., Bayer, R., Djamour, Y., Masson, F., Nankali, H., Ritz, J.F., Sedighi, M., Tavakoli, F., Deciphering oblique shortening of central Alborz in Iran using geodetic data, *Earth and Planetary Science Letters*, 223, 177-185, 2004b. 6

Weijermars, R. 1997: *Principles of Rock Mechanics*. Alboran Science Publishing. 359p.

Yassaghi.A., Madanipou.,S., 2008. Influence of a transverse basement fault on along-strike variations in the geometry of an inverted normal fault: Case study of the Mosha Fault, Central Alborz Range, Iran. *Journal of Structural Geology* 30,1507-1519

Zanchi, A., Berra, F., Mattei, M., Ghassemi, M.R., Sabouri, J., 2006. Inversion tectonics in central Alborz, Iran. *Journal of Structural Geology* 28, 2023–2037.

Hazardous waste disposal in Iran: Results
from a pre-site study of the Garmsar Salt
basin

Hazardous waste disposal in Iran: Results from a pre-site study of the Garmsar salt basin

Shahram Baikpour⁽¹⁾ Gernold Zulauf⁽¹⁾ Iraj Abdolahifard⁽²⁾

⁽¹⁾ Geoscience Department, Goethe Universität, Frankfurt a.M., Germany

⁽²⁾ Department of Geophysics, National Iranian Oil Company (NIOC), Tehran, Iran.

Abstract

Solving the problem of waste is one of the central tasks of environmental protection. It is becoming increasingly difficult to find suitable sites that are acceptable to the public. Salt and salt formations have relevant properties to be utilizing as a repository for each kind of waste. The favourable properties make rock salt highly suitable as a host rock, in particular for nonradioactive and radioactive wastes.

Tehran and suburb as an industrial state require a waste reservoir. The Great Kavir, the largest salt desert in Iran, with more than 50 salt diapirs, is surrounding the eastern and southern part of the Tehran Province. The Qom and Garmsar basins are the nearest salt diapirs to the Tehran province, and there are suitable repositories for waste disposal.

Based on surface and subsurface data, the Garmsar salt diapir has been investigated as a case example for its suitability as a host and repository for various types of waste. The data used are based on field studies, interferometry, and geophysical investigations.

The results of this study suggest the deep bedded salt of the Garmsar Salt Basin to be an appropriate host for the deposition of industrial waste. Rock salt of surficial layers or domes, on the other hand, is not regarded as an appropriate candidate for waste disposal.

Key words: Garmsar Salt Nappe, hazardous waste disposal, rock salt

Introduction

The disposal of waste is increasingly important not only for completely developed countries but also for less developed countries like Iran where improvement of economy, energy, environment, and standards of living will lead to a significant increase in industrial and artificial waste. For this reason exploration of reservoirs for disposing the waste are required. Salt formations are considered as potential host rocks for waste disposal and thus could be the answer to the waste disposal problems in the Tehran district. Rock salt is nearly impermeable, does not include much brine and is deformed viscously even at low temperature of the upper crust. The viscous behavior of deforming rock salt suppresses the opening of natural and artificial fissures where liquids and gases could migrate and leak out.

Another advantage of salt formations for the storage of waste is the fact that the formations are not affected by environmental changes. Massive deep salt deposits are common and widespread in nature. Salt has been mined for hundreds of years, and the behaviour of the mined openings has been studied and documented extensively (see e.g. references in Wallner et al., 2007). In the present paper we evaluate the salt rocks of the Garmsar area for the deposition of waste.

Geological setting

The Alborz Mountains represent a composite orogenic belt consisting of salt-bearing Neogen sediments that underwent shortening and uplift during the Cenozoic (*Alavi, 1996*). Sediments older than Miocene are not exposed at Garmsar (Fig.1). Exploration drillings have touched the top of the Eocene sediments. The lower part of the Eocene rocks consists of a variegated sequence made of sandstone, shale, marl and volcanics. The upper part consists of rock salt and anhydrite/gyprock which reflects regression (Fig. 2 A.B). This evaporate sequence continues into the Oligocene (Fig. 2A). In the Eyvanekey-Garmsar hills, the upper Eocene and lower Oligocene evaporites cannot be distinguished. These hills consist of large diapiric bodies of salt and gyprock with inclusions of mafic volcanics. Major parts of the rock salt are white and fine grained with a tight subhorizontal mylonitic foliation (*Schleder & Urai, 2006*). Thin (<2 m) beds of red, yellow, brown or black salt provide useful strain markers.

The upper part of the Oligocene sequence, the Lower Red Formation, is made of gyprock, sandy shale and some volcanics. A similar sequence, referred to as Upper Red Formation, was deposited in the Miocene. Between the Lower and Upper Red Formation

there is a sequence of limestone, marl, shale and sandstone which is called the Qom Formation (Fig. 2 A.B). The age of the Qom Formation is upper Oligocene to lower Miocene.

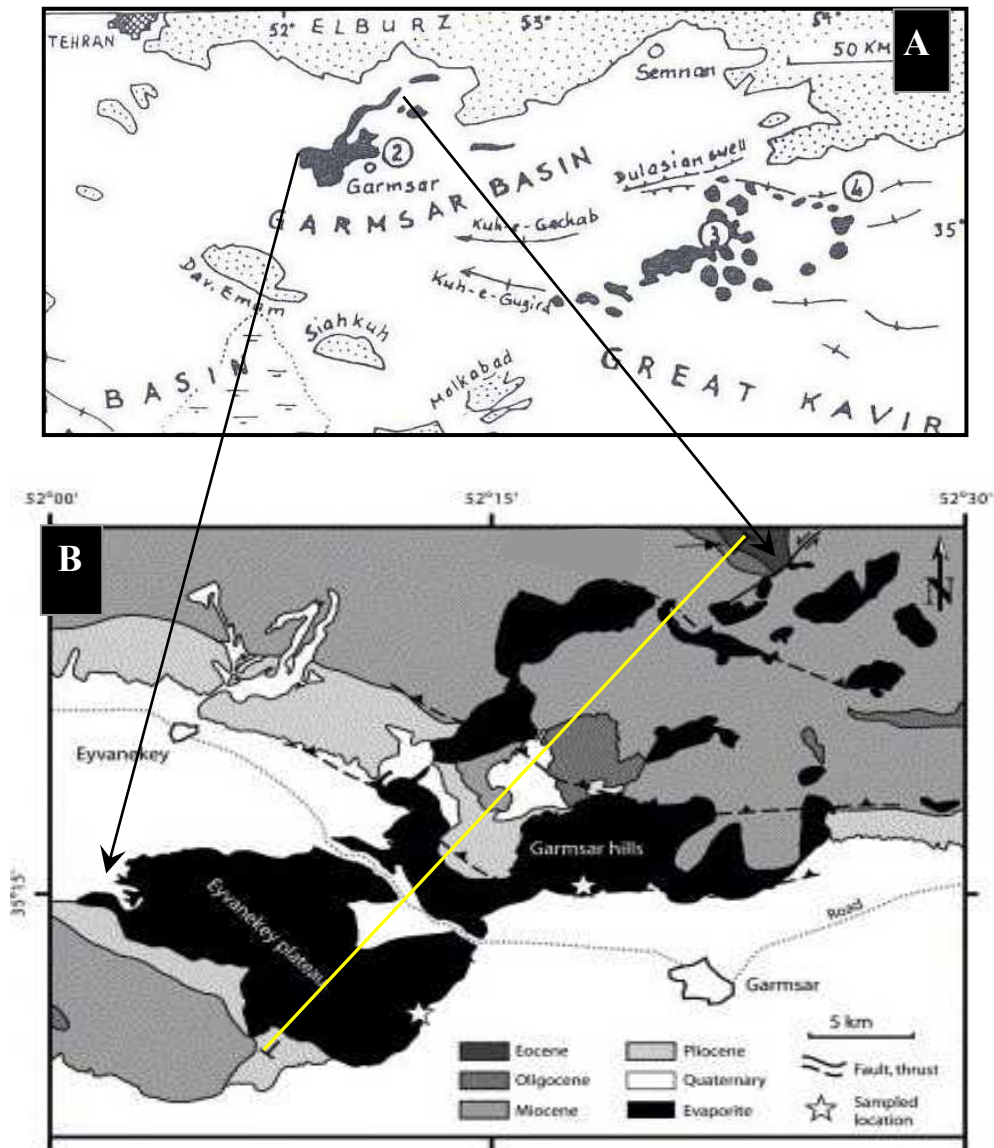


Fig.1. Simplified geological setting of Garmsar hills, Eyvanekey plateau and surroundings. (A) Cenozoic evaporites at surface in the Garmsar and Great Kavir basins (Jackson et al., 1990). (B) Geological map of Garmsar hills and Eyvanekey plateau (after Amini & Rashid, 2005). Yellow line indicates cross section shown in Fig.2.

The present surface of the Garmsar Salt Nappe is covered by several meters of barren residual insoluble soils after dissolution of the salt by rain (Talbot, 2004). Most of these soils are light green to pale brown gypsite with subordinate marl and calcareous marl (Amini and Rashid, 2005). Several authors (Jackson et al 1990) proposed that all of the salt structures in central Iran involve the same two salt sequences: (i) a relatively pure,

upper Eocene to lower Oligocene salt (base of lower Oligocene, Lower Red Formation) and (ii) a variegated, impure lower Miocene salt sequence (lower Miocene, Upper Red Formation).

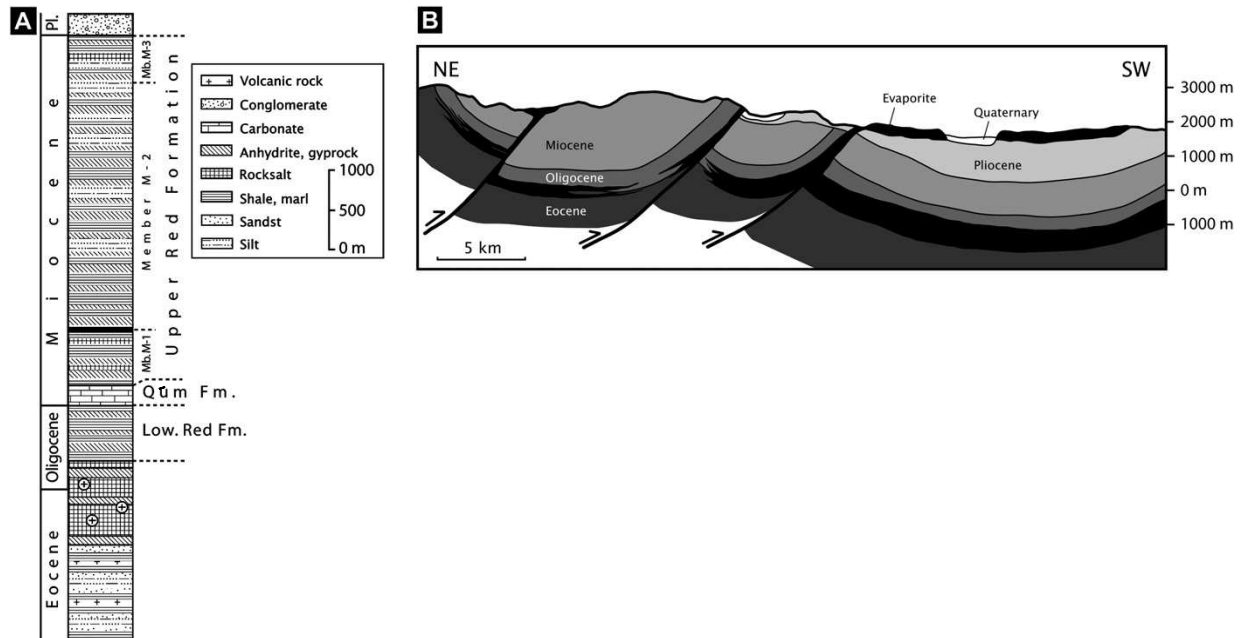


Fig. 2. (A) Stratigraphy of the rocks of the Garmsar basin (after Jackson et al., 1990). The Eocene to Oligocene rock salt is the main source for the extrusions of Garmsar hills and Eyvanekey plateau. (B) Cross section through the Garmsar hills and Eyvanekey plateau (modified after Amini and Rashid, 2005). For location of cross section, see Fig. 1.B.

Requirements and criteria for a waste repository

The finding of a waste repository is an engineered structure that requires interdisciplinary cooperation. Geoscientific and technical studies are necessary to work out a concept in which site, deposition mode, properties of the host rock, and geological situation are coordinated in a way that natural and artificial barriers are available to protect man and environment.

The factors that determine whether or not a reservoir or salt cavern will act as a suitable storage facility are both geological and geographical. The first site selection is made on the basis of geological maps, field studies and an evaluation of archival material, particularly seismic and other geophysical.

Geographically, potential sites would be relatively close to the consuming regions or industry. They must also be close to transport infrastructure, including main and trunk pipelines and distribution systems.

Moreover, recommendations for geoscientific studies of the site are to be made on the basis of the available data. In the following investigation of the site, all parameters relevant to the project must be evaluated for the final assessment of the technical feasibility and long-term safety of the repository. The first task of the site study is to define the present situation:

Determination of the rock types, stratigraphy, structure, fissure systems, and faults by field and geophysical studies. Structural studies will focus on the stability and deformability of the repository. Seismic data will be used to determine the structural edifice at deeper structural levels as well as regional earthquake activity. Hydrogeological investigations will help to constrain the type and nature of aquifers at different structural levels. Of particular interest are mine activities such as sulfur mining, salt mining, brine reduction, oil and gas activity, and any other activity which may adversely affect or be affected by waste disposal in a salt cavern.

Results

Surface deformation and subsidence pattern related to water extraction

Interferograms have been used to record the incremental ground deformation between the acquisitions dates. It is possible to produce a time series of the total surface displacement in the LOS between the starting time and each acquisition date. As there are as many linearly independent interferograms as acquisition dates in an unbroken chain (*Baikpour et al., 2010*), it is possible to use a least squares inversion to map/obtain the surface deformation for each time covered by the data (*Biggs and Wright, 2004; Bernardino, 2002*). The resulting mean displacement velocity map and plots (Fig. 3) indicate that the surface of the Eyvanekey Plateau and of the surrounding agricultural lowlands subsided continuously from 2003 to 2006. The maximum surface deformation rate is estimated to have been near 20 mm/yr in farmlands and 5 mm/yr in the centre of the sheet of allochthonous salt (*Baikpour et al., 2010*).

Almost 503 wells are present in the western part and 181 wells are present in the eastern part of the target area. Near Garmsar, east and west of the plateau, there is a correlation between the number of wells and the amount of subsidence (Fig. 3) suggesting the surface to subside most intense where the water table is significantly lowered by water extraction? Wells that cluster in areas of maximum subsidence appear to be overexploiting the groundwater. Wells in areas undergoing less subsidence may be fed more efficiently by water draining from the Alborz Range.

We attribute enhanced subsidence to fluid-controlled strain softening of rock salt by increasing the rates of dissolution/precipitation in winter when the salt is wet. The opposite case is given in summer when the salt is dry and thus much stronger.

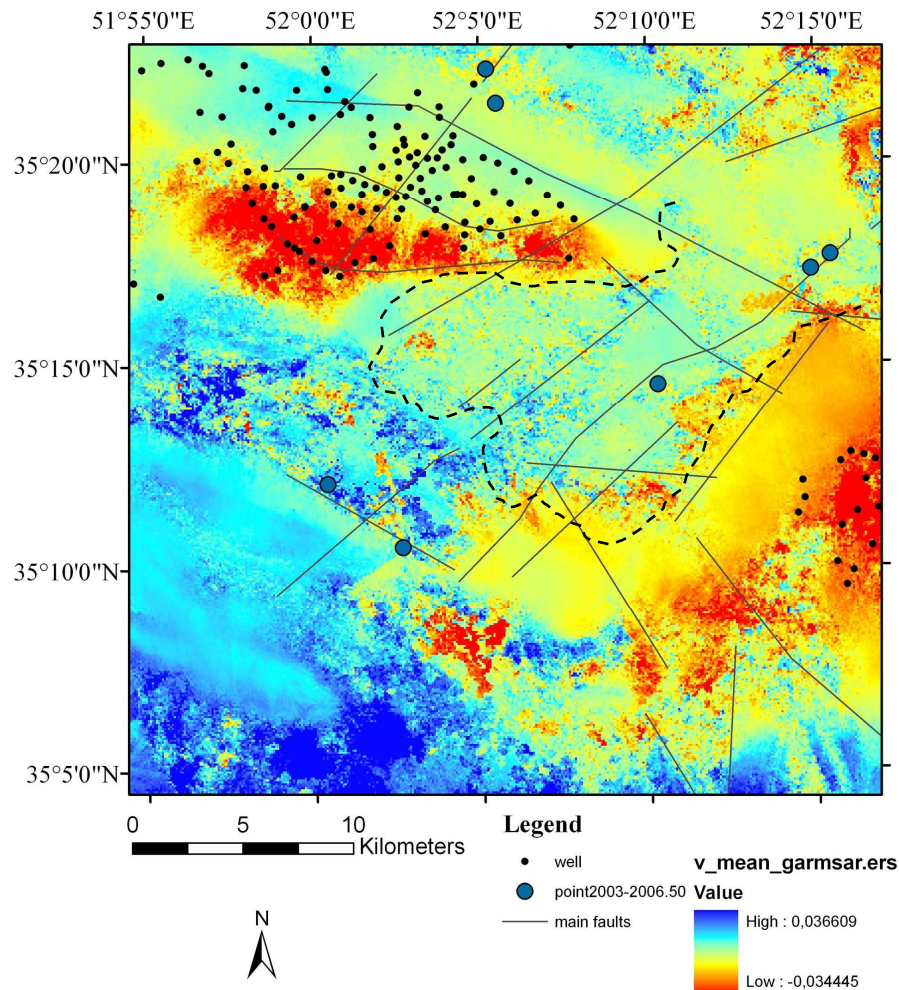


Fig.3. Mean displacement velocity map for the period 2 December 2003 to 14 June 2005. Velocity data have been calculated using MATLAB software. Blue filled circles indicate earthquake epicentres with magnitude (mb= 2 and 3) from 2003-2006 (from the IIEES catalogue). Dashed line shows the outline of salt exposed at the surface. Scaling of velocity bar is in m/yr.

Structural properties and evolution related to emplacement of salt dome

Measuring and recording the orientation of planar and linear structures was an important task during field activity. Spatial attitude of bedding and other planar and linear fabrics are collected in the study area in order to understand completely all the geological structures (i.e., folds and fractures) and analyses of geological structures help to interpret the conditions of deformation of salt rock in the study area.

We measured the structural elements (bedding, fold axes, joints, faults and fractures) in 48 outcrops (Fig. 4). The faults in the study area are probably blind faults which are covered by sediments.

Different parameters and structural elements are related to the Garmsar Basin and controlling the salt extrusion and salt flow. Several structural features related to the Garmsar Salt Basin will be presented in the present study.

Most of the lineaments in satellite images of the Garmsar Salt Nappe are interpreted as surface traces of faults. Epicentres of seven small earthquakes (ML=2 and 3; Table1) occur along some of these faults and indicate that the latter are active. All these small shocks were recorded by only 3 or 4 instruments so no kinematic solutions are available. Most of the epicentres shown are located to an accuracy of $\sim \pm 5$ km and most were at depths near 14 ± 7 km.

Most of the lineaments are straight and extend southward of the Garmsar fault but makes a conspicuous bend around the SE corner of the Garmsar Salt Nappe suggesting that fault movement stopped at the base of the salt sheet.

Date	Lat.	Lon.	Depth	Mag.	Ref.	Region
2003/09/06	35.02	52.17	15	Mb: 2.9	IIEES	S of Garmsar
2003/10/13	35.07	52.15	18	Mb: 3.5	IIEES	Garmsar
2004/10/17	35.10	52.19	14	ML: 3.2	IIEES	Garmsar
2005/02/06	35.15	52.23	14	ML: 2.7	IIEES	Garmsar
2005/02/08	35.14	52.10	14	ML: 2.2	IIEES	W of Garmsar
2005/02/08	35.17	52.14	14	ML: 2	IIEES	Garmsar
2005/03/02	35.16	52.17	14	ML: 2.1	IIEES	Garmsar
2005/04/24	35.17	52.15	34	ML: 2.2	IIEES	Garmsar
2006/05/08	35.21	52.05	14	ML: 2.7	IIEES	NW of Garmsar
2006/07/23	35.21	52.23	14	ML: 2.6	IIEES	N of Garmsar
2006/11/18	35.10	52.02	15	ML: 3	IIEES	W of Garmsar

Table 1: Earthquake data observed by the International Institute of Earthquake Engineering and Seismology (IIEES).

As the largest of the earthquakes (on salt nappe) was ML ~ 2.2 , the radii of the surfaces that underwent seismic slip can be expected to have been about 10^4 times the displacement along them (*Slunga, 1991*). The largest displacement along likely fault traces in the study area is ~ 16 mm. This implies that the slip surfaces had radii near 160 m close to the hypocenters at depths at 14 and 18 km. However, the lineaments in the area are between 1 and 32 km long (Fig. 3). This disparity implies that a large proportion

of the fault movements seen in the InSAR data must be aseismic. Other lines of evidence indicating aseismic slip in the area are: (i) the slow rates at which seismic disturbances appear to propagate, and (ii) displacements that vary in magnitude along one or both sides of many faults as though adjacent blocks are folding.

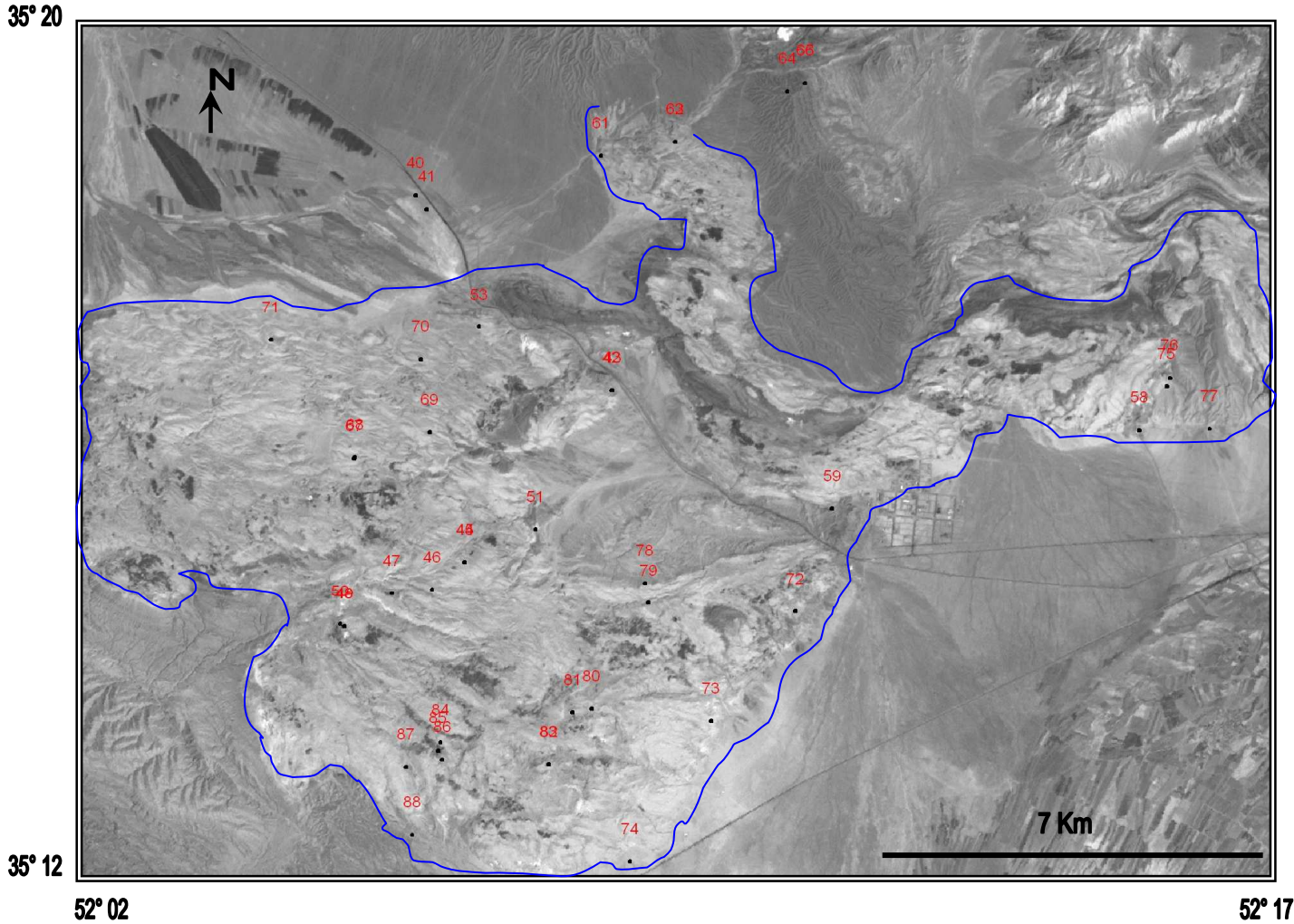


Fig.4. Map showing the localities where measurement of structural elements have been carried out. The coordinates of the stations were recorded on GPS and then plotted on georeferenced landsat image.

The interferograms reveal that, instead of the initiation of new faults, older pre-existing faults are frequently reactivated. Repeated movement along pre-existing faults within several months in advance or arrears of 10 small ($ML < 3.5$) earthquakes points to a much larger component of ductile strain than the 50 to 100% of the total deformation being seismic suggested as typical of the Alborz by Jackson and McKenzie (1988) or the 30-100% suggested by Masson et al. (2005). This assumption is reinforced by two earthquakes ($ML = 2$) with epicentres lying ~ 8 km apart moving within 220 minutes of

each other. Any communicating disturbance between these shocks travelled at ~36 m/min or 60 cm/s, very slow compared to brittle fractures that are expected to propagate at km/second. Similarly, the lengths of the faults that moved in several epochs are much longer than expected from such small earthquakes.

Joints and fractures are important structural elements that were investigated in the study area. Like all subaerial salt extrusions in Iran, the Garmsar Salt Nappe has an outer skin or carapace of brittle and broken salt, usually capped by residual soil. This dilated carapace is weak, slippery and ductile when wet, but brittle and elastic when dry. Fractures documented systematically along this Salt sheet are distinguished into several types on the basis of their orientations and inferred origins.

In almost every outcrop of salt, up to three orthogonal sets of dilational joints occur parallel and perpendicular to the local mechanical anisotropy, the latter resulting from compositional layering and/or the grain-shape fabric of salt. In most cases the long axes of the grains is parallel to the compositional layering. In fold hinges, where strong grain-shape fabrics are at high angles to the compositional layering, these anisotropy-related joints are symmetrical about both the planar and linear components of the grain-shape fabric. Apertures range from millimeter to decimeter. Some are filled with reprecipitated halite, while others have been widened by dissolution and are filled with soil. A few early joints, mineralized with salt, are steep because they were formed perpendicular to the subhorizontal compositional layering.

Another fracture system consists of relief-related joints (*Talbot, 1998*). These relate to recent free surfaces to the salt and are not quite as common as the anisotropy-related joints. Although most relief-related joints are now open, remnant salt infill survive locally in some of them. Relief-related joints occur in three sets that change in orientation around the mountain. In a few locations, vertical dilation fractures bisect two conjugate shear fractures with shared concentric strikes and opposed 45° dips. More usually, a single set of planar joints dips 45° radially outward from the dome, parallel to a formerly simple slope now fretted by dissolution.

In some parts polygonal joint systems are present which are attributed to diurnal and seasonal thermal stresses. Some of the steep fractures are not compatible with the concentric or the radial fracture patterns. Some of these master joints continue over the surface for hundreds of meters.

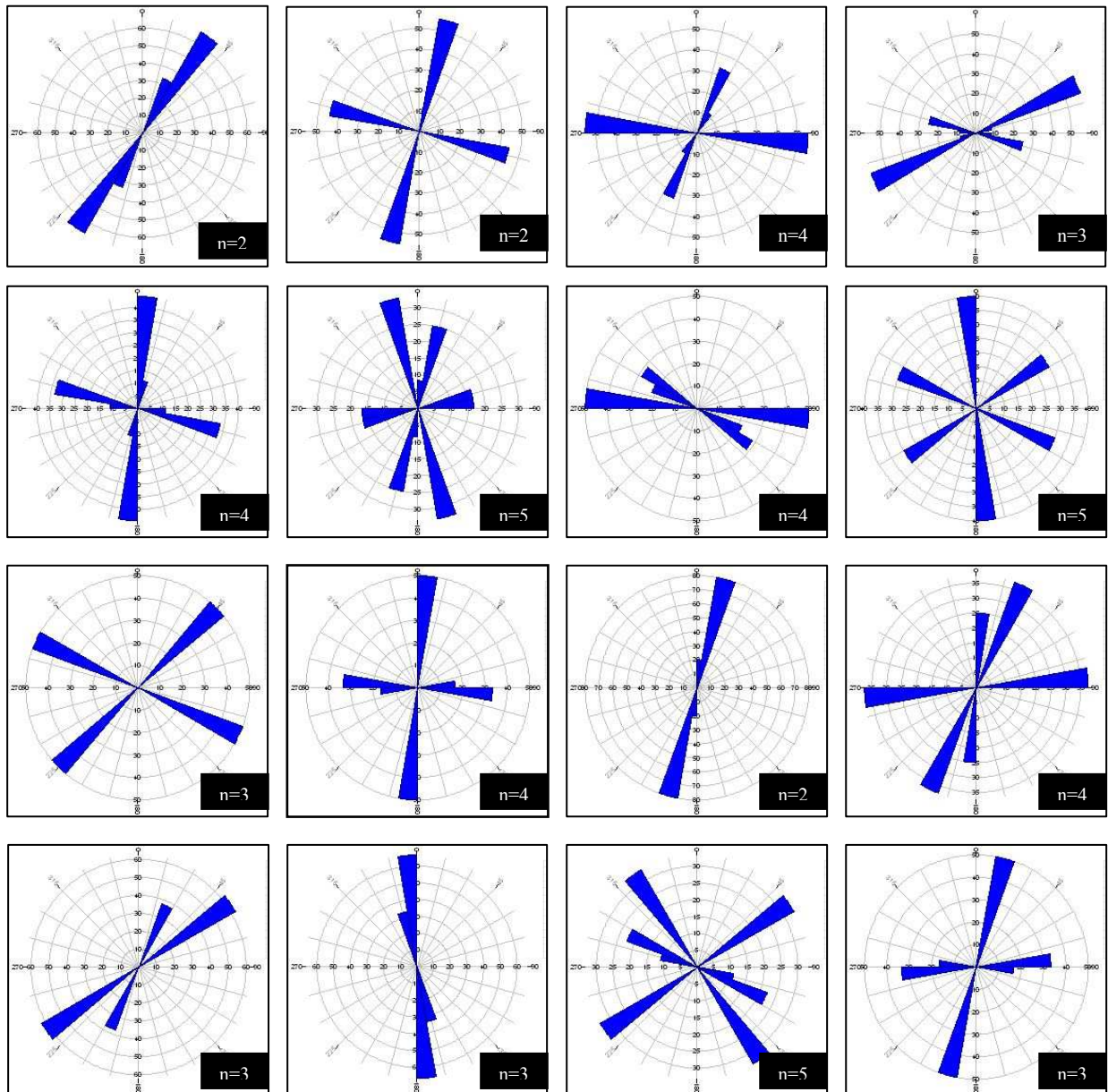


Fig.5. Rose diagrams of joint orientations at each station. Unless otherwise indicated, each rose diagram consists of data from all beds at an individual station. These are plotted on a landsat image in figure 6. Orientation of predominant joints as shown in each diagram is almost in N-S direction. (n) is number of joints acquired in the field work.

The six sets of master joints are interpreted as consisting of two sets of steep conjugate shears bisected by vertical N-S dilation fractures (Fig. 5 & 6) and another pair of steep conjugate shears is bisected by vertical E-W dilation fractures. The geometry of those shown in Fig. 6 suggests that they are due to the regional N-S shortening. Those might record temporary swaps in the regional stress axes (σ_1 for σ_3) that might drive strike-slip along the regional faults. Joints and fractures are supporting permeability in reservoirs and hence impact the productivity and recovery efficiency in those areas.

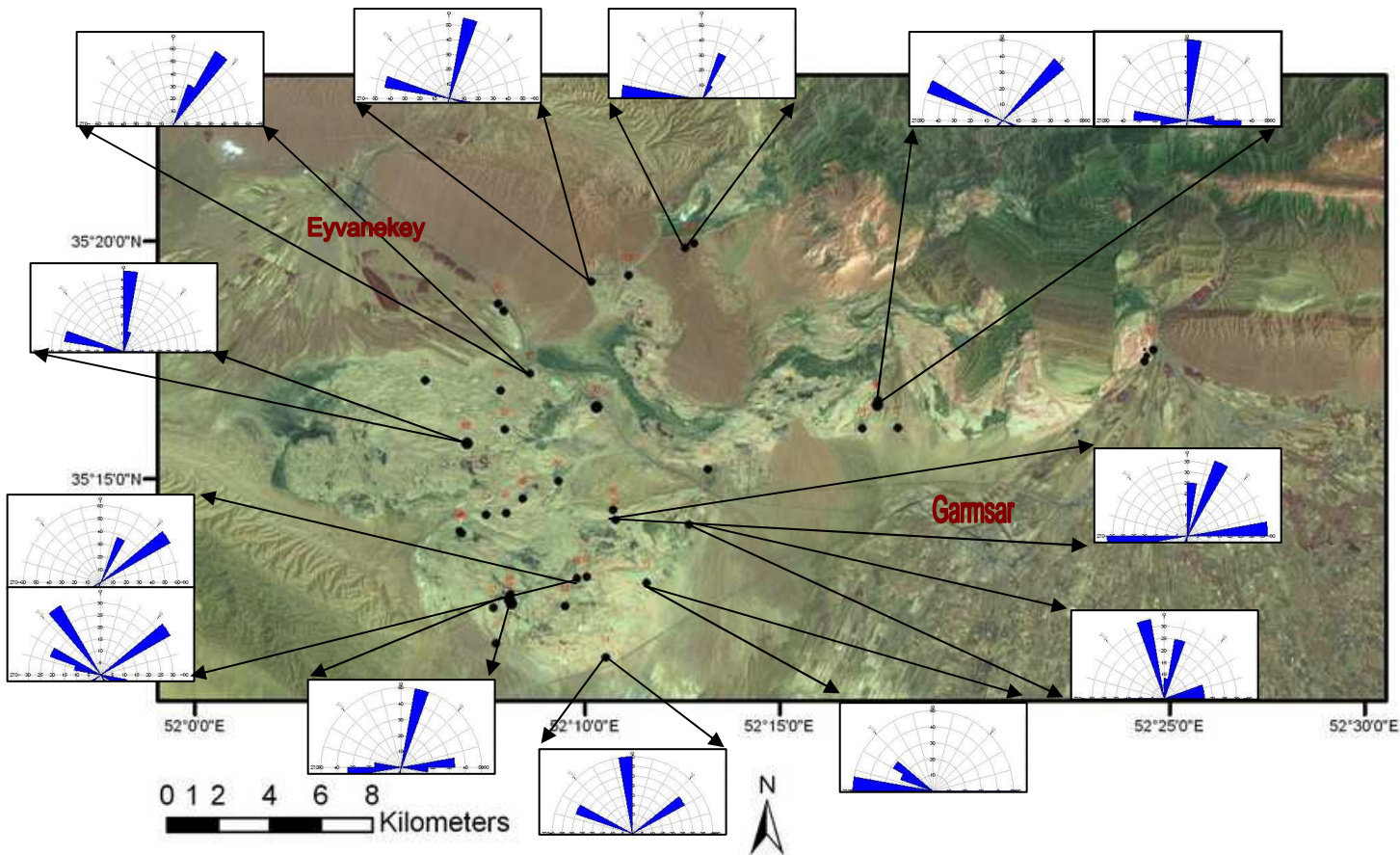


Fig.6. Orientation distribution of joints and fractures in the Garmsar salt nappe and surroundings. The joints are sub- vertical in most cases

Gravity anomalies

The Bouguer gravity map shows strong anomalies in the SW and weak anomalies in the NE (Fig.7). There are two uplifts in Bouguer gravity anomalies corresponding to the southern border of the study area, one of which is relatively strong. The strongest anomaly is at the furthest S of the study area. Anomaly values are less than in the northern weak anomaly belt (Fig. 7).

There are negative anomalies in the N and NE of the study area. Several local positive anomalies occur over relatively high anomalies toward the S of the Garmsar salt sheet, which are related to the convergence of a series of volcanic rocks trending SW. Relatively low anomalies in the open toe of the salt sheet and a vast anomaly E of the salt sheet and N of Garmsar town indicate a negative anomaly zone (Fig. 7).

The Map of Bouguer Gravity Anomaly

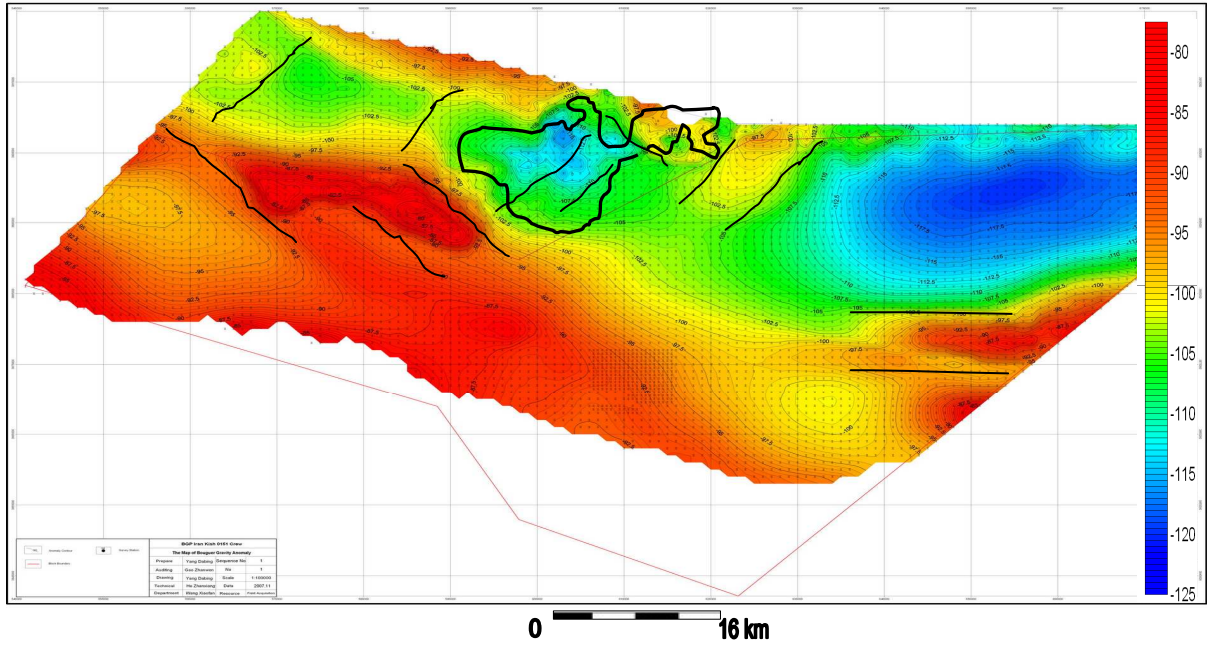


Fig.7. Bouguer gravity anomaly map. Narrow black lines show direction of extracted faults and the thicker black line shows the outline of salt exposed at the surface. Scaling of velocity bar is in mGal and Contour Interval is 2.5 mGal. (Source: NIOC)

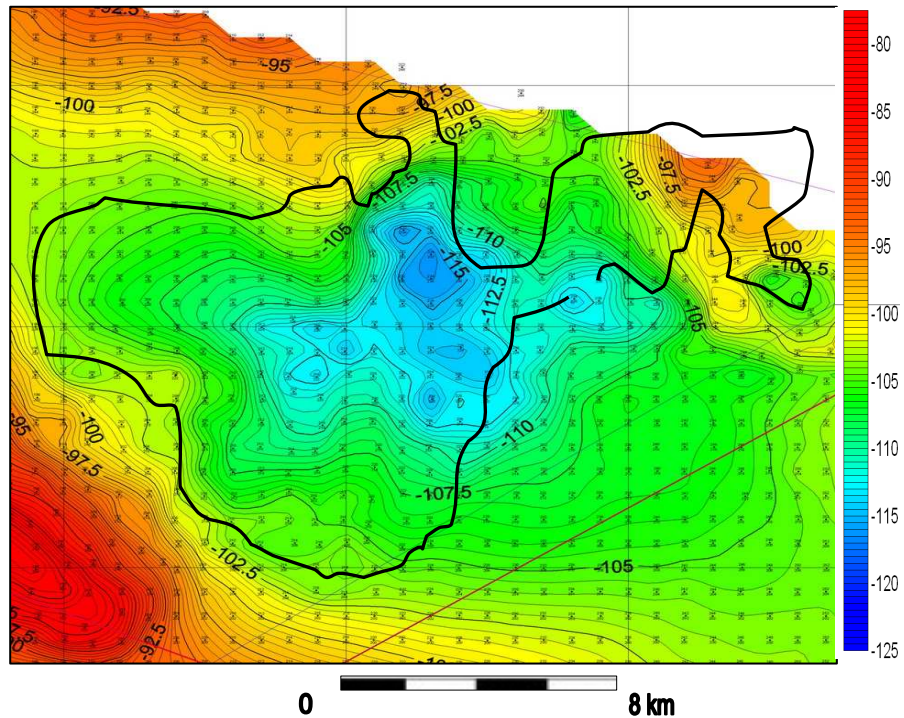


Fig.8. Bouguer gravity anomaly map of the salt nappe. The deepest line here is -116 mGal that shows the lowest anomaly in Garmsar salt (black line), it may correspond to a stem of salt inside the Garmsar salt dome.

Basement and Faults

The determination of faults is based on the Bouguer gravity anomalies, magnetic anomalies and processed plots on the base of above data, such as level total gradient gravity anomaly, the image map of gravity and magnetic anomaly and regional geology and outcrops. According to the criteria for faults identification with gravity and magnetic methods, and integrating seismic and geological data, we totally identified several faults (Figs. 7 and 8), which can be divided into (i) N-S trending master faults, and (ii) two groups of NW and NE trending faults.

According to the Bouguer gravity anomaly, the reduction of the Bouguer anomaly towards the NNE (Fig.7) indicates thicker sedimentary cover on top of the Garmsar basement (Fig.8). Gravity inversion of basement burial depth (Fig. 7) indicates that basement depth of uplift in the middle of the study area is about 2000 - 5000 m, which divides the basement into two sub-depressions. The largest buried depth of the Garmsar sub-depression in the S is >5000 m.

The timing of faulting in the study area is only badly constrained. However, most of the faults must have been active after the Eocene and were repeatedly reactivated in subsequent times.

Seismic sections

As no well data are available, the stratigraphic layers of the study area (Lower Red, Qom and Upper Red Formation) are only poorly constrained by seismic data. The seismic data were collected by Chinese contractors inside the National Iranian Oil Company in the southern part of the Garmsar Salt Nappe (Fig. 9). There are 2D and 3D seismic data. In the present paper, we are considering the 2D seismic sections only.

Our interpretation reveals a series of NE-SW, NW-SE and E-W trending faults, most of which dip to the SW except NE-SW trending faults. The NE-SW trending reverse faults are well known in the Central Iranian Basin as well as in the Alborz Mountains Range. The NW or NE trending dextral and sinistral strike-slip faults are consistent with the faults displayed on the geological map and with the lineaments derived from other studies.

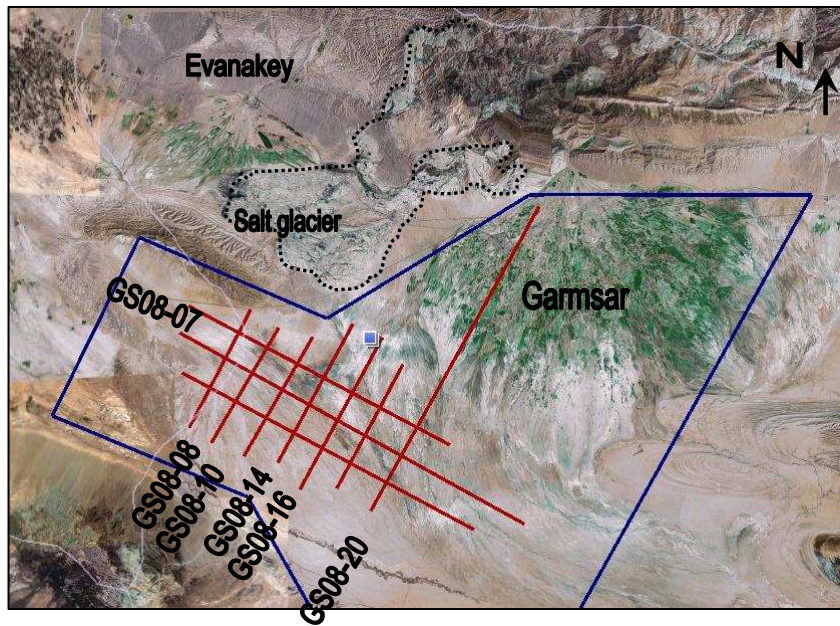


Fig.9. NE-SW and NW-SE trending seismic lines recorded by National Iranian Oil Company (NIOC) in the southern part of Garmsar salt extrusion.

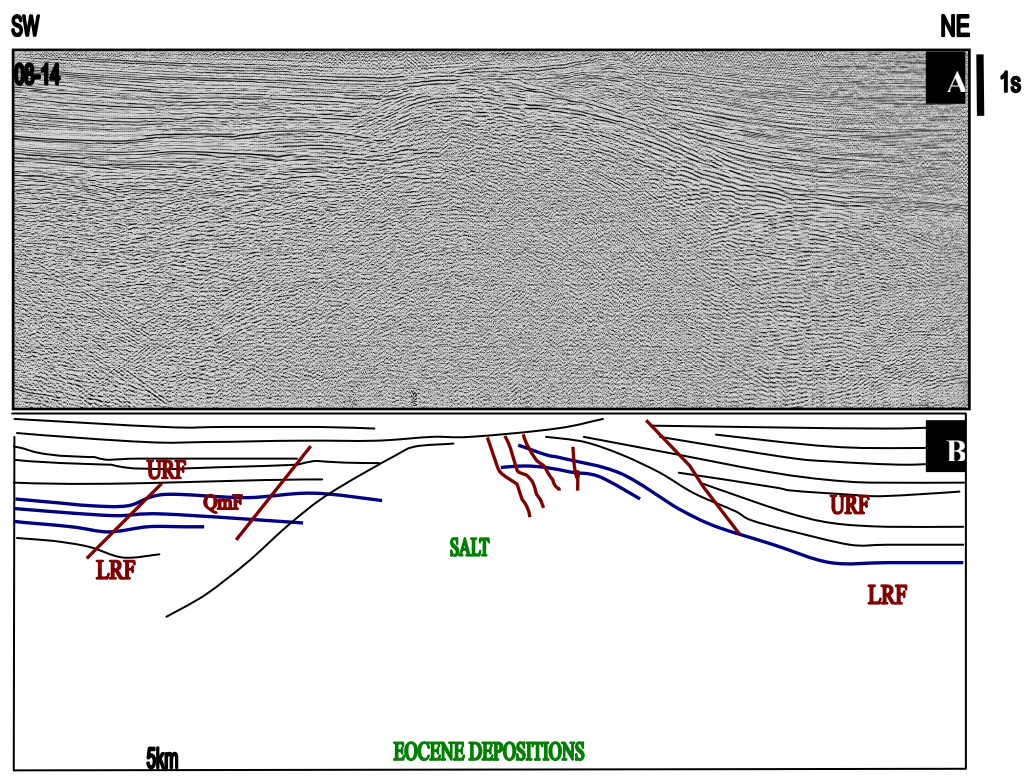


Fig.10. (A) Seismic profile and (B) line drawing showing a set of steep faults in crest and around the anticline of the salt dome. The onlapping reflectors, especially on the western flank, and thinning of the layers above the crest, indicate uplift of the salt during the Tertiary.

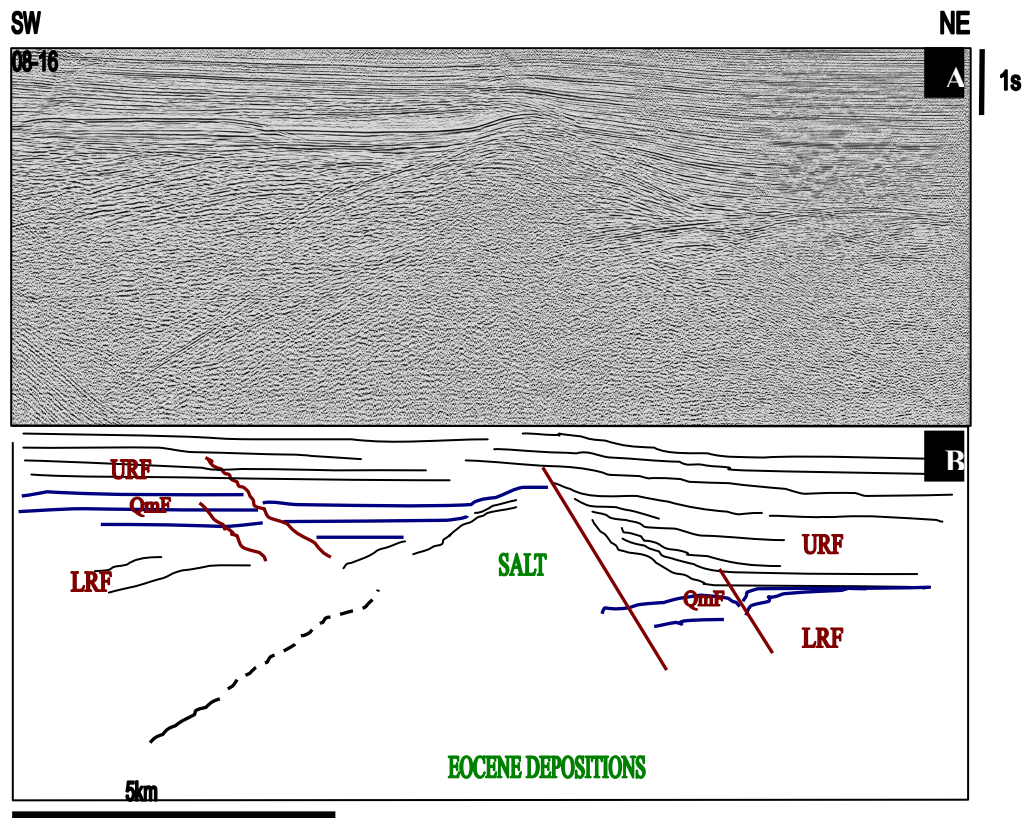


Fig. 11. NE-SW seismic profile (A) and line drawing (B) of the section showing that thinning of the URF in the central part of the seismic image is due to vertical extrusion of the salt. The LRF (Miocene) growth strata present as a young anticline above the salt dome, which was subsequently folded.

Discussion

Disposal of hazardous and radioactive waste in deep geological formations is actually not practiced, and has never practiced for high-level waste in Iran. A large body of research is required for safety and radiological aspects, migration and chemical interactions.

Environmentally compatible disposal sites must be found to avoid and reduce the generation of dangerous waste. A suitable disposal site does not depend on host rocks alone but rather on the integral geological settings that provide the required isolation potential. The selection procedure shall rather enable the identification of integral geological settings with favorable conditions for the final disposal of radioactive waste (Fig.13).

In the Garmsar Salt basin, deep geologic disposal provides the logical solution for waste with respect to near surface sites. Prior to selection of areas with favorable conditions for the disposal, at first areas with obviously unfavorable conditions shall be excluded by criteria. Based on these criteria, no uplift/subsidence of several millimeters per year and no seismic activity during the required isolation time should be observed. Based on our

applied research in Garmsar and Eyvanekey plateau, the latter might have been influenced and displaced about 9 km along the Zirab-Garmsar dextral fault. We interpret many of the lineaments of the Garmsar salt nappe to have originated as small-scale faults. Epicenters of seven small ($ML=2$ and 3) earthquakes in the region aligns along some of these faults and indicates that they are still active. On the other hand, the mean displacement velocity map and plots indicate that the surface of the Eyvanekey Plateau and the surrounding agricultural lowlands subsided continuously from 2003 to 2006.

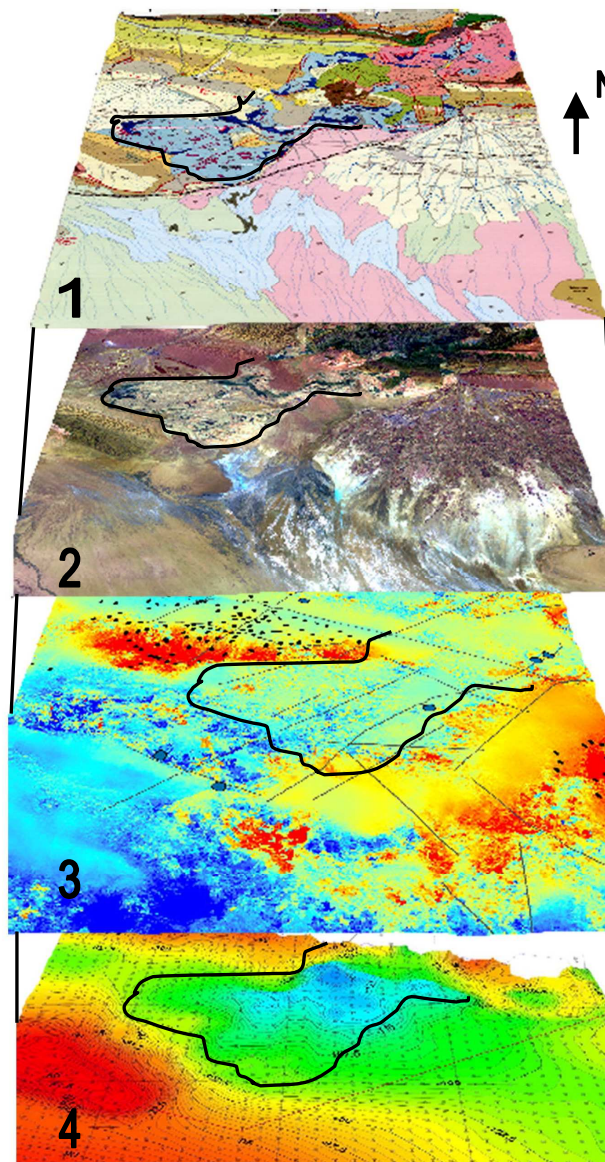


Fig.12. Sequence of overlain maps of the target area showing results of surface and subsurface studies.

Dark line shows outline of salt exposed at the surface. (1) Geological map, (2) Landsat image, (3) Mean displacement velocity map, (4) Bouguer gravity anomaly map.

The Garmsar salt nappe is a surficial sheet of allochthonous salt about 400 m thick. The InSAR results imply that the salt is dissolving at about 5 mm/y in the current rainfall. So the current low rainfall is likely to dissolve a 400 m thick salt sheet in about 80, 000 years. Radioactive waste and toxic wastes stays nasty for at least 100,000 years if not 1 million years so any deposited in the plateau is likely to be exposed before it has decayed to acceptable levels of radiation. Consequently, near surface sites obviously will not be able to satisfy the favorable conditions and criteria for high-level waste disposal (Fig. 12 & 13).

The present database of the Garmsar Salt basin suggests that chemotoxic and radiotoxic waste might be safely and permanently be disposed in the deep salt layers. Positive aspects that could make the deep salt layers of the Garmsar basin as a favorable site for waste disposal are:

- No or only slow ground water movement at repository level.
- Low tendency to build new pathways in salt layers.
- Situation which allows a good spatial characterization of the salt rock formation.
- Situation which allow a reliable prediction of the long-term stability of the favorable conditions of the salt rock formation.
- Good compatibility of the salt layers with temperature changes.

Some geo-scientific scenarios have been identified as negative aspects in deep repository areas:

- Geological or tectonic events, e.g. seismic activities in earthquake zones.
- Active disturbance zones.
- Geophysical basement faults treatments.
- Human life risks and environmental problems.

Intracrystalline inclusions and intercrystalline pockets in undisturbed rock salt contain saturated brines, each with a different chemical composition, a unique isotopic ratio, and a distinct and specific pressure. These discrete brine occurrences constitute convincing evidence for the tightness of the salt: what little formation fluid it contains has not become homogenized by internal or external force and has therefore remained isolated for tens to hundreds of millions of years (Stein and Krumhansl, 1984).

Distinctions between low, intermediate and high-level waste categories are not clear and consistent internationally. Classification schemes may be based on half-life, activity, origin or source, degree of isolation required, etc. In general, low-level waste contains radionuclides with low activities and short half lives and generates no significant heat.

Intermediate waste may contain radionuclides with low to intermediate activities and short to long half lives, generating no to negligible heat. High-level waste contains radionuclides with high activities, long or short half lives or both, and generates significant heat.

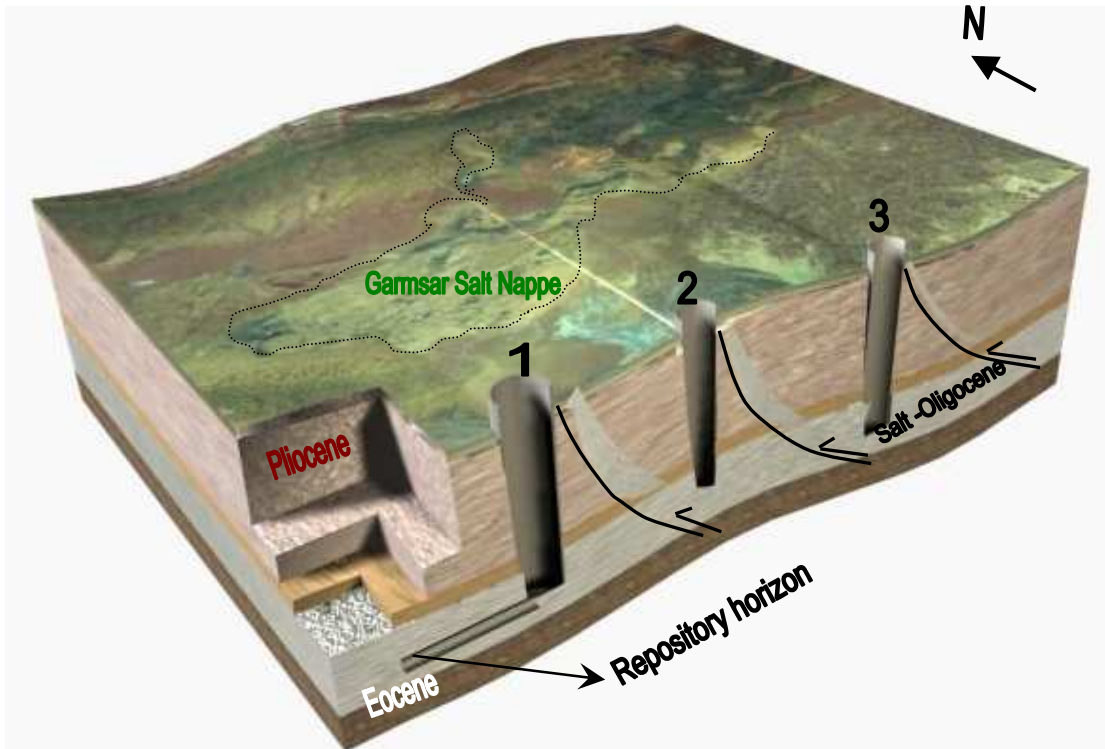


Fig.13. A 3D model through the Garmsar hills and Eyvanekey plateau. Underground bedded salt in white colour was investigated as an appropriate repository for every kind of wastes; the wells reach the bedded salt in depth 2000m below the surface. The dashed narrow line shows outline of exposed salt.

Characteristics of host salt formations dominate the cavern configuration design. Thus short, stout caverns are generally sited in bedded salts, whereas tall, slender caverns are often located in salt domes or anticlines. A horizontal caverns obviously “fit” bedded salt formations better than vertical ones (Fig.13), and bedded salt may be available where domes are not dominated.

Injection wells could be used across the Garmsar deep bedded Salt (Fig.13) for all kinds of wastes mentioned above, including industrial and municipal waste disposal, solution mining of uranium and sulfur and every kind of high-level waste.

Bedded salt formations occur in layers interspersed with such sedimentary materials as anhydrite, shale, dolomite, and other more soluble salts (e.g., potassium chloride). These

materials have varying degrees of permeability, but all are generally low (Freeze and Cherry 1979). The bedded salt deposits are tabular and can contain significant quantities of impurities.

Effects of basaltic intrusions in bedded salt formations are considerable in Garmsar deep salt basin. The mechanical and physico–chemical interactions between the volcanic magma as a source of heat and corresponding fluids with rock salt, as well as the extent of these processes should be studied.

Resulting from the complexity of the data analysis related to the storage of hazardous wastes, our knowledge is still incomplete. Focusing on the petrophysical properties of salt rock the following work is necessary.

Geophysical methods (electromagnetics, georadar, geoelectrics, seismics and sonar) are required to evaluate the safety and stability of geologic barriers in salt mines. The presence of water in the salt rock can impair the stability of the mine and the effectiveness of the salt rock as a geological barrier. Thus, information about such zones must be included in the site assessment. The reliability of the information is increased by the use of more than one method.

The thermomechanical behaviour (creep and fracture behaviour) of the various natural salt rock types, especially of evaporites such as anhydrite and carnallite, should also be investigated in more detail taking long-term effects into account.

Conclusions

The selection process for potential host rocks for hazardous waste repositories in deep geological formations in the Garmsar salt basin was based on internationally recognized geoscientific exclusion criteria and minimum requirements, as well as other criteria considered from a geoscientific point of view.

Exclusion criteria with social background will be applied to the areas with favorable integral geological settings. Areas which do not satisfy these criteria are also excluded from the procedure, as shown in Fig. 13 the near surface salt layers are out of the minimum requirements and it is impossible to safely and permanently dispose chemical and industrial waste in near surface host rocks.

The remaining possibilities such as deep geologic repositories imply favorable integral geological settings and are not excluded from planning for legal or socioeconomic reasons. In the next steps, regions within the remaining areas are identified. In order to do so, again a comprehensive set of geo-scientific and social-scientific criteria has to be

developed. The significance of the geo-scientific and social scientific criteria must be evaluated so that a ranking of the regions and sites can be performed. In this step, safety assessments have to be used to a larger extent, e.g., to be able to judge data uncertainties with regard to the isolation capability.

Acknowledgements

We thank the National Iranian Oil Company for supplying Geophysical data, and the Geological Survey of Iran GSI for supplying the hard- and software as well as logistical support when we prepared and analyzed the data. We also thank Gholamreza Peyrovian (from NIOC) for preparing the Geophysical data.

References

- Alavi, M., 1996. Tectonostratigraphic synthesis and structural style of the Alborz mountain system in northern Iran. *Journal of Geodynamics* 21, 1–33.
- Amini, B., Rashid, H., 2005. Garmsar geological map 1:100000 in scale. Geological Survey of Iran, Tehran, Iran.
- Baikpour, S., Zulauf, G., Dehghani, M. & Bahroudi, A., 2010, InSAR maps and time series observations of surface displacements of rock salt extruded near Garmsar, northern Iran, *Journal of the Geological Society, London*, 167, 171-181.
- Berardino, P., Fornaro, G., Lanari, R., and Sansosti, E. (2002). A New Algorithm for Surface Deformation Monitoring Based on Small Baseline Differential SAR Interferograms. *IEEE Trans. On Geoscience and Remote Sensing*, 40: 2375-2383.
- Biggs, J., Wright, T. (2004). Creating a time series of ground deformation using InSAR. Scientific report, Department of Earth Science, University of Oxford.
- Freeze, R.A., and J.A Cherry, 1979, *Groundwater*, Prentice-Hall, Inc., Englewood Cliffs, NJ.
- Jackson, J. & Mckenzie, D., 1988, The relationship between plate motions and seismic moment tensors, and the rates of active deformation in the Mediterranean and Middle East, *Geophysical Journal* 93, 45-73.
- Jackson, M.P.A., Cornelius, R.R., Craig, C.H., Gansser, A., Stocklin, J., Talbot, C.J., 1990. Salt Diapirs of the Great Kavir, Central Iran. Geological Society of America, Boulder 177.
- Masson, F., Chery, J., Hatzfeld, D., Martinod, J., Vernant, P., Tavakoll, F. & Ghafory-Ashtiani, M. 2005, Seismic versus aseismic deformation in Iran inferred from earthquakes and geodetic data. *Geophysical Journal International*, 160, 217-226.

- Schleder, Z., Urai, J.L. 2006. Deformation and recrystallization mechanisms in mylonitic shear zones in naturally deformed extrusive Eocene-Oligocene rock salt from Eyvanekey plateau and Garmsarhills (central Iran). *Journal of Structural Geology*, 1-15.
- Slunga, R.S., 1991: The Baltic Shield earthquakes. *Tectonophysics* 189, 323–331.
- Stein, C.L., Krumhansl, J.L., 1984. Compositions of Brines in Halite from the Lower Salado Formation, Southeastern New Mexico. SAND84e 1252A. Abstracts with Programs. Geological Society of America. 99th Annual Meeting, Reno.
- Talbot, C.J., 1998. Extrusions of Hormuz salt in Iran. In: Blundell, D.J., Scott, A.C. (Eds.), *Lyell; The Past is the Key to the Present*. Geological Society Special Publications, vol. 143, pp. 315-334.
- Talbot, C.J., Aftabi, P., 2004. Geology and models of salt extrusion at Qom Kuh, central Iran. *Journal of the Geological Society* 161, 32-334.
- Wallner, M., Lux, K.-H., Minkley, W. and Hardy, H.R., 2007. *The Mechanical Behavior of Salt. Understanding THMC Processes in Salt*. Taylor and Francis Group, London, UK., 453 pp.